



**The roles of neural cell adhesion molecules NCAM and
CHL1 in the regulation of synaptic ultrastructure in
mice (*Mus musculus* Linnaeus, 1758)**

Dissertation

Zur Erlangung des Doktorgrades des Departments Biologie der Fakultät für
Mathematik, Informatik und Naturwissenschaften an der Universität Hamburg

vorgelegt von Dmytro Puchkov

Hamburg, 2008

Genehmigt vom Department Biologie
der Fakultät für Mathematik, Informatik und Naturwissenschaften
an der Universität Hamburg
auf Antrag von Frau Professor Dr. M. SCHACHNER
Weiterer Gutachter der Dissertation:
Herr Professor Dr. L. RENWRANTZ
Tag der Disputation: 23. Mai 2008

Hamburg, den 09. Mai 2008




Professor Dr. Jörg Ganzhorn
Leiter des Departments Biologie



HPI

Heinrich-Pette-Institut für Experimentelle Virologie
und Immunologie an der Universität Hamburg

Carol Stocking, Ph.D.
FG Molekulare Pathologie
Fon (040) 480 51-273
Fax (040) 480 51-187

stocking@hpi.uni-hamburg.de

HPI · Martinistraße 52 · 20251 Hamburg

Fachbereich Biologie
Universität Hamburg
Martin Luther King-Platz 2
D-20146 Hamburg

Hamburg, 31. März 2008

Sehr geehrte Damen und Herrn,

hiermit bestätige ich, dass die von Herr Dmytro Puchkov mit dem Titel "The roles of neural cell adhesion molecules NCAM and CHL1 in the regulation of synaptic ultrastructure in mice (*Mus musculus*)" vorgelegte Doktorarbeit in korrektem Englisch geschrieben ist.

Mit freundlichen Grüßen,

Dr. Carol Stocking

Leiterin der FG Molekulare Pathologie
Heinrich-Pette-Institut
(Amerikanerin)

Heinrich-Pette-Institut
für Experimentelle Virologie
und Immunologie an der
Universität Hamburg

Martinistraße 52 · 20251 Hamburg
Telefon +49 (0) 40 480 51-0
Telefax +49 (0) 40 480 51-103
hpi@hpi.uni-hamburg.de

Bankverbindung
Haspa (200 505 50)
Konto 1001 315 959
www.hpi-hamburg.de



Mitglied der
**Leibniz
Gemeinschaft**

Content

I. INTRODUCTION	7
1. The neural cell adhesion molecule NCAM	7
1.1 Structure and general features of NCAM	7
1.2 Expression of NCAM	8
1.3 Functions of NCAM	9
1.4 Phenotype of NCAM ^{-/-} mice.....	10
2. Morphological correlates of synaptic plasticity and NCAM	11
2.1 Synapses.....	11
2.2 Synaptic plasticity.....	14
2.3 AMPA receptor recycling.....	16
2.4 Morphological correlates of synaptic plasticity.....	17
2.5 NCAM and synaptic plasticity.....	20
3. The neural cell adhesion molecule CHL1	21
3.1 Structure and general features of CHL1	21
3.2 Expression of CHL1	21
3.3 Functions of CHL1	22
3.4 Phenotype of CHL1 ^{-/-} mice.....	23
4. Synaptic vesicle recycling and CHL1	23
4.1 Synaptic vesicle recycling	23
4.2 Clathrin uncoating.....	24
4.3 CHL1 interaction with Hsc70	26
II. AIMS OF THE STUDY.....	27
III. MATHERIALS AND METHODS.....	28
1. Animals	28
2. Materials	28
2.1 Laboratory equipment.....	28
2.2 Chemicals	29
2.3 Primary antibodies	29

2.4 Secondary antibodies and imaging probes.....	31
2.5 siRNAs and cDNA of SAP90GFP.....	31
3. Methods	31
3.1 Analysis of the brain morphology.....	31
3.1.1 Brain tissue processing	31
3.1.2 Estimation of synapse density in CA1 stratum radiatum using disector method.....	33
3.1.3 Measurements of cross-sectional area of spines and number of synaptic vesicle in synaptic terminals	34
3.2 Cultures of hippocampal neurons	35
3.2.1 Preparation of dissociated hippocampal cultures.....	35
3.2.2 Processing of cultures for electron microscopy	35
3.2.3 Preembedding labelling of GluR1 receptors with Nanogold conjugates	36
3.2.4 Analysis of synapse morphology in hippocampal cultures.....	36
3.3 Treatments of hippocampal neurons	36
3.3.1 Treatments to block synaptic activity, vesicle endocytosis, and to induce actin/spectrin meshwork disassembly.....	36
3.3.2 Chemical stimulation of synaptic activity in cultures with high potassium buffer.....	37
3.3.3 Chemical LTP induction protocol.....	37
3.3.4 Transfection of hippocampal neurons.....	37
3.3.5 Loading of hippocampal neurons with β I-2,3-spectrin, β II-2,3-spectrin, HPD and QPD peptides	38
3.4 Immunocytochemistry	38
3.4.1 Confocal laser-scanning microscopy	38
3.4.2 Indirect immunofluorescence staining.....	38
3.4.3 Quantification of GluR1 and GluR2 antibody uptake	39
3.4.4 Analysis of CHL1 antibody uptake into cultured neurons.....	40
3.4.5 Time lapse imaging of SAP90-GFP transfected neurons	40
3.5 Statistical analysis.....	41
IV. RESULTS.....	42

Project 1. The role of NCAM in maintaining of the cytoskeleton-dependent structural integrity of post-synaptic densities and regulation of the AMPA receptor recycling.....	42
1.1 Number of synapses with perforated PSDs is increased in NCAM ^{-/-} mice	42
1.2 Inhibition of synaptic activity or fusion of vesicles with the plasma membrane does not reduce the number of perforated PSDs.....	44
1.3 The spectrin meshwork maintains the structural integrity of PSDs.....	46
1.4 Actin polymerisation is required for spinule formation but not for PSD perforation.....	48
1.5 Disruption of the postsynaptic spectrin cytoskeleton does not enhance PSD splitting	50
1.6 Disruption of the postsynaptic spectrin cytoskeleton increases postsynaptic endocytosis and AMPA receptor internalisation	51
1.7 LTP-associated PSD perforations are accompanied by enhanced AMPAR endocytosis.....	55
Project 2. The role of the cell adhesion molecule close homologue of L1 (CHL1) in regulation of clathrin-dependent synaptic vesicle recycling.....	58
2.1 CHL1 is accumulated in the presynaptic plasma membrane	58
2.2 CHL1 recruits Hsc70 to synapses	61
2.3 CHL1 is endocytosed to synapses in response to synapse activation.....	63
2.4 Number of clathrin-coated vesicles is increased in synaptic terminals of CHL1 ^{-/-} mice.....	66
2.5 Activity-induced formation of CCSVs is reduced in CHL1 ^{-/-} neurons	68
2.6 Activity-induced formation of CCSVs is reduced in CHL1 ^{+/+} neurons after acute CHL1/Hsc70 complex disruption	71
2.7 Disruption of CHL1/Hsc70 complex inhibits activity-induced recruitment of clathrin and Hsc70 into synaptic terminals.....	73
V. DISCUSSION	75

Project 1. The role of NCAM in maintaining of the cytoskeleton-dependent structural integrity of post-synaptic densities and regulation of the AMPA

receptor recycling.....	75
1.1 The role of NCAM/spectrin organized cytoskeleton in the regulation of PSD structure and postsynaptic endocytosis.....	75
1.2 Model of perforation formation and its role in synaptic function.....	77
 Project 2. The role of the cell adhesion molecule close homologue of L1 (CHL1) in the regulation of clathrin-dependent synaptic vesicle recycling.....	79
2.1 Role of CHL1 in the regulation of clathrin uncoating from synaptic vesicles	79
2.2 Effects of disregulated clathrin uncoating on synaptic vesicle recycling and overall synapse function in CHL1-/- synapses	81
 VI. SUMMARY.....	84
VII. REFERENCES.....	86
VIII. ACKNOWLEDGEMENTS	100
IX. APPENDIX.....	101
1. Abbreviations.....	101
2. Publications and poster presentations	102
3. Curriculum vitae	103
4. Erklärung	104

I. INTRODUCTION

1. The neural cell adhesion molecule NCAM

1.1 Structure and general features of NCAM

The neural cell adhesion molecule (NCAM) belongs to the immunoglobulin superfamily of cell adhesion molecules. Immunoglobulin cell adhesion molecules are transmembrane or membrane-bound molecules containing one or more immunoglobulin like domains (Fig.1). The extracellular part of NCAM contains five Ig-like domains (Ig1-5) and two fibronectin type III-like domains (FNIII1-2) (Maness and Schachner, 2007). Fasciclin II of *Drosophila melanogaster* and the cell adhesion molecule from *Aplysia californica* (apCAM) are homologous to the mouse and human NCAM. In vertebrates, NCAM exists in three major membrane-bound isoforms produced by alternative splicing: NCAM-120, NCAM-140 and NCAM-180. They are named after their approximate molecular weight. NCAM-140 and NCAM-180 are transmembrane proteins that differ by the length of their intracellular domain. NCAM-180 contains additional 261 amino acid insert in its intracellular domain. NCAM-120 completely lacks intracellular and transmembrane domains and is linked to the membrane via a glycosylphosphatidylinositol (GPI) anchor (Fig. 1). In addition, soluble forms of NCAM could be generated by truncation, proteolysis or shedding from the plasma membrane (Olsen et al., 1993). Several posttranslational modifications of NCAM proteins are known, such as phosphorylation of serine and threonine residues (Mackie et al., 1989), palmitoylation of cysteine residues in the cytoplasmic domain (Niethammer et al., 2002) and glycosylation of asparagine residues in the extracellular domain. Very important posttranslational modification of NCAM is glycosylation with an oligosaccharide polysialic acid (PSA) which mediates some NCAM functions in cell migration and synaptic remodelling; therefore NCAM is mentioned as PSA-NCAM in some studies (Muller et al., 1996). NCAM could also carry some other carbohydrates, for example a sulphated glycan HNK-1 epitope (Kruse et al., 1984; Schachner and Martini, 1995).

1.2 Expression of NCAM

NCAM is widely present in developing brain, however during maturation of nervous system, NCAM expression, and in particular expression of its polysialylated form, decreases being more prominently present only in regions of the brain with higher levels of neuronal plasticity like hippocampus and olfactory bulbs. NCAM isoforms have different expression profiles. NCAM-120 is usually expressed on glial cells whereas NCAM-140 is present on both glial cells and neurons (Maness and Schachner, 2007). NCAM-180 is more prominently expressed on neurons (Schachner, 1997; Schuster et al., 1998). At the subcellular level, NCAM-180 is more prominently accumulated at the postsynaptic membrane of synapses whereas NCAM-140 tends to be preferentially expressed on axons and axonal terminals. Noteworthy, NCAM-180 is prominently concentrated only in certain subpopulations of synapses indicating dynamic nature of NCAM concentration at synapses that might be important for synaptic remodelling (Schuster et al., 2001). Number of synapses positive for NCAM and overall NCAM expression becomes up-regulated after the induction of long term potentiation (LTP) (Schuster et al., 1998).

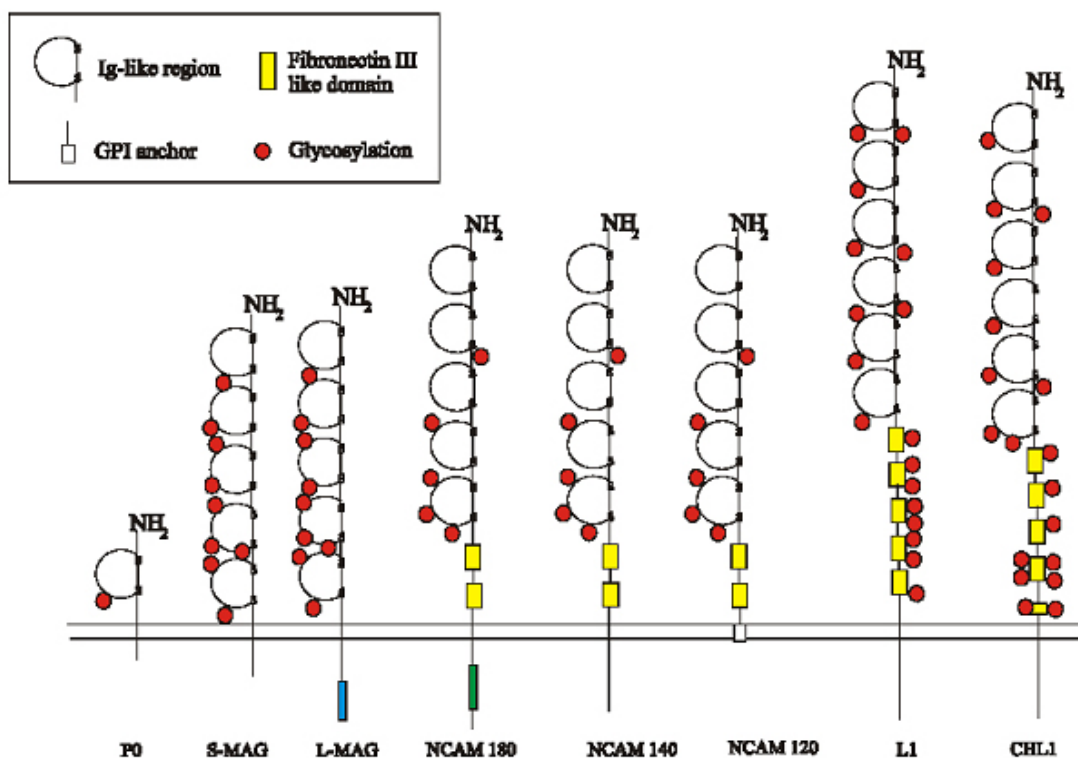


Figure 1. Examples of members of the immunoglobulin superfamily. Neuronal cell adhesion molecules NCAM and CHL1 belong to the immunoglobulin superfamily. P0, MAG isoforms, NCAM isoforms, CHL1 and L1 are shown. Extracellular domains of all immunoglobulin cell adhesion

molecules contain for at least one immunoglobulin-like domain. Additionally cell adhesion molecules could contain fibronectin type III repeats, a single transmembrane region and intracellular domain or alternatively GPI anchor. Glycosylation sites are present in all cell adhesion molecules shown above.

1.3 Functions of NCAM

NCAM is involved in the number of processes like cell proliferation, cell migration, neurite outgrowth, axon fasciculation, and synaptic remodelling (Schachner, 1997; Doherty and Walsh, 1992; Jorgensen, 1995; Kiss and Muller, 2001; Maness and Schachner, 2007). The extracellular part of NCAM plays a role of receptor or co-receptor for different cell adhesion and extracellular matrix molecules. The intracellular part of NCAM is involved in signal transduction functions and anchoring of proteins via its interaction with the cytoskeleton (Sytnyk et al., 2006; Maness and Schachner, 2007). As all members of immunoglobulin superfamily, extracellular domain of NCAM interacts with its binding partners in calcium independent manner. Homophilic binding of NCAM is very strong thus a twofold increase in NCAM concentration raises adhesiveness of beads coated with NCAM more than 30 folds (Hoffman and Edelman, 1983). In vivo molecules of NCAM readily interact with each other. Thus NCAM is the main physiological binding partner of itself, and its self-interaction can take place either on the same (cis-interaction) or apposing (trans-interaction) membranes (Crossin and Krushel, 2000). In heterophilic interactions, NCAM can bind heparin, a key component of the extracellular matrix (Cole and Akeson, 1989). Soluble NCAM, derived by proteolytic cleavage at the membrane, can bind to collagen I- VI and IX (Probstmeier et al., 1989). Furthermore, NCAM assists homophilic binding of another cell recognition molecule (L1) positioned on the same cell membrane in “cis” configuration (Kadmon et al., 1990). NCAM also binds to phosphacan/RPTP ζ/β (Milev et al., 1994), TAG1/axonin-1 (Milev et al., 1996), RPTP- α (Bodrikov et al., 2005) and other molecules.

NCAM mediated signalling is important for promoting neurite outgrowth via homophilic or heterophilic engagements with other molecules on adjacent cell surfaces and in the extracellular matrix (Crossin and Krushel, 2000). NCAM serves both, as a ligand and as a signal transducing receptor. NCAM mediation of neurite outgrowth requires fibroblast growth factor receptor (FGF-R), which serves as a necessary co-factor for NCAM mediated signalling (Williams et al. 1995). NCAM mediated signalling is

transduced via different kinase cascades among them PKC and Fyn kinase pathways (Leshchyns'ka et al., 2003; Bodrikov et al., 2005). Despite of FGF-R receptor contribution to NCAM mediated neurite outgrowth, FGF-R might not be the only mediator of NCAM-dependent signal transduction (Kolkova et al., 2000).

NCAM is important for formation and stabilization of synapses. Thus in heterogenic cultures, where neurons obtained from NCAM^{+/+} and NCAM^{-/-} mice were grown together, synapses were more likely to be formed on NCAM^{+/+} neurons (Dityatev et al., 2000). NCAM accumulated in synapses recruits via spectrin TGN organelles that are important for trafficking of synaptic components providing growth and stabilization of newly formed synapses (Sytnyk et al., 2002). NCAM is also involved in the function of mature synapses. Amount of synaptic NCAM increases following LTP induction (Schuster et al., 1998). NCAM can act on synaptic plasticity via regulation of AMPA and NMDA receptor number and/or activity at synapses (Dityatev et al., 2000; Kiss and Muller, 2001; Bukalo et al., 2004; Sytnyk et al., 2006). Ligand action of PSA carried by NCAM could contribute to NCAM function in synaptic remodelling (Dityatev et al., 2004). LTP in the CA1 region of hippocampus is abolished in hippocampal slices treated with endoneuraminidase (endo-N), a bacterial enzyme that removes PSA, therefore reflecting LTP abolishment observed in NCAM deficient mice (Muller et al., 1996). However, NCAM function can not be simply reduced just to the function of the carrier of polysialic acid. The intracellular domain of NCAM directly binds and recruits spectrin to the postsynaptic membrane. Spectrin is a key organisational element of the membrane-associated cytoskeleton in the cell in general and PSD in particular (Ziff, 1997) where it anchors synaptic proteins and stabilize synaptic contacts (Pielage et al., 2005). The reduced amount of spectrin at NCAM^{-/-} synapses is likely to be responsible for the loss of NMDA receptors at PSDs of NCAM^{-/-} mice (Sytnyk et al., 2006). Present study investigates how NCAM/spectrin associated cytoskeleton influences morphology of synapses and which other proteins are dysregulated at synapses in NCAM^{-/-} mice.

1.4 Phenotype of NCAM^{-/-} mice

Knockout of the NCAM gene in mice evokes only moderate morphological changes in the adult nervous system in spite of multiple roles of NCAM in central nervous system (CNS) development and function (Cremer et al., 1994; Cremer et al., 1997). The

olfactory bulbs of NCAM deficient mice are reduced in size as a result of disturbed cell migration. Reduced sizes of olfactory bulbs and abnormal cell migration have been reported for wild type mice treated with endoneuraminidase N in order to remove NCAM-associated polysialic acid (Ono et al., 1994), indicating that normal NCAM-PSA expression is important for granule cell migration and normal development of olfactory bulbs. Published data also report disorganized structure of pyramidal cell layer in the CA3 hippocampal area and reduction in fasciculation and number of mossy fibre bundles in NCAM^{-/-} mice (Cremer et al., 1994; Cremer et al., 1997).

NCAM deficient mice exhibit abnormal behaviour. A modest alteration of exploratory activity, deficits in spatial learning and strongly increased intermale aggression have been previously observed (Cremer et al., 1994; Stork et al., 1997). Furthermore, NCAM^{-/-} mice show increased anxiety-like behaviour compared to wild type mice. Anxiety-related behavioural alterations in NCAM deficient mice could be reduced by agonists of serotonin namely buspirone and 8-OH-DPAT (Stork et al., 1999). This finding relates anxiety-related behavioural abnormalities to dysregulations of serotonergic system. Study of Delling and colleagues (2002) has clearly shown that alterations in serotonergic system in NCAM^{-/-} mice are due to alterations in delivery of Kir3 channels (inward-rectifying potassium channel) to the cell surface membrane in NCAM^{-/-} neurons. NCAM-180 and -140 decrease localisation of Kir3 in the plasma membrane of neurons. Thus absence of NCAM leads to the accumulation of Kir3 channels in the neuronal surface membrane and inhibition of serotonergic neurons.

As described above, NCAM^{-/-} mice show abnormalities in function of mature synapses. Electrophysiological parameters characterising some forms of synaptic plasticity are impaired in NCAM^{-/-} mice: LTP and LTD induction are severely inhibited in CA1 stratum radiatum of NCAM^{-/-} mice (Bukalo et al., 2004). Furthermore, lack of NCAM is accompanied by reduced amounts of spectrin, NMDA receptors and CAMkinaseII at synapses (Sytnyk et al., 2006).

2 Morphological correlates of synaptic plasticity and NCAM

2.1 Synapses

Chemical synapses are specialized cellular junctions through which neurons signal to each other or to non-neuronal cells. A typical chemical synapse consists of a presynaptic

terminal containing synaptic vesicles that are filled with the neurotransmitter and the postsynaptic membrane where receptor-coupled ion channels are accumulated. The information from presynaptic membrane is transmitted by release of neurotransmitters that activate ionotropic and/or metabotropic receptors located at postsynaptic membrane. The presynaptic terminal has a specialized membrane region where vesicles dock and release neurotransmitter into the synaptic cleft. This part is called an active zone. Opposing postsynaptic membrane is also highly specialized and contains high concentration of ion channels, receptors, signalling, cell-recognition, anchoring and cytoskeleton molecules. This protein accumulation could be seen at the electron microscope as the electron-dense material associated with the postsynaptic membrane and is called a postsynaptic density (PSD).

Synapses in the nervous system could be classified in dozens of classes depending on the neurotransmitter type, inhibitory or excitatory action on the innervated cell, type of innervated cell and position on it. The main excitatory input in the central nervous system is represented by glutamatergic synapses formed on dendrites of neurons. Depending on the position of a synapse on the dendrite of neuron there are spiny, shaft and stubby synapses. Shaft synapses are situated directly on the surface of dendritic branches. Spiny synapses are positioned on the specialized, short protrusions of dendrites, which are called spines (Fig. 2). These protrusions consist of a tiny neck and relatively wide head. Spines are able to move and also dynamically change the size over the time. Stubby spines are short and do not have neck. There is a third kind of dendrite protrusions, so called filopodia. These are very long thin protrusions. Filopodia are usually observed in big amounts in the immature brain and have been shown to be involved in the formation of new synapses (Fiala et al., 1998). In the immature brain, most of synapses are formed on filopodia and dendrite shafts. The number of spiny synapses increases with development and the majority of excitatory synapses providing electrical input to the principal pyramidal neurons in adult brain are formed on spines.

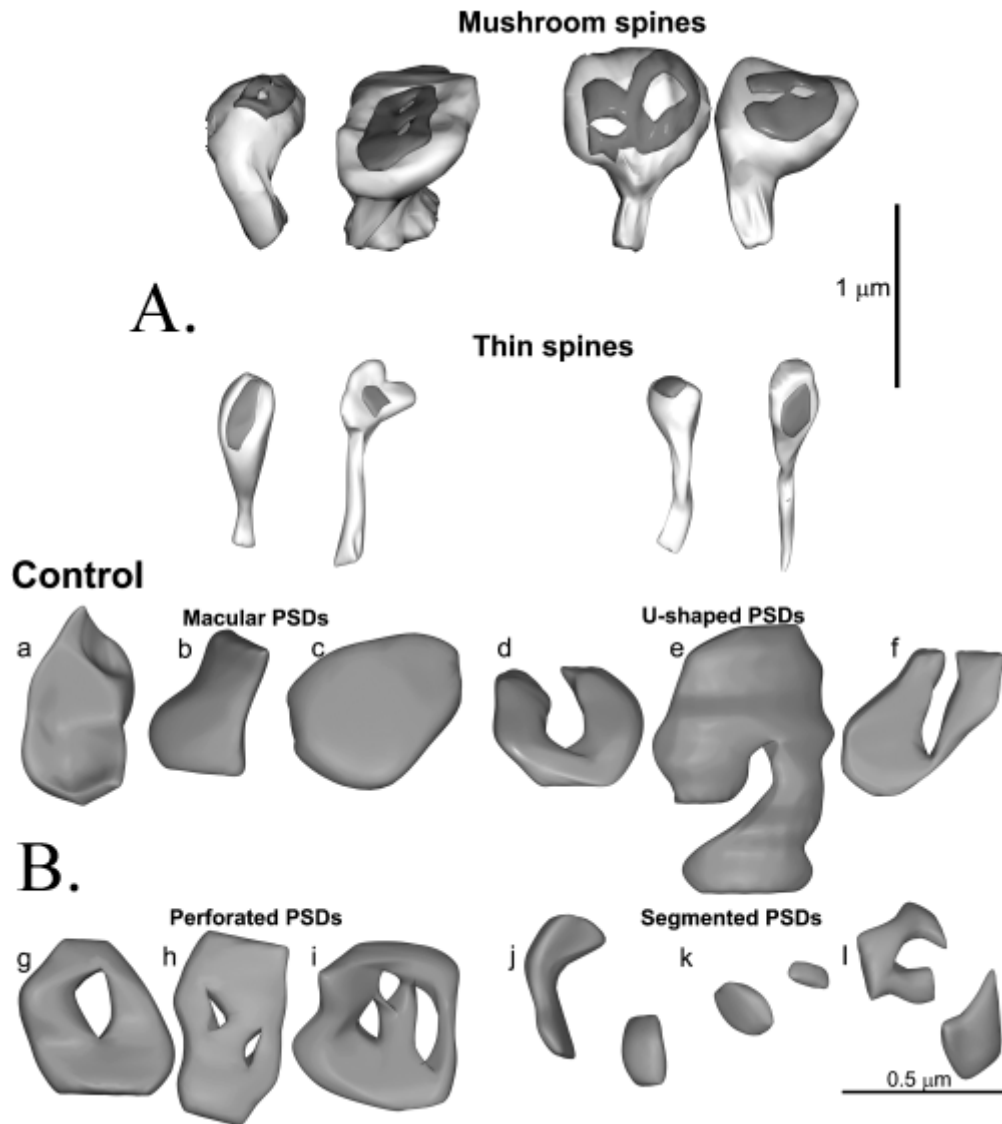


Figure. 2. Examples of three dimensional structure of dendritic spines (A) and postsynaptic densities located on mushroom spines (B). A. - 3-D reconstructions of mushroom and thin spines including their PSDs. B. - Four categories of PSDs located on mushroom spines: (a–c) macular PSDs; (d–f) U-shaped PSDs; (g–i) perforated PSDs with one (g), two (h), and three (i) perforations. Scale bars, 1 μm (A); 0.5 μm (B) (Image is taken from Stewart et al., 2005).

Glutamatergic synapses are heterogeneous in function and structure. Larger, mushroom-like spines contain more glutamate receptors (first of all AMPA receptors) and thus have higher transmission efficacy (Nicholson et al., 2006). Another interesting structural variation is the shape of the postsynaptic density. PSDs of 90 % of synapses are compact disk-like structures. Such synapses are called macular synapses. However some synapses possess PSDs of more complex shapes. Such PSDs consists of partially or even

completely segmented parts (Fig. 2). On two-dimensional sections they appear as two or more electron-dense parts separated by short regions of the normal plasma membrane. The shape of such complex PSD can be reconstructed in 3 dimensions analysing serial sections of the brain (Toni et al., 2001; Stewart et al., 2005). Reconstructions reveal that such complex PSDs can have following shapes: horse-shoe like, fenestrated, and completely segmented (Fig. 2). The site of “perforation” may contain so called spinules. A spinule is a long thin protrusion of the plasma membrane that goes deep into the neighbouring neurite.

Perforation of PSD and spinule formation attracted much of attention since these structural changes in the PSD were shown to be associated with LTP induction. However until now there is a controversy about the functional role of such PSD reorganizations and mechanisms inducing them.

2.2 Synaptic plasticity

The functioning of the nervous system is based on the ability of neurons to form neuronal networks, which are able to analyse and process incoming information from the outside world. This process is accompanied by ongoing restructuring of connections between neurons resulting in dynamic changes in transmission efficacy between individual elements of neuronal networks. Changes in transmission efficacy between neurons are referred to as synaptic plasticity.

Many forms of synaptic plasticity were discovered in the brain. They differ by directivity of changes (enhancement or, in opposite, depression of synaptic efficacy), by experimental or behavioural conditions that are necessary to induce a certain plasticity change, by duration (short or long-term changes) and by different molecular pathways underlying these changes. Interestingly, different types of neurons have their own specific patterns of synaptic plasticity changes (Bliss and Collingridge, 1993; Nicoll and Malenka, 1995; Sanes and Lichtman, 1999).

Long-term potentiation (LTP) is the form of synaptic plasticity that has been the most extensively studied so far in the central nervous system (Luscher et al., 2000; Derkach et al., 2007). The long-term potentiation (LTP) is a persistent increase in the efficiency of synaptic transmission between two neurons induced by certain stimulation protocol. LTP has been found by Bliss and Lomo in 1973 at synapses in the hippocampal dentate gyrus. However, later, it has been found in all excitatory pathways of the

hippocampus and also in the cerebellum and cortex (Sanes and Lichtman, 1999). Although the relation of LTP to learning and memory is not universally accepted, it nicely relates to neuronal network theories of brain function. LTP is widely used as a paradigm for long-term plasticity at the central synapse and was very helpful to elucidate the relation between morphological and functional parameters of synapses in different regions of the brain (Yuste and Bonhoeffer, 2001).

Different ways are used to induce LTP: high frequency stimulation; theta burst stimulation, which is thought to resemble the naturally occurring theta rhythm in the hippocampus; paired stimulation and pharmacological treatments (Sanes and Lichtman, 1999). Chemicals used to induce LTP include picrotoxin, a blocker of inhibitory GABA receptors, potassium channel blocker TEA, NMDA agonist glycine in combination with Mg^{2+} free solution, high potassium chloride concentration for general depolarization and others (Stewart et al., 2005; Park et al., 2004). Although chemical induction of LTP is considered to be less “physiological” than electrical induction protocols, in some experiments chemical LTP induction offers some advantages, for example, activation of larger sample of neurons than it is possible with electrical stimulation.

LTP is divided into 4 phases: the induction phase and the following initial LTP (short term potentiation (STP) and post-tetanic potentiation (PTP)), the early expression phase and the late expression phase. LTP is induced by Ca^{2+} influx in combination with other factors like concentration and pattern of Ca^{2+} influx itself, level of depolarisation of neuron, availability and pre-activation of molecules involved in signalling cascades, etc. Early expression phase of LTP is maintained by events on the local dendritic level including insertion of new AMPA receptors into the PSD and modification of pre-existed synaptic proteins by phosphorylation, for example. The later phases are characterized by the induction of gene transcription, protein expression and formation of new synapses. LTP exhibited by neurons is underlied by changes that occur both in the pre and postsynaptic parts of a synapse (Bliss and Collingridge, 1993; Malenka and Nicoll, 1999; Sanes and Lichtman, 1999). Presynaptic changes include enhancement of synaptic vesicle release probability and efficiency of glutamate uptake. Postsynaptic changes are associated with the increase of the number of glutamate receptors and their modification in the PSD of activated synapses.

2.3 AMPA receptor recycling

Majority of excitatory synapses in the central nervous system are glutamatergic. AMPA (α -amino-3-hydroxy-5-methyl-4-isoxazolepropionic acid) and NMDA (N-methyl-D-aspartate) are the main ionotropic glutamate-gated receptors accumulating in postsynaptic densities of excitatory glutamatergic synapses. AMPA and NMDA receptors are tetramers consisting of four alternative subunits, GluR1–GluR4 for AMPA receptors and NR1, NR2A, NR2B, NR3 for NMDA receptors. Subunit composition has a strong influence on properties of glutamate-gated channels (Derkach et al., 2007). In contrast to AMPA receptors, NMDA receptors cannot be directly opened by glutamate because the pore of the channel formed by NMDA receptor subunits is blocked by ion of magnesium (Mg^{2+}). Therefore opening of the NMDA receptor requires two steps. The first step requires the depolarisation of the plasma membrane that changes the conformation of NMDA receptors allowing removal of Mg^{2+} from the channel pore. The second step is binding of glutamate that can open the channel. Another important difference between NMDA and AMPA receptors is calcium permeability. The size of the pore formed by NMDA subunits allows not only sodium but also calcium ions to enter the cell whereas AMPA receptors in subunit composition present in pyramidal neurons, allow only sodium to enter the cell in response to glutamate binding (Derkach et al., 2007). These two differences underlie different functional specialisation of two channels. Thus majority of fast excitatory transmission in the central nervous system is mediated by AMPA receptors whereas NMDA receptors are primarily involved in modulation of synaptic function via calcium signalling (Malenka and Nicoll, 1999).

The amount of AMPA receptors at the PSD directly correlates with the strength of a synapse (Nicholson et al., 2006). Synapses lacking significant amounts of AMPA receptors and thus containing mainly NMDA receptors are called “silent synapses” (Malenka and Nicoll, 1999). Regulation of the amount of AMPA receptors at synapses along with their modification are mechanisms underlying such forms of synaptic plasticity as LTP and LTD (Malinow and Malenka, 2002). Repetitive activation of synapses, which occurs during LTP induction, activates synaptic NMDA receptors that induce up-regulation of AMPA receptors in PSD via activation of the CamKII-ras-MAPK pathway (Zhu et al., 2002). New AMPA receptors are supplied by exocytosis of transport vesicles from recycling endosomes present in dendrites in the vicinity of activated spines (Park et al., 2004; 2006). This explains earlier experiments emphasizing crucial role of postsynaptic exocytosis for

LTP formation (Maletic-Savatic and Malinow 1998; Lledo et al., 1998).

Endocytosis of AMPA receptors results in a decrease in the synaptic strength. NMDA receptors signaling from extra synaptic sites induce LTD via the internalisation of AMPA receptors (Snyder et al., 2001; Hsieh et al., 2006). NMDA dependent regulation of the AMPA receptor concentration at synapses is involved in long-term depression (LTD) and long-term potentiation in many neuron types. The internalisation of AMPA receptors is mediated by clathrin-dependent pathway and endocytosed AMPA receptors are targeted to recycling endosomes (Carroll et al., 1999; Ehlers, 2000).

The regulation of cytoskeleton composition at synapse is another important way to regulate numbers of AMPA receptors at the PSD. AMPA receptors undergo free lateral diffusion in the neuronal plasma membrane. However in the PSD, receptors are getting accumulated since their diffusion is limited via high affinity association with the postsynaptic cytoskeleton (Tardin et al., 2003; Adesnik et al., 2005; Sharma et al., 2006). Depolymerisation of F-actin in spines by latrunculin A reduces spine localization of AMPA receptors (Allison et al., 1998). The role of the cytoskeleton in the regulation of AMPA receptor anchoring at synapses is also supported by findings showing that long-term depression associated AMPA receptor internalisation requires a reduction in their association with the scaffold proteins accumulated in the PSD (Lu and Ziff, 2005).

2.4 Morphological correlates of synaptic plasticity

Since the time of Ramon y Cajal two alternative mechanisms underlying synaptic plasticity were suggested. Ramon y Cajal himself speculated that learning required novel neuronal growth. At the same time Tanzi argued that changes in existing connections might underlie information storage in the brain (Yuste and Bonhoeffer, 2001). Later both ideas were combined by Hebb in 1949 in the postulate that alteration in synaptic strength of existing connections and formation of novel synapses might be responsible for learning and memory. Discovery of various forms of synaptic plasticity confirmed Hebb's suggestions. However there were difficulties in finding morphological correlates for observed functional changes. There are reports showing no alteration in the number or structure of synapses following long term potentiation induction or memory inducing paradigms. For example, Harris et al., (1992) indicates no change in the number of synapses as well as their structure at two hours following theta burst stimulation of

hippocampal slices. However later studies revealed that structural remodelling of synapses induced by LTP is a temporal process that takes place in just first hour following stimulation under experimental conditions used (Geinisman et al., 1991; Buchs and Muller, 1996; Toni et al., 2001). Creation of new synapses de novo is observed following LTP induction as well, however formation of new synapses occurs only in the vicinity of activated synapses and is probably accompanied by retraction of synapses in other dendrite regions thus maintaining overall amount of synapses on the same level as before stimulation (Toni et al., 2001). This process might be associated with activity-dependent scaling of the strength of synaptic currents received by the individual neuron (Turrigano et al., 1998). Activity-dependent scaling allows elimination of weak inputs in response to the strengthening of others, therefore contributing to synaptic competition and elimination. Interestingly, neurons increase the number of glutamatergic receptors in synapses and induce a compensatory synaptogenesis in response to the blockade of synaptic activity by low calcium or tetrodotoxin application trying to compensate for the loss of synaptic input (Turrigano et al., 1998; Kirov and Harris, 1999).

Time-lapse fluorescent confocal video microscopy shows that spines are motile structures. They perform oscillation-like movements within minutes. Application of AMPA leads to the “freezing” of this movement (Fischer et al., 2000). This nicely correlates with the stabilization of actin cytoskeleton that is important for anchoring of AMPA receptors in the PSD (Allison et al., 2000). Insertion of new AMPA receptors from the intracellular depot in the PSD of activated synapses does also occur (Zhu et al., 2002), and this insertion is absolutely crucial for further LTP expression.

The electron microscopy analysis revealed remodelling of individual stimulated synapses at the ultrastructural level (Fig. 3). Toni and colleagues (2001) used calcium precipitation protocol, which specifically marked synapses that were stimulated during LTP induction of the brain slices. Authors revealed that in 15 minutes following LTP induction, labelled spines in stimulated slices were increased in the size comparing with labelled spines from control non-stimulated slices. 30 minutes following LTP induction, nearly 45% of all labelled synapses turned into perforated synapses. However, the observed increase in the number of perforated synapses was only transient. 60 minutes following stimulation the number of perforated synapses dropped down to the basal level. However, at 60 minutes following LTP induction another morphological alteration could be seen. In LTP stimulated slices appearance of “multiple spine boutons” was observed.

Multiple spine boutons are groups of two or more closely positioned spines that arise from the same dendrite and form synapses with the same axonal bouton (Toni et al., 2001). Authors suggested that these neighbouring spines were created via splitting of the perforated synapses, and that perforated synapses represented an intermediate step of the synapse splitting (Toni et al., 2001; Nikonenko et al., 2002). Harris and colleagues (2002) conducted a similar experiment to validate this conclusion. This study also revealed an increase in the number of multiple spine boutons following LTP induction. However, authors showed that these multiple spine boutons could not be formed via synapse splitting since the gap between neighbouring spines of multiple spine boutons was often filled by stable structures like long mature axons and myelinated fibres, that should had been pre-existed long before LTP induction and appearance of additional spines. It was more likely that new spines in the vicinity of activated synapses appeared not due to the splitting of pre-existed synapses but as an independent act of synaptogenesis in the vicinity of activated synapses.

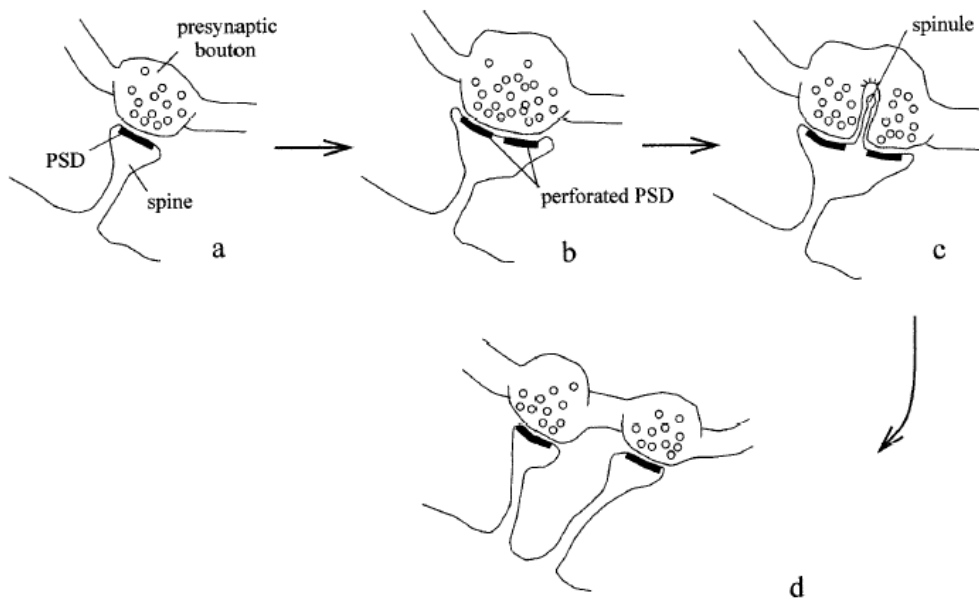


Figure 3. A time-line for morphological changes following long-term potentiation. a: A macular synapse before LTP stimulation. b and c: Size of postsynaptic density increases and perforation forms in the macular synapse at 30 to 60 min following LTP induction. d: The formation of multiple spine boutons occurs at 60 min to 120 min following LTP induction due to the locally induced synaptogenesis (Image adapted from Sorra et al., 1998).

The role of the PSD perforation is widely discussed in the literature (Geinisman et al., 1993; Edwards 1995; Nikonenko et al., 2002; Toni et al., 2001; Yuste and Bonhoeffer, 2001; Spaseck and Harris 2004). Basing on the fact that perforations are usually formed on big mushroom synapses with the large amount of AMPA receptors (Ganeshina et al., 2004) some studies suggest that the PSD perforation creates compartmentalized releasing sites that might increase efficacy of the perforated synapse comparing with non-perforated one. As it was discussed above, Toni and colleagues (2001), Nikonenko and colleagues, (2002) and others offered a hypothesis that a perforated synapse might be an intermediate step of the spine synapse division. Spacek and Harris (2004) suggested that the fusion of synaptic vesicles with the presynaptic membrane and the insertion of new material in the postsynaptic membrane causes mechanical tensions that may lead to the partial dissociation of the PSD, suggesting that the PSD perforation can be just a result of the exocytotic activity linked to the synapse restructuring but by itself having no direct implementation in the efficiency of synaptic transmission. However all these speculations on the role and mechanisms of PSD perforation are weakly supported by experimental data.

2.5 NCAM and synaptic plasticity

NCAM and associated with this molecule PSA are long-time known for their involvement in synaptic plasticity. NCAM gets accumulated in synapses in activity dependent manner and also expression of NCAM gene itself is up-regulated after LTP induction (Schuster et al., 1998). NCAM is important for formation of synapses (Dityatev et al., 2000) probably via recruiting trans-Golgi network (TGN) organelles to the sites of axo-dendritic contacts (Sytnyk et al., 2002). NCAM conditional and constitutive knockout mice exhibit reduced NMDA-dependent LTP and LTD (Bukalo et al., 2004). Mechanisms of how NCAM is influencing LTP and LTD are not completely understood though a study of Sytnyk and colleagues (2007) illustrated that postsynaptic densities from NCAM^{-/-} mice contain less β I-spectrin, CAMkinase II α and NMDA receptors. The study demonstrated that NCAM, organizing spectrin cytoskeleton at synapses, produces a scaffold to anchor proteins involved in synaptic plasticity. The goal of the present study is to further elucidate the role of NCAM/spectrin complex in the assembly and maintenance of PSD and synaptic accumulation and turnover of the PSD associated synaptic proteins.

3. The neural cell adhesion molecule CHL1

3.1 Structure and general features of CHL1

The close homologue of L1 (CHL1) is a cell adhesion molecule of the immunoglobulin superfamily. Typical structural components of the L1 subfamily, the member of which is CHL1, are six immunoglobulin (Ig)-like domains, four to five fibronectin type III (FNIII)-like domains, a single transmembrane stretch and a highly conserved intracellular domain of approximately 110 amino acids. Mouse CHL1 protein and the human analogue of this protein – (CALL) - display only a half of the fifth FNIII-like repeat (Fig.1).

CHL1 was discovered during screening of a λ gt11 expression library for cDNA clones encoding the cell adhesion molecule L1 with a polyclonal anti L1 antibody. Screening showed that one of clones revealed only 34.1 % homology to L1 (Lipman and Pearson, 1985). A particular DNA fragment derived from this clone was used for screening a different cDNA library and subsequently six independent clones were isolated. Two clones of 4.2 kb and 4.4 kb inserts contained the entire coding region of a new immunoglobulin cell adhesion molecule that was called a close homologue of L1 (CHL1) (Holm et al., 1996). CHL1 is composed of 1081 amino acids containing 18 potential N-glycosylation sites and more than 60 possible sites for O-glycosylation. Similar to other cell adhesion molecules, CHL1 can contain HNK-1 epitope. A single transmembrane segment consists of 23 amino acids followed by an intracellular portion that is composed of 105 amino acids. The immunoglobulin part of the extracellular domain consists of 585 amino acids and fibronectin-type III repeats composed of 472 amino acids.

3.2 Expression of CHL1

CHL1 expression in different neuronal cell types often coincides with L1 expression. For example, in primary cultures, both molecules are detectable in subpopulations of hippocampal neurons, cortical neurons, mesencephalic neurons and neurons derived from the dorsal root ganglia. However although both proteins are expressed in spinal cord neurons, CHL1 is only weakly detectable comparing with strong L1 expression. Granular cells from cerebellum express only L1. Conversely, astrocytes express CHL1 and no L1. Non-mature oligodendrocytes also show CHL1 expression that

becomes down-regulated during development to mature oligodendrocytes (Hillenbrand et al., 1999).

3.3 Functions of CHL1

In contrast to many other adhesion molecules like NCAM, L1, neuroglian or TAG-1, CHL1 does not show homophilic interactions (Kadmon and Altevogt, 1997; Hortsch et al., 1996). The cell aggregation assays could neither demonstrate a homophilic interaction between CHL1-CHL1 molecules nor a heterophilic interaction between CHL1 and L1 (Hillenbrand et al., 1999). The extracellular domain of CHL1 contains putative sites for interaction with integrins (Ruoslahti and Pierschbacher, 1987). The identification of extracellular binding partners of CHL1 is still an open field for research since no extracellular binding partner of CHL1 has been isolated so far. As a substrate for neurite outgrowth, CHL1 stimulates neuritogenesis of cultured hippocampal and cerebellar neurons (Hillenbrand et al., 1999). CHL1 regulates neuronal migration (Buhusi et al., 2003). CHL1-Fc fusion protein has a positive effect on the survival of cultured murine cerebellar granular and hippocampal neurons of rat embryos (Chen et al., 1999). The serum deprivation induces apoptosis that can be prevented by either soluble or substrate-coated CHL1 fusion protein. Addition of CHL1 increased the number of surviving neurons by about 45 % (Chen et al., 1999). Several studies show that CHL1 is involved in the regeneration of nervous system. Crush or cut and subsequent ligation of the sciatic nerve provoke a strong upregulation of CHL1 mRNA levels in the injured motor and small sensory neurons. Interestingly, no CHL1 upregulation was observed in large primary sensory neurons of DRG (dorsal root ganglia) after sciatic nerve crush. The CHL1 upregulation was also observed in putative Schwann cells and astrocytes following dorsal root injury (Zhang et al., 2000).

A human analogue of CHL1 - CALL gene is mapped to the chromosome 3p26 locus, a region that is associated with mental retardation in "3p-syndrome". Thus loss or mutations of CHL1 (or CALL in human) may contribute to mental impairment associated with the "3p-syndrome" (Angeloni et al., 1999) and mental retardation (Frints et al., 2003). Moreover, mutations in CHL1 in humans correlate with occurrence of schizophrenia (Sakurai et al., 2002; Chen et al., 2005), a neuropsychiatric disorder associated with abnormal neurocircuits and functioning of synapses (Harrison and Weinberger, 2005).

Abnormalities observed in CHL1 deficient mice have relation to the abnormalities associated with schizophrenia, suggesting that CHL1 knockout mice can be used as one of animal models for schizophrenia (Irintchev et al., 2005; Nikonenko et al., 2006).

3.4 Phenotype of CHL1^{-/-} mice

CHL1 deficient mice were generated by Montag-Sallaz and colleagues (2002). Animals are vital and fertile. CHL1^{-/-} mice show alterations in hippocampal mossy fibre organization and olfactory axon projections. Behaviour of CHL1^{-/-} mice in the open field, the elevated plus maze, and the Morris water maze indicates deficits in information processing in the brain. Further studies showed abnormalities in apical dendrite branching and orientation of neurons in the cortex and cerebellum (Demyanenko et al., 2004). CHL1 deficiency in mice leads to reduced prepulse inhibition of the acoustic startle response, a measure of the ability of the central nervous system to gate the flow of sensorimotor information (Irintchev et al., 2004). Enhanced perisomatic inhibition was registered in CA1 pyramidal cells of the hippocampus accompanied by impaired long-term potentiation induction in the CA1 stratum radiatum (Nikonenko et al., 2006). Expression of the mRNA of the NCAM-180 isoform was upregulated in adult CHL1-deficient mice, while mRNA levels of several other recognition molecules were not changed (Montag-Sallaz et al. 2002). Although these findings suggest that CHL1 regulates synapse functioning, the exact role of CHL1 in the organization of the synaptic machinery has not been yet analysed.

4. Synaptic vesicle recycling and CHL1

4.1 Synaptic vesicle recycling

Synaptic vesicle is probably the most studied organelle in the cell biology. It is a small organelle with diameter of just 40 nm consisting of approximately 10000 phospholipid molecules and 200 protein molecules that provide pumping of the neurotransmitter, regulate the fusion of vesicle with the active zone of presynaptic bouton and regeneration of the synaptic vesicle after neurotransmitter release. In the case of intensive stimulation synaptic vesicle pool in the axonal terminal would be rapidly depleted, if there would be no mechanism that insure local reconstruction of vesicles in the

synaptic bouton. Synaptic vesicle reconstruction occurs predominantly via endocytosis of synaptic vesicle membrane following synaptic vesicle endocytosis. Many proteins, including different adaptor proteins like AP2, AP180, AP3, synaptojanin and others, regulate the process of synaptic vesicle endocytosis. Synaptic vesicles could pinch either directly from the plasma membrane or from larger endosomal compartments internalised into the neuronal terminal. These two possible routes may explain observations showing that there are rapidly and slowly regenerating vesicles in synaptic terminals (Richards et al., 2000). Furthermore, vesicles from slow and rapid endocytosis pathways seem to differ in adaptor proteins involved in endocytosis: rapid endocytosis requires AP2 whereas slow endocytosis relies on AP3 (Voglmaier et al., 2006). Experiments with clathrin siRNA, used to knock down clathrin expression in neurons, show that clathrin is crucial for all “physiological” endocytotic pathways involved in synaptic vesicle formation. Inhibition of the clathrin dependent endocytosis by clathrin siRNA blocked synaptic vesicles retrieval (Granseth et al., 2006). During endocytosis, adaptor proteins initiate clathrin coat formation on the presynaptic membrane and recruit synaptic vesicle proteins to the site of endocytosis. Dynamin induces pinching of clathrin coated membrane pockets from the plasma membrane hereby forming clathrin-coated vesicles. Afterwards, clathrin dissociates from the vesicles and new synaptic vesicles can be refilled with the neurotransmitter to be ready for the next fusion round.

4.2 Clathrin uncoating

Clathrin mediated synaptic vesicle retrieval from the plasma membrane is extremely rapid, it could last less than 30 seconds (Gaidarov et al., 1999). Shedding of the clathrin has to be therefore very fast to allow further processing of endocytosed vesicles. Formation of the clathrin coat at the plasma membrane is induced by adaptor proteins under ATP-poor and ADP-rich conditions. Clathrin shedding is ATP consuming and catalyzed by variety of factors including auxilin and Hsc70 (Fig. 4). Hsc70 is a protein possessing the chaperon activity. Chaperones are the family of proteins that regulate folding and maintenance of correct protein conformations, participate in refolding and sorting of proteins and thus are involved in numerous functions in cells (Young et al., 2004). Processes that involve changes of the protein conformation such as clathrin coat

disassembly also often require chaperone assistance. Thus Hsc70 catalyses the release of clathrin from clathrin-coated vesicles as the final step of receptor mediated endocytosis in *in vitro* and *in vivo* experiments (Newmyer and Schmid, 2001). A similar function is attributed to Hsc70 in synapses where Hsc70 regulates uncoating of synaptic vesicles in the clathrin-dependent synaptic vesicle recycling pathway (Zinsmaier and Bronk, 2001). During the process of synaptic vesicle uncoating, Hsc70-ATP complex binds to clathrin-coated synaptic vesicles (CCSV) via auxilin (Jiang et al., 2000). Following ATP hydrolysis, auxilin is released from CCSV whereas Hsc70-ADP form a complex with clathrin triskelions of the clathrin-coat, thereby inducing the dissociation of the clathrin cage. Clathrin, Hsc70 and ADP molecules remain in the complex, which under certain experimental conditions can be shown on FPLC (fast performance lipid chromatography). In the presence of ATP, complex of clathrin and Hsc70-ADP is then transformed to a steady-state complex between Hsc70, ATP and clathrin that can bind to the membrane for further endocytosis rounds.

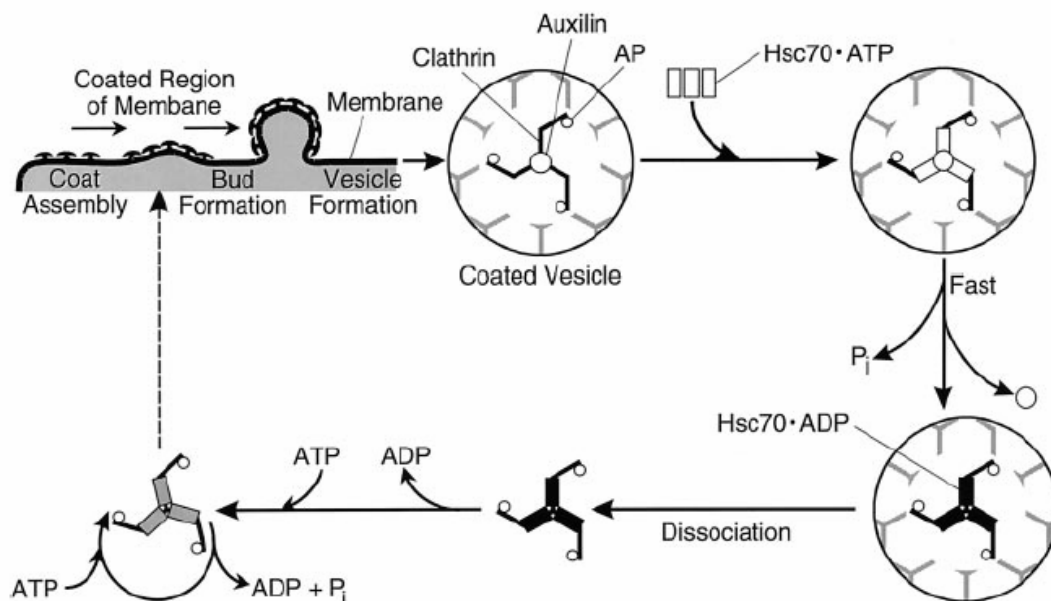


Figure 4. A model for the interaction of Hsc70 with clathrin-coated vesicles. In this model of the uncoating reaction, auxilin induces Hsc70-ATP to bind to the clathrin-coated vesicles, and then, following ATP hydrolysis, a complex is formed between Hsc70-ADP and a clathrin triskelion in the clathrin-coated vesicle. This lead to the dissociation of the clathrin coat. However, complex of Hsc70-ADP and clathrin triskelion is still maintained even after clathrin coat dissociation. Clathrin-Hsc70-ADP complex in the ATP rich surrounding is then transformed to a steady-state complex between Hsc70, clathrin, and ATP. This steady state complex dissociates very slowly. However, if stripped vesicles are added to this steady-state

complex, the clathrin rebinds to the stripped vesicles (arrow with dotted line) and is again uncoated by Hsc70 (Adapted from Jiang et al., 2000).

4.3 CHL1 interaction with Hsc70

Biochemical experiments from our laboratory show that CHL1 interacts with the 70 kDa heat shock cognate protein (Hsc70) via the intracellular domain of CHL1 which contains the recognition site comprising of HPD tripeptide for shaperon proteins of Hsp70 family (Tsai and Douglas, 1996). CHL1 is able to recruit Hsc70 to the membrane. CHL1 deficiency leads to reduced levels of Hsc70 on synaptic vesicles. Clathrin-coated synaptic vesicles purified from the CHL1^{-/-} brain homogenates show severely inhibited rates of clathrin release in in vitro uncoating assay (Leschyns'ka et al., 2006).

This fact suggests that CHL1 is an important player for Hsc70 mediated vesicle uncoating. In the present project we intended to further analyse how CHL1 deficiency influences synaptic vesicle recycling in excitatory glutamatergic synapses.

II. AIMS OF THE STUDY

Project 1. The role of NCAM in maintaining of the cytoskeleton-dependent structural integrity of post-synaptic densities and regulation of the AMPA receptor recycling.

β I-spectrin is a major scaffold organiser at the postsynaptic density (Ziff 1997). The β I-spectrin-associated cytoskeleton is involved in the protein anchoring and can influence endo- and exocytosis of many synaptic proteins thus modulating properties of individual synapses. NCAM is involved in accumulation of β I-spectrin to synapses, as shown by experiments demonstrating that NCAM^{-/-} PSDs contain less spectrin than those of NCAM^{+/+} mice (Sytnyk et al., 2006). The aim of the present study is to analyse how NCAM deficiency and associated with it loss of spectrin influence synaptic morphology and function. Our preliminary experiments revealed an increased number of synapses with partially or completely segmented PSD in CA1 stratum radiatum of NCAM^{-/-} mice. These synapses with PSDs of complex shape are often referred as perforated and their function is not completely understood. Therefore the second question addressed in this study is how formation of perforated synapses is regulated and what functional significance such structural alteration of PSD might possess.

Project 2. The role of the cell adhesion molecule close homologue of L1 (CHL1) in the regulation of clathrin-dependent synaptic vesicle recycling.

Mutations in human analogue of murine CHL1 gene, CALL, correlate with the occurrence of schizophrenia (Sakurai et al., 2002; Chen et al., 2005). Schizophrenia is a neuropsychiatric disorder associated with abnormal neurocircuits and functioning of synapses (Harrison and Weinberger, 2005). Therefore CHL1 is very likely to be involved in synaptic function. Pilot experiments demonstrated that the intracellular domain of CHL1 interacts with Hsc70. Hsc70 plays an important role in the regulation of clathrin-coated vesicle uncoating. In the present study we analyse how deficiency in CHL1 influences clathrin uncoating and synaptic vesicle recycling at synapses. We also directly evaluate the functional importance of CHL1-Hsc70 interaction using an acute block of CHL1-Hsc70 interactions via peptide competing for Hsc70 binding site of CHL1. The goal of the study is to reveal CHL1 contribution to synapse functioning in normal and pathological conditions.

III. MATERIALS AND METHODS

1. Animals

Mice of two NCAM^{-/-} lines and one CHL1^{-/-} line and their corresponding controls (littermates) were used in the study.

The first, constitutive NCAM^{-/-} mouse strain was obtained from Cremer et al. (1994). The second, conditional NCAM^{-/-} mouse strain was generated in our laboratory (Bukalo et al., 2004) on the C57bl background. NCAM gene is disabled postnatally in these animals thus allowing to distinguish the developmental role of NCAM from its contribution to the function of postembryonic nervous system. This is achieved by inactivation of NCAM gene in differentiated neurons following activation of CAMkinase II promoter using floxP – cre recombinase system. CAMkinase II is a marker of differentiated neurons and its promoter is activated postnatally in forebrain neurons in first weeks after birth. In hippocampus and cortex, NCAM expression is significantly down-regulated already on the second week after birth in NCAMfloxP cre positive (NCAM knockout) mutants compared with control NCAMfloxP cre negative mice (without cre-recombinase, floxed NCAM gene is not cut out and is expressed as in wild type mice). Animals for experiments were obtained in heterozygous breedings. Knockout mice were compared with their wild type littermates. We used adult animals of 2 to 6-months age.

CHL1 knockout mice used in experiments were obtained from the line produced in our laboratory (Montag-Sallaz et al., 2002). We used 5 month-old animals.

All experimental protocols and handling of the animals were approved by the local authorities of the city of Hamburg.

2. Materials

2.1 Laboratory equipment

Vibrotome – Reichart Leica VT 1000S

Ultramicrotome - Reichart Leika Ultracut UCT

Confocal microscope – Zeiss LSM510

Transmission electron microscope - Zeiss EM10C

Further instruments and materials for immunofluorescence and electron microscopy were obtained from PLANO (Wetzlar, Germany), Carl Roth (Karlsruhe, Germany), Merck (Darmstadt, Germany) and Sigma-Aldrich (Deisenhofen, Germany).

2.2 Chemicals

All chemicals unless stated different were obtained in p.a. quality from the following companies: GibcoBRL (Life technologies, Karlsruhe, Germany), Macherey-Nagel (Düren, Germany), Merck (Darmstadt, Germany), Serva (Heidelberg, Germany) and Sigma-Aldrich (Deisenhofen, Germany), Carl Roth (Karlsruhe, Germany), Invitrogen GmbH, (Karlsruhe, Germany).

Concentrations and providers of the chemicals used for experiments with cultured neurons:

Latrunculin A 5 μ M (BIOMOL Research Laboratories, Hamburg, Germany)

Tetrodotoxin (TTX) 1 μ M (Sigma-Aldrich Deisenhofen, Germany)

Vincristine 5 μ M (Sigma-Aldrich Deisenhofen, Germany)

Tetanus toxin 10 nM (Sigma-Aldrich Deisenhofen, Germany)

Antimycin A 0.1 μ M (Sigma-Aldrich Deisenhofen, Germany)

MDL 28170 100 μ M (Sigma-Aldrich Deisenhofen, Germany)

Cell culture plastic ware and reagents were obtained from Invitrogen (Karlsruhe, Germany), Nunc (Roskilde, Denmark) or Life Technologies (Karlsruhe, Germany).

2.3 Primary antibodies

Rabbit polyclonal antibodies against the extracellular domain of mouse CHL1 (Buhusi et al., 2003);

Rat monoclonal antibody 555 against the extracellular domain of L1 (Appel et al., 1993);

Mouse monoclonal antibodies against SV2 (Developmental Studies Hybridoma Bank, Iowa City, IA, USA);

Mouse monoclonal antibodies against the clathrin heavy chain (BD Biosciences, San Jose, CA, USA);

Goat polyclonal antibodies against synaptophysin, Hsp70, and Hsc70 (Santa Cruz Biotechnology, Santa Cruz, CA, USA);

Mouse monoclonal antibodies against PSD95 (Upstate Biotechnology, Lake Placid, NY, USA);

Mouse monoclonal antibodies against MAP2 (Sigma, St. Louis, MO, USA);

Nonspecific rabbit Ig (Sigma, St. Louis, MO, USA);

Rabbit polyclonal antibodies against synaptophysin were a generous gift from Reinhard Jahn (Max-Planck-Institute for Biophysics, Gottingen, Germany);

Rabbit polyclonal antibodies against CSP were a generous gift from Guido Meyer (Max-Planck-Institute for Experimental Medicine, Gottingen, Germany);

Mouse monoclonal antibody recognizing the extracellular domain of GluR1 was a generous gift from Dr. Peter Streit (Brain Research Institute, University of Zurich, Zurich, Switzerland);

Mouse monoclonal antibody against β I spectrin (Santa Cruz Biotechnology, Santa Cruz, CA, USA);

Mouse monoclonal antibody recognizing the extracellular domain of GluR2 (Chemicon (Temecula, USA, CA).

2.4 Secondary antibodies and imaging probes

Cyanine dyes (Cy2, Cy3 or Cy5) conjugated with donkey anti-mouse, anti-rabbit, anti-goat or anti-rat immunoglobulins were obtained from Dianova (Hamburg, Germany) and used in a dilution of 1:200.

Nanogold ® anti-mouse-Fab conjugates and Nanogold-enhancement kit were obtained from Nanoprobes (Nanoprobes, Yaphank, NY, USA)

2.5 siRNAs and cDNA of SAP90GFP

Spectrin β I siRNA was obtained from Santa Cruz Biotechnology, Inc. (Santa Cruz, CA, USA)

Control (nonsilencing) siRNA was purchased from QIAGEN GmbH, (Hilden, Germany).

cDNA encoding green fluorescent protein-tagged postsynaptic marker protein SAP90 (SAP90GFP) was generously provided by Dr. Stefan Kindler (Institute for Cell Biochemistry and Clinical Neurobiology, University Hospital Hamburg-Eppendorf, Hamburg, Germany)

3. Methods

3.1 Analysis of the brain morphology

3.1.1 Brain tissue processing

Mice were deeply anaesthetized with sodium pentobarbital and perfused transcardially with a mixture of 2% formaldehyde and 2.5% glutaraldehyde in 0.1 M phosphate buffer (pH 7.4). After perfusion, brains were dissected free and postfixed overnight at 4°C in 4% formaldehyde and 5% glutaraldehyde in the same buffer. On the next day, brains were cut into 400 μ m thick slices on the Leica vibrotome. Tissue slices were post-fixed in 0.1 M cacodylate buffer containing 1% OsO₄. Slices were rinsed, dehydrated in methanol and flat embedded in Epoxy resin. Brains were coded to ensure

evaluation in a blinded manner. Semithin sections from the brains were stained with a mixture of 1% methylene blue and 1% toluidine blue and analysed under the light microscope to locate CA1 stratum radiatum of the hippocampus. The third outer part of the stratum radiatum of the dorsal hippocampus was then trimmed (Fig.5). Ribbons of serial 90 nm-thick sections were made from the trimmed blocks on a Reichart Leika Ultramicrotome. Ribbons of sections were mounted on Formavar coated grids with a 125 μm slot. Blocks from two slices of dorsal hippocampus were used per animal. Sections were stained with uranyl acetate and lead citrate. Images from sections were obtained on Zeiss EM10C transmission electron microscope at x7000 magnification for synapse number analysis and at x30000 for counting vesicles.

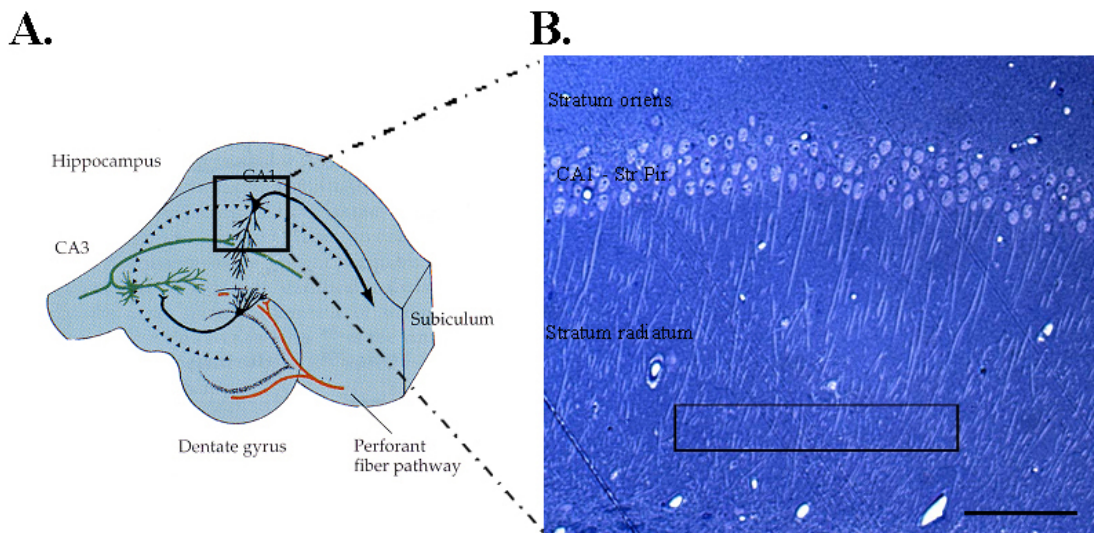


Figure 5. A Scheme of the hippocampus indicating the region of the CA1 stratum radiatum used for the ultrastructural analysis of synapses. (A). Schematic illustration of the hippocampus. Informational input from the entorhinal cortex enters the hippocampus through the perforant pathway (in red), which terminates on the dendrites of granule cells in the dentate gyrus. Axons of granule cells – mossy fibers (black) – relay information to apical dendrites of pyramidal cells in area CA3. Information is subsequently relayed by the axons of area CA3 neurons – the Schaffer collaterals (green) – to apical dendrites of pyramidal neurons in stratum radiatum of CA1. (B) Micrograph of the 1 μm thick semithin section from the CA1 region of the hippocampus. Black box represents a distal part of the CA1 stratum radiatum where further ultrathin sectioning and electron microscopical estimation of the synapse number was performed. The semithin section was stained with methylene/toluidine blue. Scale bar 200 μm .

3.1.2 Estimation of the synapse density in the CA1 stratum radiatum using a disector method.

We applied an unbiased stereological method of the disector for estimation of synaptic density in the outer part of the CA1 stratum radiatum (Sterio, 1984). This method allows estimation of the numerical density of objects per unit volume using two dimensional images obtained from analysed volume without a complete three dimensional reconstruction of this volume. In our case using the disector method we estimate number of synapses per unit volume of the CA1 stratum radiatum. Disector method is based on the partial serial sectioning of the volume of interest that allows taking three dimensional “probes” in which density of particles of interest could be counted and then extrapolated on the rest of the investigated volume. This method gives more precise estimation than more traditional profile counting of synapses and also gives numerical estimate relevant to the volume. Briefly, the disector consists of a pair of serial sections collected at a known distance apart representing small volume samples from the original big volume that we analyse. Comparing upper and lower sections we could estimate number of particles (for example synapses) in the volume of disector according to appearance/disappearance of the particles of interest on the upper “looking up” section relevantly to the lower “reference” section (Fig. 6). By collecting numerical estimates in a representative number of small disector volumes we may extrapolate mean estimates of the density (in our case density of synapses) on the whole volume we analyse.

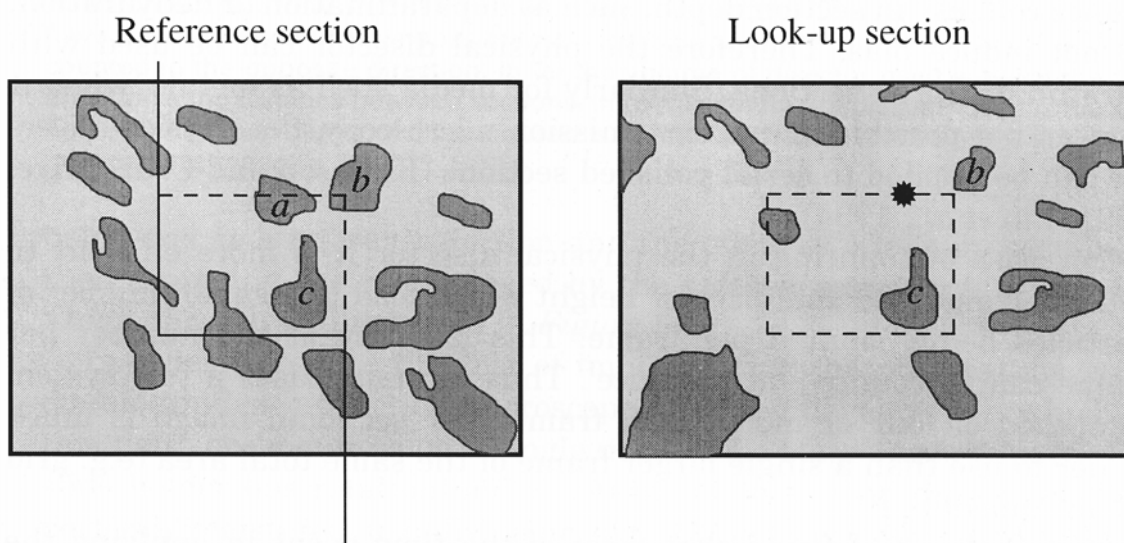


Figure 6. An illustration of the disector counting rule. The left hand section contains a 2D counting frame and is known as the “reference” section. The right hand section is known as the “look-up”

section. For each of transects correctly sampled by the counting frame in the reference section (a, b and c) a corresponding transect is sought in the look-up section. If no corresponding transect is found anywhere in the look-up section (in this example transect “a” is missing, indicated by the asterisk) this particle is counted in 3D. Note that although the transect from particle “b” that is seen in the look-up section is outside the dashed line this particle is not counted in 3D because it is still present in the look-up section. Scheme was adopted from Howard and Reed (1998).

Pairs of electron micrographs of the CA1 stratum radiatum from adjacent sections were taken at a magnification of 7000 and, afterwards, images were printed on photopaper with final magnification of x15720. Images were aligned with each other and unbiased counting frame was superimposed on matched fragments from both disector sections. The volume of the disector used was $144 \mu\text{m}^3$. Numerical density values were expressed as the number of synapses/ μm^3 . 40 disector sample pairs were analysed per animal. Asymmetric synapses were identified by the presence of a prominent postsynaptic density (PSD) and at least three presynaptically localized clearly recognisable vesicles in the presynaptic bouton apposing the PSD. As a “counting cap” (Sterio, 1984) for asymmetrical synapses with non-perforated PSD we used appearance of a top of the synapse. Perforated synapses were defined as only synapses with clearly seen non-electron dense gap in their postsynaptic density.

3.1.3 Measurements of the cross-sectional area of spines and the number of synaptic vesicles in synaptic terminals

Cross-sectional area of spines and the number of vesicles were calculated on digital images obtained at x30000 magnification. Profiles of spine heads and terminals were outlined using free software program Image Tool (UTHSCSA Image-Tool program (University of Texas, San Antonio, TX; available from <ftp://maxrad6.uthscsa.edu>)).

Clathrin coated vesicles were distinguished from other vesicles in the synaptic terminal and spines by the presence of clearly seen clathrin coat.

The densities of synaptic vesicle profiles were quantified in digital electron micrographs of spine synapses from the CA1 stratum radiatum. Electron micrographs were taken at the magnification of 30,000x. The density of synaptic vesicles was quantified as the number of vesicle profiles per synaptic terminal.

3.2 Cultures of hippocampal neurons

3.2.1 Preparation of dissociated hippocampal cultures

Cultures of hippocampal neurons were prepared from one- to three-day-old C57BL/6J, constitutive NCAM^{-/-} mice and CHL1^{-/-} mice. Cultures were maintained on glass coverslips for immunocytochemistry or on coverslips made of ACLAR embedding film (Plano, Wetzlar, Germany) for electron microscopy for 2-3 weeks in hormonally supplemented culture medium containing 5% of horse serum (Sigma, St. Louis, MO, USA) (Leshchyn'ska et al., 2003). Every 3 days half of the culture medium was replaced with a freshly prepared one. Coverslips were coated overnight with poly-L-lysine (100 µg/ml) in conjunction with laminin (20 µg/ml).

3.2.2 Processing of cultures for electron microscopy

Cultures were processed for electron microscopy essentially as described (Neuhoff et al., 1999). Cultures were fixed with 3% glutaraldehyde in PBS for 15 minutes, postfixed in 1% OsO₄ in water for 30 minutes, rinsed in water three times. Afterwards cultures were incubated in 1% aqueous uranyl acetate for 30 minutes, rinsed in water three times and dehydrated in increasing concentrations of methanol in water, pure methanol and, finally, propylene-oxide. Cultures were embedded in epoxy resin mix (51% of Epon 812, 32% of MNA hardener, 16% of DDSA hardener and 1% of DPS-30 accelerator). Glass or ACLAR coverslips with cultures were attached to the self made resin blocks (from Epoxy resin). Following polymerisation, ACLAR coverslips were removed by razor from embedded cells. To remove glass coverslips we had to subsequently immerse blocks with cultures to liquid nitrogen and hot (90⁰ C) water. Rapid change of temperature induced cracking of the glass leaving however embedded cells intact and attached to the resin blocks. Resin blocks with cultures attached to their surface were trimmed and cut parallel to the culture surface on a Reichart Leika Ultramicrotome. Sections (90 nm) were stained with aqueous uranyl acetate and lead citrate. Sections were analysed on Zeiss transmission electron microscope. Synapses were randomly photographed at x30000 magnification with Mega View II camera (Soft Imaging System, Münster, Germany) attached to the microscope.

3.2.3 Preembedding labelling of GluR1 receptors with Nanogold conjugates

Neurons were incubated for 15 min in a CO₂ incubator with the mouse monoclonal antibody 8A1 recognizing the extracellular domain of GluR1 obtained from Dr. Peter Streit (Brain Research Institute, University of Zurich, Zurich, Switzerland), washed with culture media 3 times and incubated with Nanogold anti-mouse-Fab conjugates (Nanoprobes, Yaphank, NY, USA) for 15 min in a CO₂ incubator. After washing with media neurons were allowed to recover for 5 min, fixed in 3% glutaraldehyde in PBS, treated with Gold-enhance-EM Formulation (Nanoprobes) to enlarge nanogold particles and processed for electron microscopy as described above.

3.2.4 Analysis of synapse morphology in hippocampal cultures

Percentage of perforated synapses in hippocampal cultures was quantified relative to the number of all synapses analysed. For this analysis, 100 individual asymmetric synapses were digitally photographed at x30000 magnification from each culture. All experiments were performed at least two times with 4-6 cultures per experimental value. All estimations were performed in a blinded manner. Only asymmetric synapses were analysed. Perforated synapses were defined as synapses with clearly seen non-electron dense gap in their postsynaptic density.

The area of synaptic bouton profiles, number of synaptic vesicles and size of active zones were quantified with Image Tool program (UTHSCSA Image-Tool program (University of Texas, San Antonio, TX; available from <ftp://maxrad6.uthscsa.edu>)). Clathrin coated vesicles were distinguished from other vesicles in the synaptic terminal by the presence of the clearly seen clathrin coat.

3.3 Treatments of hippocampal neurons

3.3.1 Treatments to block synaptic activity, vesicle endocytosis and to induce actin-spectrin meshwork disassembly.

Drugs were added directly to the culture medium from a concentrated DMSO or methanol stock solutions. Latrunculin A (5 μ M,) was applied for 2 or 24 hours before fixation of cultures (Allison et al., 2000). In both cases the same experimental effect was observed. Tetrodotoxin (TTX) (1 μ M) and tetanus toxin (10 nM; Maletic-Savatic and

Malinow, 1998) were applied for 1 and 24 hours. Vincristine (5 μ M; Allison et al., 2000), antimycin A (0.1 μ M; Molitoris et al., 1996), and MDL 28170 (100 μ M; Faddis et al., 1997) were applied for 2 hours. None of the reagents or vehicle resulted in any evident cell death, cell degradation or abnormal changes in overall synapse morphology. The number of the apoptotically active caspase-3 positive neurons was similar in control non-treated and treated neurons and did not exceed 7%.

3.3.2 Chemical stimulation of synaptic activity in cultures with high potassium buffer

In order to induce synaptic vesicle exo- and endocytosis in synapses of cultured neurons, cultures were exposed to stimulation solution represented by modified Tyrode buffer with 47mM potassium concentration obtained by equimolar substitution of KCl for NaCl and later referred to as high potassium buffer. Control Tyrode buffer with nominal potassium concentration contained 150 mM NaCl, 4 mM KCl, 2 mM MgCl₂, 10 mM glucose, 10 mM HEPES and 2 mM CaCl₂ (pH 7.4, ~310 mOsm) (Virmani et al., 2003). High potassium buffer was applied to neurons for following time durations: 10s, 30s, 90s or 90s and rinsing with nominal potassium buffer for 1 or 5 min. In control cultures media was changed to Tyrode buffer with nominal 4mM potassium concentration. Subsequently experimental and control cultures were fixed in 3% glutaraldehyde in PBS for 20 min at 36 degree and processed further for electron microscopy analysis.

3.3.3 Chemical LTP induction protocol

To induce LTP, neurons were treated with 200 μ M glycine for 3 min in Mg²⁺-free extracellular solution containing (in mM): 150 NaCl, 2 CaCl₂, 5 KCl, 10 HEPES, 30 glucose, 0.0005 TTX, 0.001 strychnine, 0.02 bicuculline methiodide, pH 7.4 (Lu et al., 2001; Park et al., 2004, 2006). Following stimulation, neurons were kept in extracellular solution without glycine for 15, 45 and 120 minutes before fixation for electron microscopy.

3.3.4 Transfection of hippocampal neurons

Neurons were transfected 12 days after plating with control non-silencing siRNA or β I spectrin siRNA (Santa Cruz Biotechnology, Santa Cruz, CA, USA) or SAP90GFP cDNA using Lipofectamine 2000 (GIBCO Invitrogen, Carlsbad, CA, USA) according to

the manufacturer's instructions and analysed 14 days after plating. Knock-down of β I spectrin expression was confirmed by labelling neurons with polyclonal antibodies against β I spectrin (Santa Cruz Biotechnology) as described (Sytnyk et al., 2006).

3.3.5 Loading of hippocampal neurons with β I-2,3spectrin, β II-2,3spectrin, HPD and QPD peptides

Peptides were introduced to neurons 12 days after plating using Chariot (Active Motif, Rixensart, Belgium) or Pulsin (Biomol, Hamburg, Germany) according to the manufacturers' instructions. Both reagents provided similar results.

3.4 Immunocytochemistry

Immunocytochemistry studies presented in the current study were performed in collaboration with Vladimir Sytnyk

3.4.1 Confocal laser-scanning microscopy

All images of hippocampal neurons were obtained with a Zeiss LSM510 confocal laser-scanning microscope equipped with a 60x oil-immersion objective. Images were scanned with a resolution of 512x512. Detector gain and pinhole were adjusted to give an optimal signal to noise ratio.

3.4.2 Indirect immunofluorescence staining

Cultured hippocampal neurons were fixed for 15 minutes in 4% paraformaldehyde in phosphate buffered saline (PBS), pH 7.3. Previously it was shown that this type of fixation does not result in membrane permeabilization (Sytnyk et al., 2002). To detect CHL1 and L1 at the cell surface only, neurons were then blocked with 3% bovine serum albumin (BSA, Sigma), incubated with corresponding primary and secondary antibodies and then post-fixed in 2% paraformaldehyde in PBS for 5 minutes. To label intracellularly localized proteins, neurons were then permeabilized with 0.25% Triton X-100 in PBS applied for 5 minutes and blocked with 3% BSA in PBS applied for 20 min. Primary antibodies were applied to cells for 2 hours and detected with fluorochrome-coupled secondary antibodies applied for 45 minutes. All steps were performed at room temperature. Coverslips were embedded in Aqua-Poly/Mount (Polysciences, Inc.,

Warrington, PA, USA). Images were acquired at room temperature using a confocal laser scanning microscope LSM510 (Zeiss, Jena, Germany). Contrast and brightness of the images were further adjusted in Corel Photo-Paint 9 (Corel Corporation, Ottawa, Ontario, Canada).

3.4.3 Quantification of GluR1 and GluR2 antibody uptake

Neurons were incubated for 15 min in a CO₂ incubator with the mouse monoclonal antibody 8A1 recognizing the extracellular domain of GluR1, washed with culture media 3 times and incubated with Cy3-conjugated goat anti-mouse antibodies for 15 min in a CO₂ incubator. After washing with media, neurons were allowed to internalise GluR1/Cy3 complexes for 1 hour in a CO₂ incubator. Then neurons were fixed with 4% formaldehyde in PBS, washed with PBS, blocked with 3% BSA in PBS and labelled with Cy2-conjugated donkey anti-goat antibodies (Jackson ImmunoResearch laboratories, Inc.) for 30 min at room temperature to visualize surface GluR1/Cy3 complexes. In control experiments, when non-immune mouse immunoglobulins were used instead of the anti-GluR1 antibody, no Cy3 or Cy2 labelling was observed indicating that non-specific binding and uptake of secondary antibodies was negligible. Images of labelled neurons were acquired with the LSM510 laser scanning microscope and used to quantify internalisation of GluR1/Cy3 complexes. For each analysed neurite, Cy3-labeled clusters were automatically outlined using a threshold function of Scion Image software (Scion Corporation, Frederick, Maryland, USA), and mean intensities of Cy3 and Cy2 labeling were measured within the outlines. Cy3-labeled clusters containing Cy2 labeling with mean intensity higher than background that was measured near the neurite were considered to be surface accumulations of GluR1, while Cy2-negative Cy3-labeled clusters were considered to be intracellular GluR1 accumulations. For each Cy3-labeled GluR1 cluster, accumulation of Cy3 labelling was defined as a product of mean intensity of Cy3 labelling within the cluster multiplied by the cluster area. The index of GluR1 internalisation along a neurite was then calculated as the sum of all intracellular Cy3-labeled GluR1 accumulations along the neurite normalized to the sum of all Cy3-labeled GluR1 accumulations including both surface and intracellular GluR1 accumulations:

$$\text{GluR1}_{\text{intern.}} = \frac{\sum(\text{area}_{\text{GluR1intr.}} \times \text{mean}_{\text{GluR1intr.}})}{(\sum(\text{area}_{\text{GluR1intr.}} \times \text{mean}_{\text{GluR1intr.}}) + \sum(\text{area}_{\text{GluR1surf.}} \times \text{mean}_{\text{GluR1surf.}}))}$$

Analysis of GluR2 endocytosis was performed as described for GluR1 using mouse monoclonal antibody recognizing the extracellular domain of GluR2.

3.4.3 Analysis of CHL1 antibody uptake into cultured neurons

Neurons were incubated with rabbit anti-CHL1 antibodies (5 µg/ml) applied for 15 minutes in culture medium at 37°C in a CO₂ incubator, washed and exposed for 90 seconds to modified Tyrode solution containing nominal or high potassium concentration (for details see section 3.3.2) to induce synaptic vesicles exo- and endocytosis (Virmani et al., 2003). Neurons were then chilled on ice for 2 minutes and incubated in 0.5 M NaCl / 0.2 M acetic acid for 6 minutes. This procedure selectively strips bound antibody from the cell surface and leaves cellular morphology and intracellular antibody-protein complexes intact (Wilde et al., 1999; Carroll et al., 1999). Neurons were then washed extensively with ice-cold PBS and fixed in 4% paraformaldehyde in PBS. To verify efficiency of stripping, neurons were then incubated with donkey anti-rabbit Cy5 conjugate and were found to be not fluorescently labelled. Cells were then permeabilized with 0.25% Triton X-100 in PBS for 5 minutes, blocked with 4% BSA in PBS, and incubated with donkey anti-rabbit Cy3 conjugate to detect acid-resistant and thus non-cell surface bound immunoreactivity representing internalised CHL1. The incubation with non-specific rabbit Ig (10 µg/ml) for 30 min did not result in any detectable uptake of immunoglobulins indicating the specificity of CHL1 antibody uptake.

3.4.5 Time lapse imaging of SAP90-GFP transfected neurons

For live cell imaging, cultures were placed in a CO₂ incubator (Zeiss, Jena, Germany) and maintained at 37°C and 5% CO₂. Time lapse recordings were done with a LSM510 laser scanning microscope (Zeiss) with a 10 s interval between frames for 10-20 min. Intensity of the 488 nm argon laser was set to a minimal value. No photobleaching was observed under these conditions. The pinhole was maximally opened to reduce focus fluctuations.

3.5 Statistical analysis

Statistical analysis was performed with Statistica 5 (StatSoft, Tulsa, OK). Values are presented as mean \pm standard deviation. The statistical significance of differences between sample groups was assessed with T-test. $P < 0.05$ was considered as statistically significant.

IV. RESULTS

Project 1. The role of NCAM in maintaining of the cytoskeleton-dependent structural integrity of post-synaptic densities and regulation of the AMPA receptor recycling

1.1 Number of synapses with perforated PSDs is increased in NCAM^{-/-} mice

We started by comparing the density and ultrastructure of excitatory synapses in ultrathin sections of the CA1 stratum radiatum of wild type (NCAM^{+/+}) and conditional NCAM deficient (NCAM^{-/-}) mice. NCAM was conditionally ablated predominantly in the hippocampus under the control of the CAM kinase II promoter starting from postnatal day 22 in order to minimise developmental defects (Bukalo et al., 2004). The overall density of excitatory synapses was not different in NCAM^{-/-} versus NCAM^{+/+} animals. In NCAM^{-/-} mice, however, the percentage of synapses with perforated PSDs was increased by approximately 30% indicating that NCAM is important for maintaining the structural integrity of PSDs (Fig. 7). Measurements of spine head area showed no changes in NCAM^{-/-} mice, indicating that abnormal spine swelling was not the reason for increased percentage of perforated PSDs in these mice (Fig. 1). A similar effect was observed when constitutively deficient NCAM^{-/-} mice (Cremer et al., 1994) were analysed (synaptic density was 2.14 ± 0.19 and 2.12 ± 0.27 synapses per μm^3 in NCAM^{+/+} and NCAM^{-/-} littermates, respectively; perforated synapses constituted 8.66 ± 1.58 % and 12.04 ± 3.69 % in NCAM^{+/+} and NCAM^{-/-} littermates, respectively).

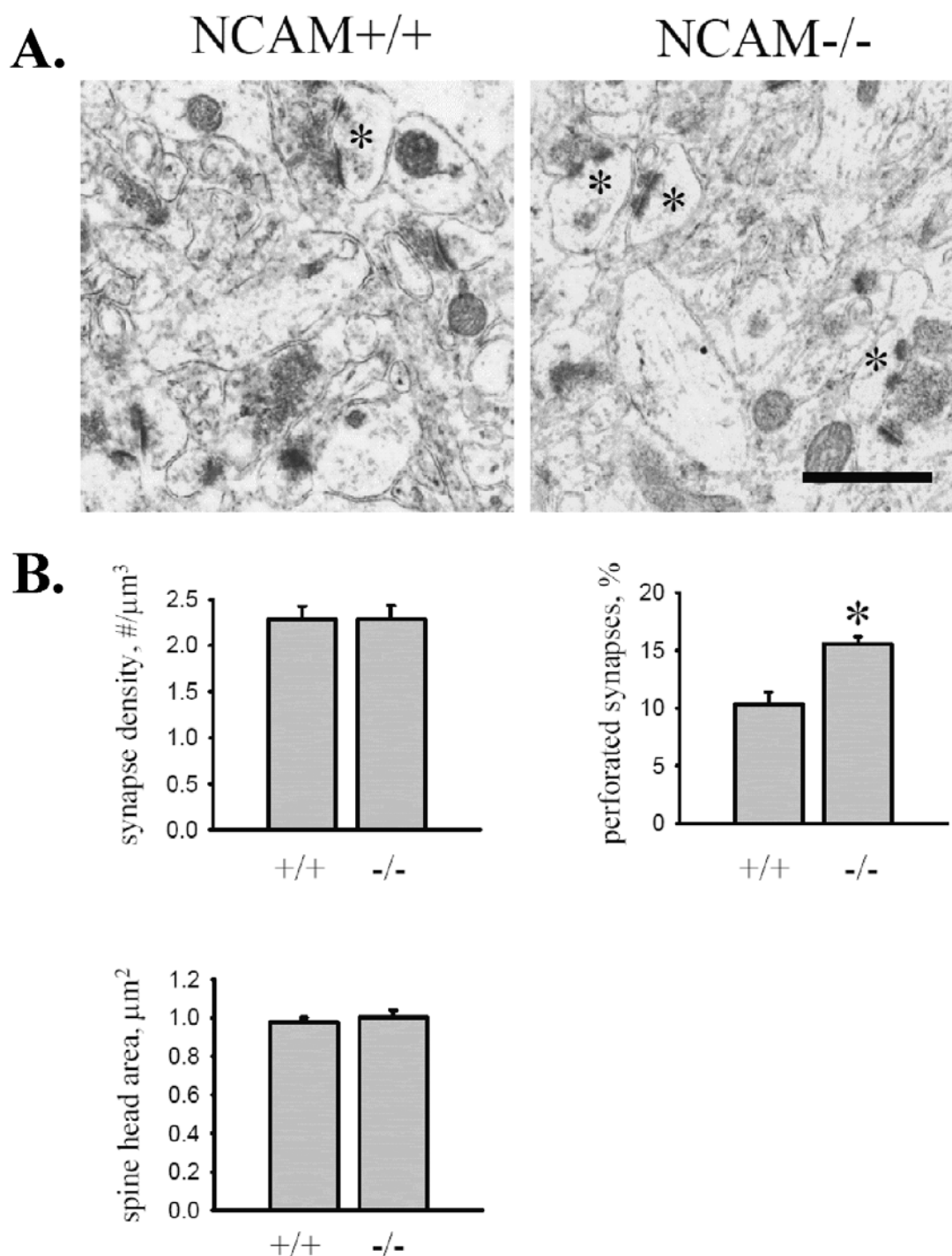


Figure 7. Ablation of NCAM increases the percentage of perforated synapses. A. – Representative electron micrographs of CA1 stratum radiatum in NCAM^{+/+} and conditionally deficient NCAM^{-/-} mice. Examples of perforated synapses are marked with asterisks. Bar = 1 μm. B. – Graphs show synapse density, spine head area and percentage of perforated synapses in NCAM^{+/+} and NCAM^{-/-} mice. Mean values ± SEM are shown. Six (N=6) animals were analyzed for each genotype. The percentage of perforated synapses is increased in NCAM^{-/-} brains. *P<0.05, paired t-test.

1.2 Inhibition of synaptic activity or fusion of vesicles with the plasma membrane does not reduce the number of perforated PSDs

Increased number of perforated synapses has been correlated with increased synaptic activity (Nikonenko et al., 2002). Intensive fusion of synaptic vesicles with the presynaptic plasma membrane and transport vesicles with the PSD were also considered as a possible mechanisms for PSD perforation (Luscher et al., 2000; Spacek and Harris, 2004), i.e. PSD disruption may result from expansion of synaptic membranes during exocytosis. Since NCAM is involved in the regulation of synaptic efficacy (Cremer et al., 1994; Muller et al., 1996; Bukalo et al., 2004) and anchoring of transport and synaptic vesicles at synapses (Sytnyk et al., 2002, 2004), we investigated whether abnormalities in these may result in increased densities of perforated PSDs in NCAM^{-/-} mice by using cultures of dissociated hippocampal neurons as an easy-to-manipulate system. In cultures of NCAM^{-/-} neurons, the percentage of synapses with perforated PSDs was increased when compared to NCAM^{+/+} neurons (Fig. 8), in agreement with the observations in intact tissue of constitutively and conditionally NCAM^{-/-} mice. To analyse whether an increase in the percentage of perforated synapses is related to enhanced synaptic activity in NCAM^{-/-} neurons, the number of perforated synapses was quantified following inhibition of neuronal activity by tetrodotoxin (TTX), which blocks voltage-dependent Na⁺ channels, thereby inhibiting action potential propagation. To compare possible contribution of vesicle exocytosis to the formation of perforated synapses in NCAM^{+/+} versus NCAM^{-/-} neurons, vesicle fusion was blocked by tetanus toxin (tetTX), which proteolytically inactivates VAMP2, a component of the SNARE complex (Maletic-Savatic et al., 1998). Inhibition of neuronal activity for 60 min (Fig. 8) by TTX or block of vesicle exocytosis by tetanus toxin neither decreased the percentage of perforated PSDs in NCAM^{+/+} neurons nor did they reduce the percentage of perforated PSDs in NCAM^{-/-} neurons to the levels seen in NCAM^{+/+} neurons (Fig. 8). Thus perforated synapses are formed and/or maintained in the absence of synapse activation and independently of exocytosis. Moreover, prolonged inhibition of synaptic activity up to 24 hours by TTX and to lesser extent by TetTX even increased the number of perforated synapses in NCAM^{+/+} but not in NCAM^{-/-} neurons.

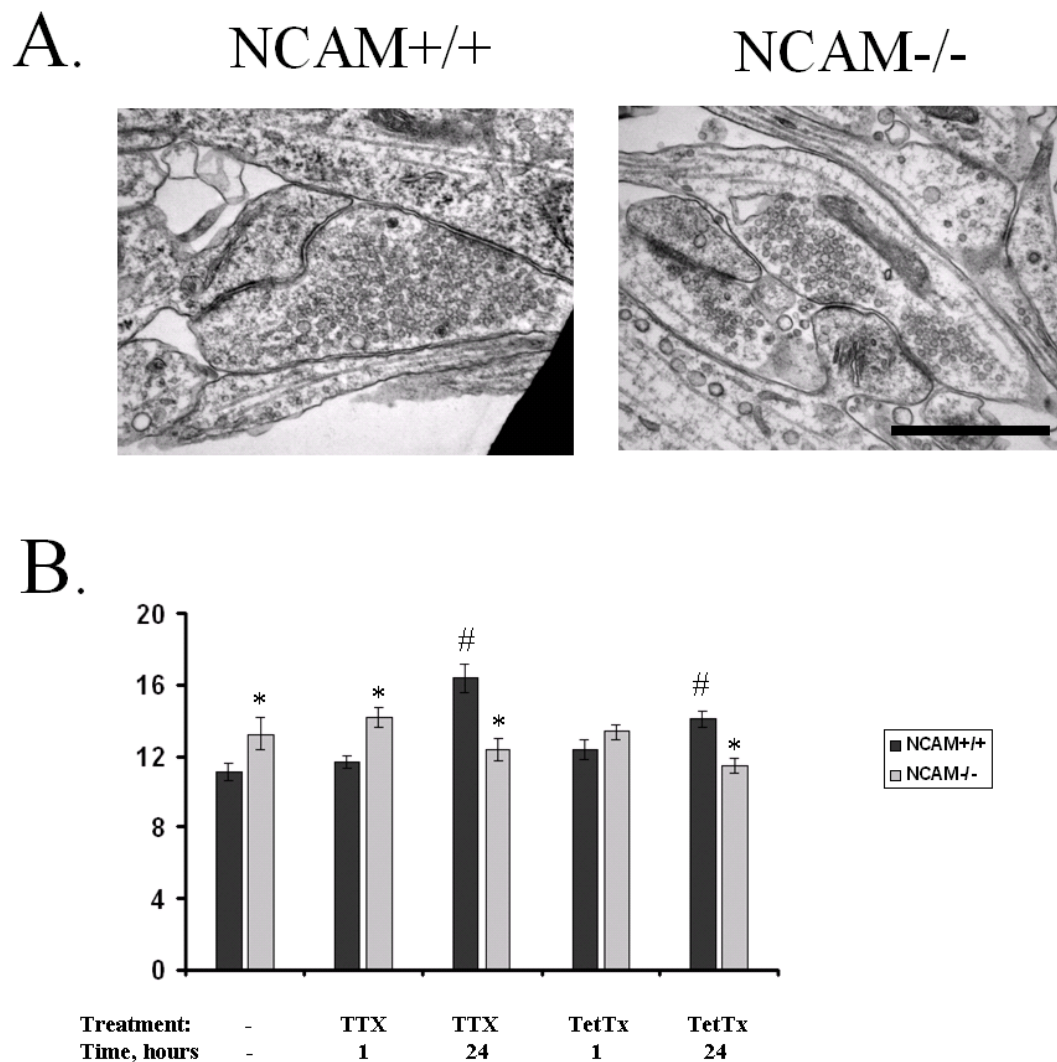


Figure 8. Inhibition of neuronal activity or vesicle fusion does not decrease percentages of perforated synapses in NCAM+/+ and NCAM-/- neurons. A. – Representative electron micrographs of perforated synapses in NCAM+/+ and NCAM-/- cultured hippocampal neurons. Bar = 1 μ m. B. – NCAM+/+ and NCAM-/- neurons were treated with tetrodotoxin (TTX) or tetanus toxin (TetTx). Graph shows the percentage of perforated synapses in control untreated and toxin-treated neurons of both genotypes. Symbol (*) indicates statistically significant differences ($p < 0.05$, t test) between CHL1-/- and CHL1+/+ neurons and (#) shows statistically significant difference ($p < 0.05$, t test) when neurons of a particular genotype are compared with the control group of neurons of this genotype. Note that inhibition of synaptic activity with TTX or block of vesicle fusion with TetTx does not decrease the percentage of perforated synapses neither in NCAM+/+ nor NCAM-/- neurons. Mean values \pm SEM are shown. At least seven cultures ($N \geq 7$) were analyzed for each group.

1.3 The spectrin meshwork maintains the structural integrity of PSDs

A web-like scaffold formed by spectrin and actin filaments is a prominent feature of PSDs (Baines, et al., 2001; Landis and Reese, 1983; Ziff, 1997). NCAM promotes the assembly of the spectrin meshwork in PSDs and up-regulates the overall expression of the spectrin protein in the brain (Leshchyns'ka et al., 2003; Sytnyk et al., 2006). To analyze the contribution of the spectrin meshwork to maintenance of PSD integrity, we disrupted this meshwork in cultured neurons by antimycin A, an ATP-depleting agent that induces dissociation of spectrin from the actin filaments leading to dispersion of spectrin (Molitoris et al., 1996), but not to depolymerisation of actin microfilaments (Atkinson et al., 2004). We also used latrunculin A that binds to monomeric actin with a 1:1 stoichiometry, thus sequestering G-actin and resulting in net actin microfilament depolymerisation and disruption of the spectrin meshwork cross-linked to actin filaments (Allison et al., 2000). None of the reagents or vehicle resulted in any evident cell death, cell degradation or abnormal changes in overall synapse morphology (not shown). Disruption of the spectrin meshwork by antimycin A or latrunculin A, but not microtubule depolymerisation by vincristine (Allison et al., 2000), increased the number of synapses with perforated PSDs in NCAM^{+/+} neurons (Fig. 9A). Furthermore, when β I spectrin levels were reduced in NCAM^{+/+} neurons by transfection with β I spectrin siRNA, the number of synapses with perforated PSDs increased in these neurons to levels seen in NCAM^{-/-} neurons, while transfection with control siRNA did not affect the percentage of perforated synapses (Fig. 9C). Thus, abnormal spectrin meshwork assembly in NCAM^{-/-} neurons is a prominent cause for the increased density of perforated synapses.

The presence of perforated synapses in untreated NCAM^{+/+} neurons suggests that mechanisms inducing PSD perforations are also active at the basal levels of neuronal activity. Remodelling of the spectrin meshwork in neurons is achieved through proteolytic digestion of actin and spectrin by proteases, among which the calcium-activated cysteine proteases, called calpains, partially degrade spectrin in response to synapse activation (Lynch and Baudry, 1987; Jourdi et al., 2005). To analyse whether calpains regulate PSD perforation in NCAM^{+/+} neurons under basal synaptic activity, we treated cultures with the cell-permeable calpain inhibitor MDL28170 (Faddis et al., 1997). Inhibition of calpain activity reduced the percentage of perforated synapses in NCAM^{+/+} neurons (Fig. 9B). MDL28170 had little effect on the number of synapses with perforated PSDs in NCAM^{-/-}

neurons (Fig. 9B), indicating that inhibition of spectrin proteolysis can not compensate for inefficient spectrin accumulation in PSDs of these neurons (Sytnyk et al., 2006).

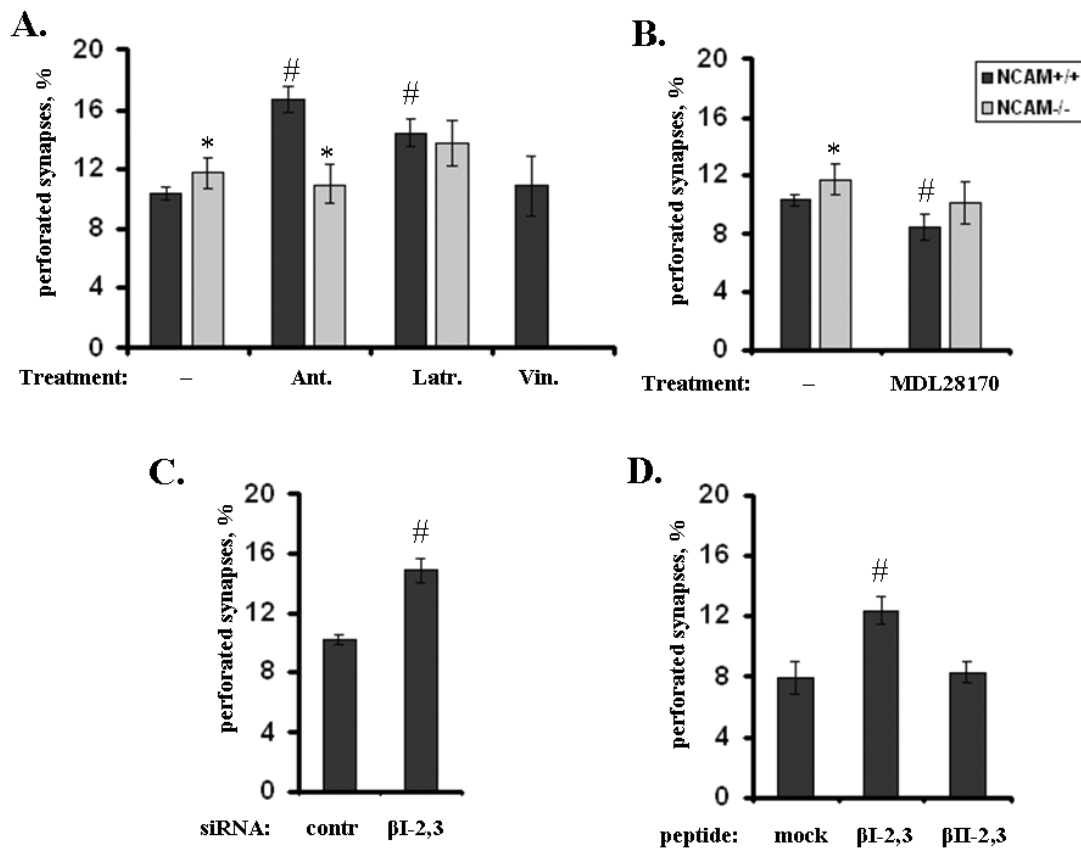


Figure 9. Disassembly of the spectrin meshwork increases whereas inhibition of spectrin meshwork remodelling reduces the percentage of perforated synapses. A. – The percentage of perforated synapses was quantified in control untreated NCAM+/+ and NCAM-/- neurons and NCAM+/+ and NCAM-/- neurons treated with antimycin A (Ant.), latrunculin A (Latr.) or vincristine (Vin.) (the latter only NCAM+/+ neurons); B. – The percentage of perforated synapses was quantified in control untreated NCAM+/+ and NCAM-/- neurons and neurons of both genotype treated with the calpain inhibitor MDL28170. C. – The percentage of perforated synapses was quantified in spectrin β I siRNA transfected neurons and control siRNA transfected neurons. D. – The percentage of perforated synapses was quantified in neurons loaded with β I-2,3 spectrin peptide, β II-2,3 spectrin peptide or in neurons treated only with transfection reagent (mock). Graphs show mean values \pm SEM. Five or more than five cultures ($N \geq 5$) were analysed for each group with more than 100 synapses analysed for each culture. Symbol (*) indicates statistically significant differences ($p < 0.05$, t test) between NCAM-/- and NCAM+/+ neurons and (#) shows statistically significant difference ($p < 0.05$, t test) when neurons of a particular genotype are compared with the control group of neurons of this genotype. Note that NCAM deficiency or disruption of the spectrin meshwork with antimycin A, latrunculin A or β I spectrin siRNA, as well as disruption of NCAM-mediated recruitment of β I spectrin into PSD by β I-2,3 spectrin peptide increase the percentage of perforated

synapses, while inhibition of calpain activity reduces the percentage of perforated synapses in NCAM^{+/+} neurons.

Direct inhibition of NCAM-mediated recruitment of β I spectrin by loading NCAM^{+/+} neurons with peptide derived from β I-2,3 spectrin fragment also increased the number of perforated synapses further indicating the role of NCAM/spectrin complex in the maintenance of structural integrity of the PSD. β I-2,3 peptide loaded neurons were compared with β II-2,3 loaded and only transfection reagent treated neurons.

1.4 Actin polymerisation is required for spinule formation but not for PSD perforation

Elongation of actin microfilaments towards PSDs resulting in PSD disruption by newly-formed spinule was also considered to cause PSD perforation (Edwards et al., 1995). Disruption of actin microfilaments by latrunculin A, however, did not reduce the percentage of perforated synapses, indicating that actin polymerisation is not required for PSD perforation (Fig. 9). Nevertheless, the density of perforated synapses with spinules was drastically reduced by latrunculin A (Fig. 10), indicating that actin polymerisation is required for spinule formation and that spinules mark sites of active microfilament formation. Interestingly, inhibition of calpain activity also reduced the percentage of perforated synapses with spinules (Fig. 10) suggesting that partial digestion of the spectrin meshwork is required for spinule formation. Taking into the account that spinules in PSDs are formed exclusively at sites free of electron-dense material (Spacek and Harris, 2004; and our own observations), our findings indicate that local disassembly of the spectrin meshwork may also remove a physical barrier preventing formation of a spinule. Partial disassembly of the spectrin meshwork by calpains can also results in the release of spectrin subunits and short F-actin microfilaments that could serve for further growth of actin filaments involved in spinule formation. In β I spectrin siRNA treated neurons, the number of perforated synapses with spinules was reduced (Fig. 10) further suggesting a role for β I spectrin as an actin nucleation and spinule initiation signal.

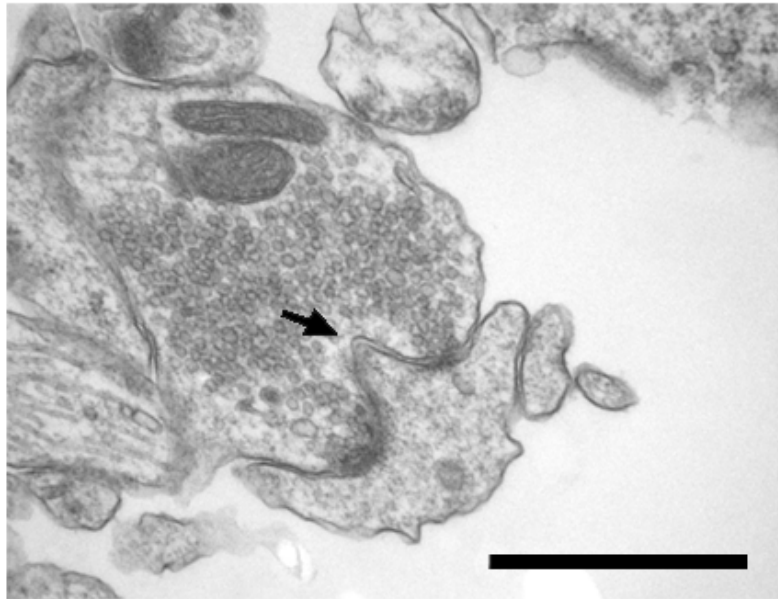
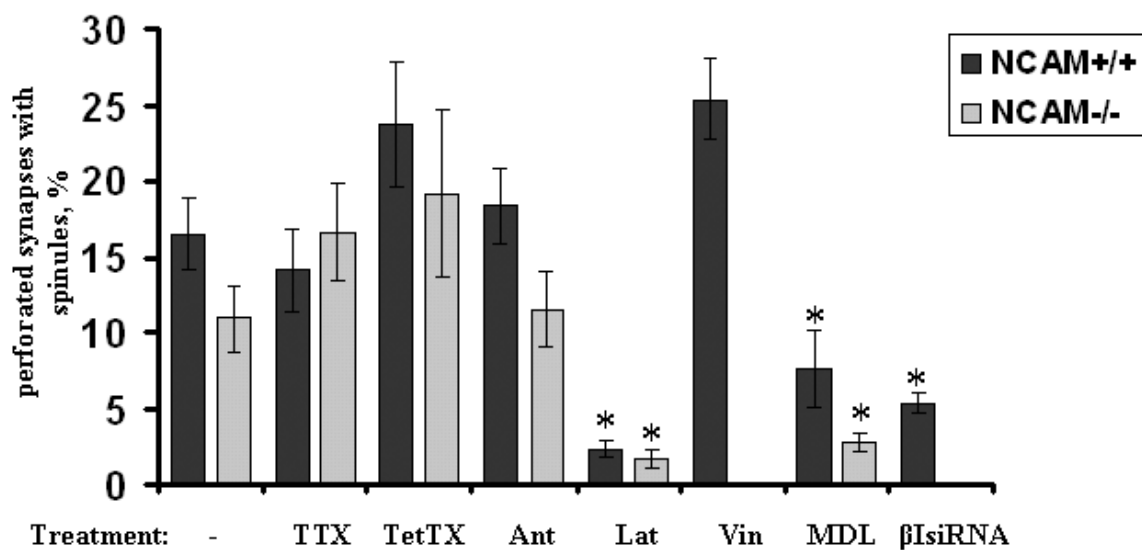
A.**B.**

Figure 10. Actin polymerisation is required for spinule formation. A. – representative electron micrograph of perforated synapses with spinule at the site of perforation (arrow). Bar = 0.5 μ m. B. – The graph shows percentage of perforated synapses with spinules in control untreated neurons or neurons treated with tetrodotoxin (TTX), tetanus toxin (TetTx), antimycin A (Ant.), latrunculin A (Latr.), vincristine (Vin.) (only for NCAM+/+ neurons), calpain inhibitor MDL28170 or transfected with β I spectrin siRNA (only for NCAM+/+ neurons). NCAM+/+ and NCAM-/- neurons were analysed. Asterisks indicate statistically significant differences ($p < 0.05$, t-test) when compared to control untreated NCAM+/+ or NCAM-/-neurons. Note that the percentage of perforated synapses with spinules is reduced in cultures treated with latrunculin A, MDL28170 or β I spectrin siRNA.

1.5 Disruption of the postsynaptic spectrin cytoskeleton does not enhance PSD splitting

PSD perforation has also been suggested as an initial step in PSD splitting and new synapse formation (Geinisman et al., 1993; Toni et al., 2001). To analyse this possibility, we visualized PSDs in live NCAM^{+/+} and NCAM^{-/-} neurons by transfecting them with green fluorescent protein tagged postsynaptic marker protein SAP90 (SAP90GFP) and recorded SAP90GFP clusters in live neurons for 10-20 min. The majority of SAP90GFP clusters (more than 95%) remained immobile for the total recording time with only occasional clusters which fused with each other, split away from each other, formed de novo, disappeared or moved with no difference between the genotypes (Fig. 11). Similarly, co-transfection of NCAM^{+/+} neurons with the β I2-3 spectrin fragment that disrupts the association between NCAM and β I spectrin (Leshchyns'ka et al., 2003) did not increase splitting rates of SAP90GFP clusters. Although we cannot exclude that in these experiments smaller clusters of SAP90GFP, which were below the resolution of our confocal microscope, were detaching from larger clusters, our data indicate that higher percentage of synapses with perforated PSDs in NCAM^{-/-} neurons is not accompanied by higher rates of complete PSD disassociation or splitting.

	NCAM ^{+/+}	NCAM ^{+/+} & β I2-3	NCAM ^{-/-}
N clusters	237	93	126
N neurites	30	16	19
N neurons	16	12	11
time, sec	23085	11156	16782
fuse	0 (0.0000 \pm 0.0000)	1 (0.0016 \pm 0.0015)	0 (0.0000 \pm 0.0000)
split	2 (0.0013 \pm 0.0009)	2 (0.0040 \pm 0.0026)	0 (0.0000 \pm 0.0000)
disappear	2 (0.0007 \pm 0.0005)	1 (0.0016 \pm 0.0015)	0 (0.0000 \pm 0.0000)
form	1 (0.0003 \pm 0.0003)	0 (0.0000 \pm 0.0000)	1 (0.0004 \pm 0.0004)
move	0 (0.0000 \pm 0.0000)	3 (0.0050 \pm 0.0027)	3 (0.0012 \pm 0.0009)

Figure 11. Increased number of PSD perforation in NCAM^{-/-} neurons or NCAM^{+/+} neurons with reduced spectrin concentration at the PSD due to NCAM/spectrin

complex disruption by β I-2,3 spectrin peptide are not accompanied by increased PSD splitting rates. NCAM+/+ and NCAM-/- neurons were transfected with SAP90GFP, or NCAM+/+ neurons were co-transfected with SAP90GFP and the β I_{2,3} spectrin fragment. Behaviour of SAP90GFP clusters in transfected neurons was then analysed by time lapse recordings. The table shows numbers (N) of clusters, neurites and neurons analysed, the total recording time, and the total numbers of events when SAP90GFP clusters fused, split, disappeared, formed de novo, or moved. Average numbers of these events per neurite per second are given in brackets (mean values \pm SEM are shown). No statistically significant differences were observed in these parameters for neurons of the two genotypes.

1.6 Disruption of the postsynaptic spectrin cytoskeleton increases postsynaptic endocytosis and AMPA receptor internalisation

In glutamatergic synapses, stable clathrin zones, so called endocytic zones, normally lie laterally to PSDs (Blanpied et al., 2002). It has been postulated that, as a consequence, synaptic receptors and other membrane proteins must be translocated to these endocytic sites before internalisation (Blanpied et al., 2002). Clathrin coated pits and budding clathrin coated vesicles (CCVs) have, however, also often been observed at sites of PSD perforations (Fig. 12A; Toni et al., 2001). We suggest that PSD perforations may represent formation of additional endocytic zones. In accordance with this idea, in dendritic spines in the CA1 stratum radiatum of NCAM-/- hippocampi, numbers of CCVs located in the vicinity of PSDs (within 0.3 μ m from the PSD) were increased (Fig. 12B). Similarly, increased numbers of CCVs were observed postsynaptically in cultured NCAM-/- neurons and in NCAM+/+ neurons transfected with β I spectrin siRNA (Fig. 12), suggesting that PSD perforations induced by NCAM/spectrin complex disassembly increase endocytosis at the postsynaptic membrane.

Although CCV numbers in the vicinity of NCAM-/- PSDs were increased by only 15-30%, they could reflect a significantly increased degree of endocytosis rates given the fact that endosomes reside only transiently in the PSD vicinity and rapidly translocate and fuse with larger endosomal pools in dendrites (Cooney et al., 2002; Park et al., 2006).

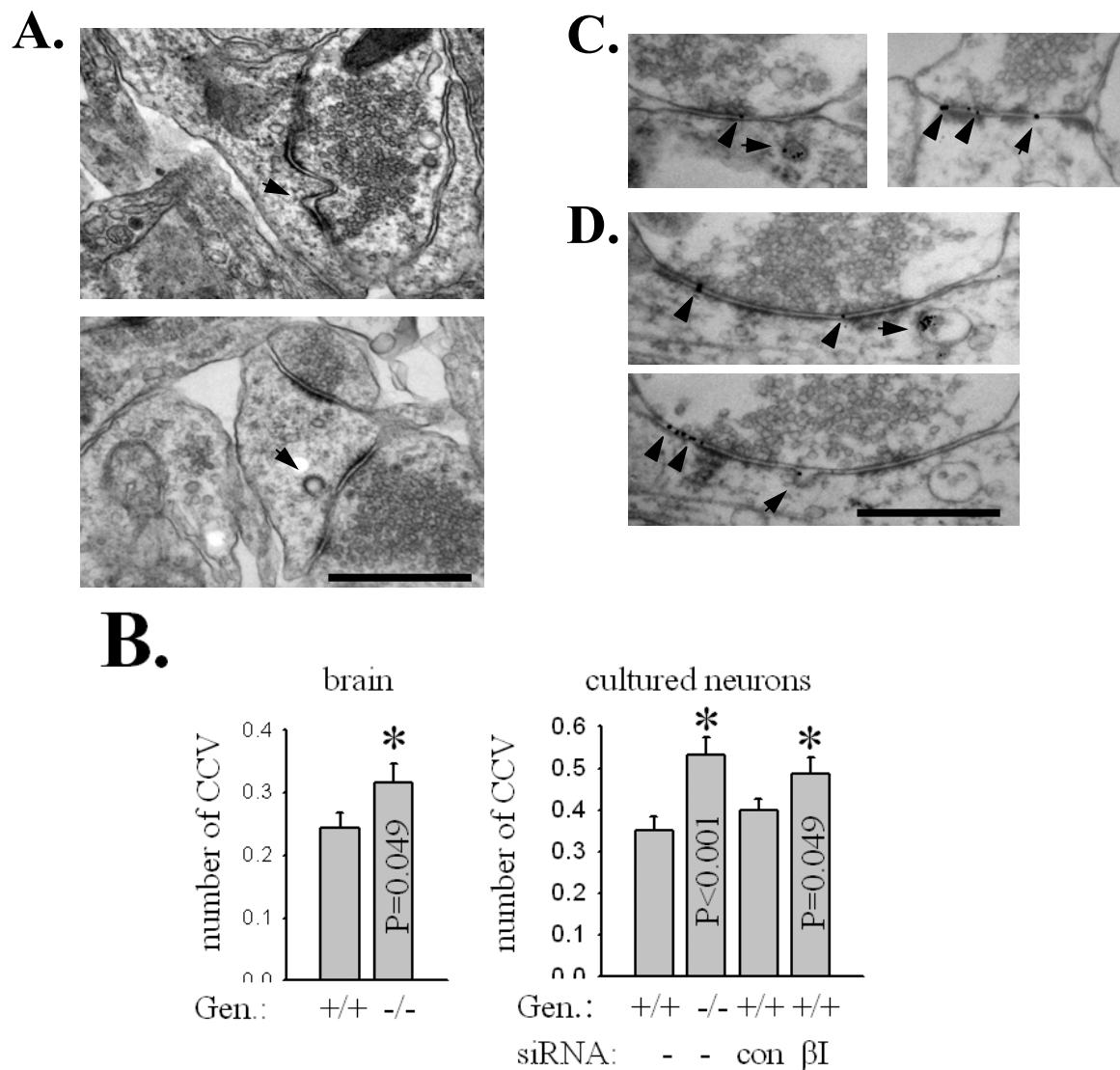


Figure 12. Perforations are sites of active membrane recycling. A. - Representative electron micrographs of perforated synapses in NCAM^{+/+} hippocampal neurons with clathrin-coated vesicles budding from the plasma membrane at the sites of perforations (arrows, left panel) or observed near the site of perforation (arrow, right panel). Bar = 0,5 μ m. B. - Graphs show mean numbers \pm SEM of clathrin-coated vesicles (CCV) per postsynaptic profile counted within 0.3 μ m from PSDs in the CA1 stratum radiatum in NCAM^{+/+} and conditionally deficient NCAM^{-/-} brains (N=400 synapses from 5 NCAM^{+/+} animals and 300 synapses from 4 NCAM^{-/-} animals were analysed) or in cultured NCAM^{-/-} or NCAM^{+/+} neurons non-treated or treated with control or β I spectrin siRNA (N>300 synapses from 5 cultures were analysed in each group). Asterisks indicate statistically significant differences (t-test, p as indicated on the graphs) when compared to NCAM^{+/+} brains (for brain) or to untreated NCAM^{+/+} neurons or control siRNA transfected neurons (for cultured neurons). C, D - Live cultured hippocampal neurons were incubated with antibodies against the extracellular domain of GluR1 followed by nanogold-Fab conjugates, incubated for 5 minutes, fixed and processed for electron microscopy. Representative images of synapses are shown. C. (left panel) -

An example of a non-perforated synapse is shown with the nanogold particles observed in the synaptic cleft (arrowhead) and in the budding vesicle adjacent to the PSD (arrow). C. (right panel) – An example of a perforated synapse is shown with the nanogold particles observed in the synaptic cleft apposed to the PSD (arrowheads) and to the PSD perforation (arrow). D. – Two sections separated by approximately 200 nm through the perforated synapse are shown with nanogold particles observed in the synaptic cleft (arrowheads). The upper section shows a continuous PSD. An endosome containing the nanogold particles is marked with an arrow. The lower section reveals a perforation in the PSD with a clathrin coated invagination at the perforation site containing a nanogold particle (arrow). Bar = 0.5 μm (for A, C and D).

To investigate whether PSD perforations play a role in endocytosis of the postsynaptic membrane proteins, we visualized sites of AMPA receptor endocytosis in synapses by applying to live cultured neurons the antibodies against the extracellular domain of the GluR1 subunit of AMPA receptors followed by nanogold-Fab conjugates to visualize GluR1-antibody complexes. After five minute recovery followed by fixation and gold enhancement, neurons were processed for electron microscopy. In GluR1 antibody labelled neurons, GluR1-nanogold complexes were observed in synaptic clefts above PSDs (Fig. 12C,D), while no labelling was present when non-specific immunoglobulins were used instead of GluR1 antibodies (not shown) indicating the specificity of the labelling. In non-perforated synapses, clathrin coated membrane invaginations and budding vesicles containing GluR1-nanogold complexes have been found aside of PSDs (Fig. 12C,D) in accordance with previous reports on endocytic zone localization (Blanpied et al., 2002). Interestingly, in perforated synapses GluR1-nanogold complexes have been found in the synaptic cleft both above the PSD and at perforation sites (Fig. 12C,D), indicating that AMPA receptors enter membrane of PSD perforations. Furthermore, GluR1-nanogold complexes have been observed in clathrin coated membrane invaginations formed at PSD perforations (Fig. 12D) suggesting that PSD perforations participate in AMPA receptor endocytosis by opening additional endocytic zones.

Taking in consideration over observations that NCAM^{-/-} mice contain more perforated synapses containing additional endocytic zones and more clathrin coated vesicles we investigated whether changes in clathrin coated vesicles numbers correlate with the endocytosis of postsynaptic proteins. We compared endocytosis rates of the AMPA receptor GluR1 subunit in NCAM^{+/+} neurons and NCAM^{-/-} neurons by estimating GluR1-mediated uptake of cell surface bound anti-GluR1 antibodies to endosomes (Carroll et al., 1999). Neurons pre-incubated with the mouse anti-GluR1 antibodies visualized with

the Cy3-conjugated goat anti-mouse Ig antibodies were allowed to take up the GluR1/antibody complexes for one hour. After fixation, surface GluR1/antibody complexes were visualized with the Cy2-conjugated anti-goat Ig antibodies. Cy3-positive/Cy2-negative internalised GluR1 complexes formed bright accumulations in dendrites that were clearly distinguishable from surface Cy3/Cy2-positive GluR1 clusters in accordance with previous reports showing that the major endosomal pool in dendrites is located several micrometers apart from PSDs (Cooney et al., 2002; Park et al., 2006; Fig13A). GluR1 internalisation index ($\text{GluR1}_{\text{intern.}}$) defined as a ratio of internalised Cy3 immunofluorescence to the total Cy3 immunofluorescence along neurites was increased in NCAM^{-/-} versus NCAM^{+/+} neurons (Fig. 13B). Similarly we compared endocytosis rates of another AMPA receptor subunit – GluR2. Its endocytosis was also significantly increased in NCAM^{-/-} neurons (Fig. 13C,D). Knock-down of β I spectrin expression in NCAM^{+/+} neurons with β I spectrin siRNA resulted in significantly increased $\text{GluR1}_{\text{intern.}}$ (Fig. 13B) confirming that spectrin meshwork disassembly promotes AMPAR internalisation.

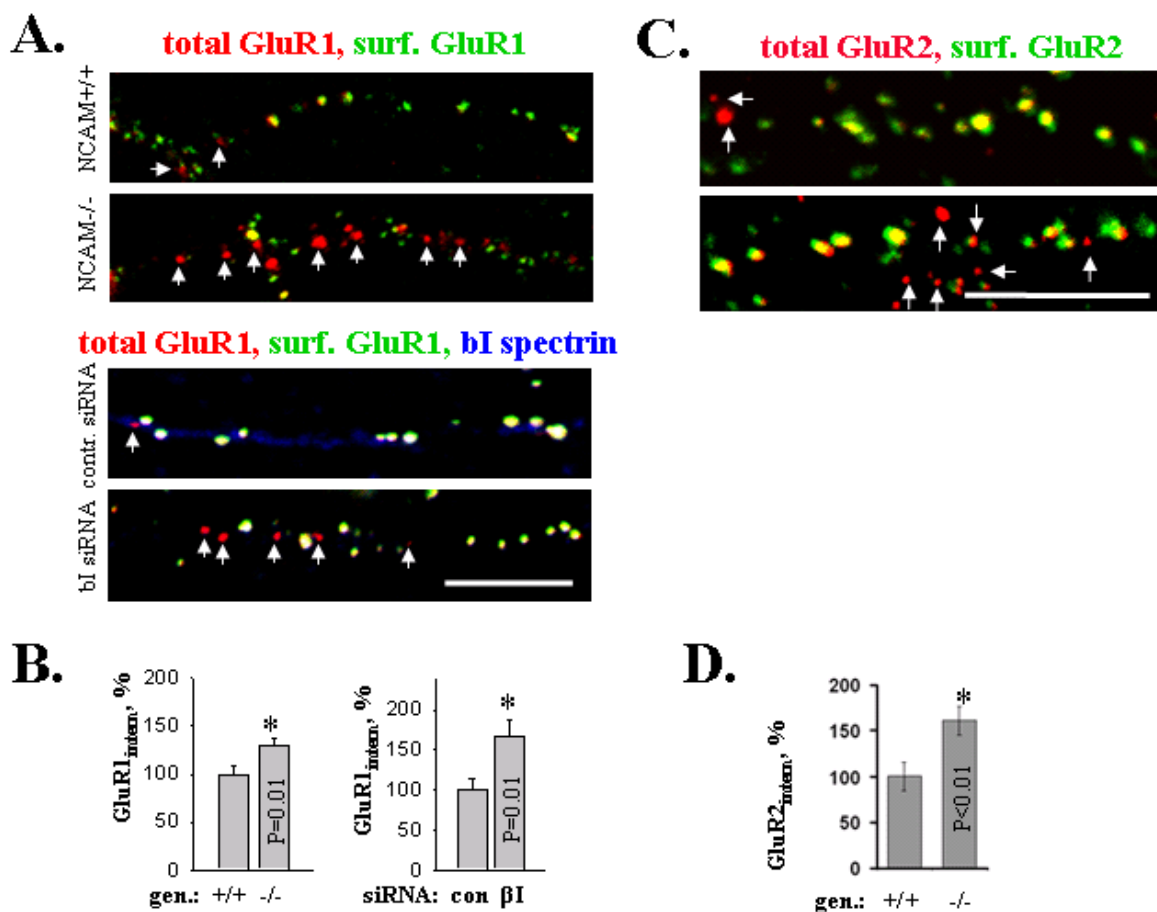


Figure 13. Increased number of perforated synapses in NCAM^{-/-} neurons and NCAM^{+/+} neurons transfected with β I spectrin siRNA correlates with increased endocytosis of AMPA receptors.

A. – Live cultured NCAM^{+/+} and NCAM^{-/-} hippocampal neurons or control and β I spectrin siRNA transfected NCAM^{+/+} neurons were labelled with antibodies against the extracellular domain of GluR1 followed by Cy3 conjugated secondary antibodies (red). After one hour, neurons were fixed and surface Cy3/GluR1 complexes were visualized with Cy2 conjugated secondary antibodies (green). siRNA transfected neurons were co-labelled with β I spectrin antibodies (blue). Representative neurites are shown. Note increased numbers of Cy3-positive/Cy2-negative internalised GluR1 accumulations (arrows) in NCAM^{-/-} and β I spectrin siRNA transfected NCAM^{+/+} neurons. Bar = 10 μ m. B. - Graphs show mean GluR1 internalisation index ($\text{GluR1}_{\text{intern.}}$, see text for the definition) \pm SEM along neurites of NCAM^{+/+} and NCAM^{-/-} neurons and NCAM^{+/+} neurons treated with control or β I spectrin siRNA with the mean $\text{GluR1}_{\text{intern.}}$ in non-treated or control siRNA transfected NCAM^{+/+} neurons set to 100%. C. - Live cultured NCAM^{+/+} and NCAM^{-/-} hippocampal neurons were labelled with antibodies against the extracellular domain of GluR2 followed by Cy3 conjugated secondary antibodies (red). After one hour, neurons were fixed and surface Cy3/GluR2 complexes were visualized with Cy2 conjugated secondary antibodies (green). Representative neurites are shown. Note increased numbers of Cy3-positive/Cy2-negative internalised GluR2 accumulations (arrows) in NCAM^{-/-}. D. - Graph shows mean GluR2 internalisation index ($\text{GluR2}_{\text{intern.}}$) \pm SEM along neurites of NCAM^{+/+} and NCAM^{-/-} neurons with the mean $\text{GluR2}_{\text{intern.}}$ in NCAM^{+/+} neurons set to 100%. At least 100 neurites were analysed in each group from 45 neurons from 3 cultures. Experiments were performed twice with the same effect. Asterisks indicate statistically significant differences when compared to untreated NCAM^{+/+} neurons or control siRNA transfected neurons (p as indicated on the graphs, t-test).

1.7 LTP-associated PSD perforations are accompanied by enhanced AMPAR endocytosis

Long-term potentiation (LTP) of synapses is associated with an increase in the rate of PSD perforations that appear after a certain delay following LTP induction (Geinisman et al., 1991; Buchs and Muller, 1996; Yuste and Bonhoeffer, 2001). To analyse whether these activity associated changes in the number of perforated synapses correlate with the changes in the AMPA receptor endocytosis, we treated neurons with 200 μ M glycine for 3 min to activate synaptic NMDA receptors, a protocol used to induce chemical LTP in cultured hippocampal neurons (Lu et al., 2001; Park et al., 2004, 2006). In stimulated NCAM^{+/+} neurons, the number of perforated synapses remained unchanged at 15 and 45 min following glycine stimulation and increased by approximately 100% when compared to control mock treated neurons at 120 min following glycine stimulation (Fig. 14A.). To

dissect activity-related changes in the AMPA receptor internalisation rate, $\text{GluR1}_{\text{intern}}$ in neurons stimulated with glycine ($\text{GluR1}_{\text{intern.Gly}}$) was normalized to $\text{GluR1}_{\text{intern}}$ in mock treated neurons analysed in parallel ($\text{GluR1}_{\text{intern.control}}$). At 15 and 75 min following glycine stimulation, $\text{GluR1}_{\text{intern.Gly}}$ was reduced in NCAM^{+/+} neurons when compared to $\text{GluR1}_{\text{intern.control}}$ ($\text{GluR1}_{\text{intern.Gly}}/\text{GluR1}_{\text{intern.control}} = 61.8 \pm 7.4 \%$ and $54.5 \pm 9.9 \%$, respectively, Fig. 14B), suggesting that AMPA receptor endocytosis was inhibited immediately after LTP induction. However, $\text{GluR1}_{\text{intern.Gly}}/\text{GluR1}_{\text{intern.control}}$ ratio steeply increased by approximately 200% at 120 min after glycine stimulation (Fig. 14B), indicating that an increase in the number of perforated synapses correlates with higher AMPA receptor internalisation rates. In NCAM^{-/-} neurons, glycine stimulation did not change the number of perforated synapses and AMPA receptor internalisation rate (Fig. 14B). A plausible mechanism contributing to this phenomenon could be that poorly assembled spectrin meshwork in NCAM^{-/-} PSDs could not be further disassembled by LTP-associated cytoskeleton restructuring within PSD that, in turn, would result in unchanged AMPAR endocytosis rates. In accordance with this idea, while $\text{GluR1}_{\text{intern.Gly}}$ was 2.48 ± 0.3 and 1.78 ± 0.27 times higher in NCAM^{-/-} neurons than in NCAM^{+/+} neurons at 15 min and 75 min, respectively, $\text{GluR1}_{\text{intern.Gly}}$ was similar in NCAM^{+/+} and NCAM^{-/-} neurons at 120 min after glycine stimulation, that is at the time of active PSD perforation formation in stimulated NCAM^{+/+} neurons (Fig. 14).

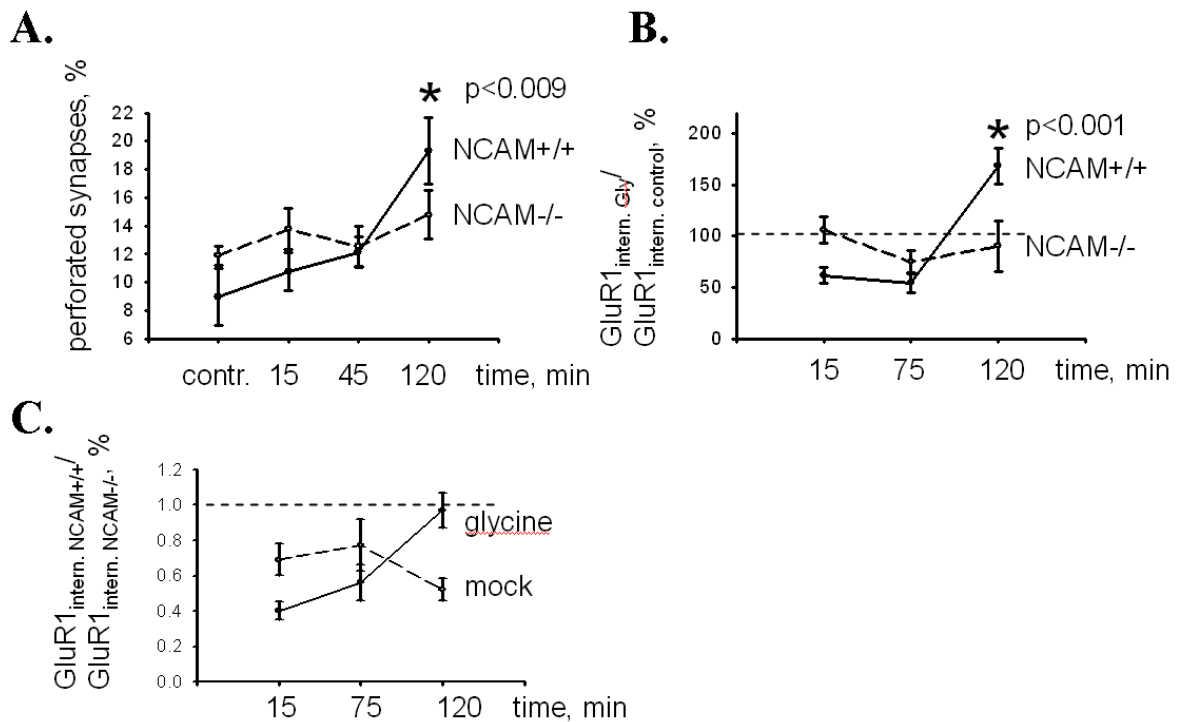
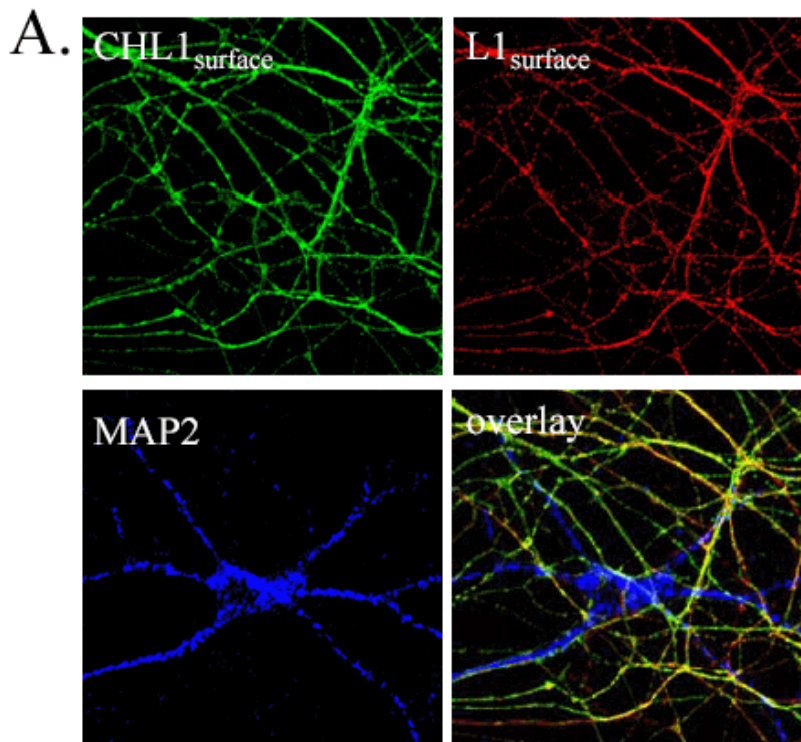


Figure 14. Glycine-induced LTP induces PSD perforations and enhances AMPA receptor endocytosis at 2 hours following glycine application. A. – Numbers of perforated synapses were estimated in NCAM^{+/+} and NCAM^{-/-} neurons treated with 200 μ M glycine for 3 min and fixed at the indicated time points. Graphs show mean percentages \pm SEM. T-test shows a statistically significant increase in the number of perforated synapses in NCAM^{+/+} neurons at 120 min following glycine stimulation when compared to NCAM^{+/+} control group that is indicated by asterisk. $N \geq 6$ cultures were analysed in each group. B.; C. – GluR1_{intern.} was analysed in NCAM^{+/+} and NCAM^{-/-} neurons that were mock-treated or stimulated with 200 μ M glycine for 3 min and fixed at the indicated time points following glycine stimulation. The ratio of GluR1_{intern.} in stimulated neurons (GluR1_{intern.Gly}) to GluR1_{intern.} in mock-treated neurons (GluR1_{intern.control}) (B.) and the ratio of GluR1_{intern.} in NCAM^{+/+} neurons (GluR1_{intern.NCAM+/+}) to GluR1_{intern.} in NCAM^{-/-} neurons (GluR1_{intern.NCAM-/-}) (C.) is shown. Straight dashed lines show the GluR1_{intern.} level in mock-treated neurons (B.) and NCAM^{-/-} neurons (C.). * - The t test shows statistically significant increase in the GluR1_{intern.Gly}/GluR1_{intern.control} ratio in NCAM^{+/+} neurons at 120 min following glycine stimulation when compared to NCAM^{+/+} neurons that were fixed at 15 and 75 min after glycine stimulation (B.). Note that GluR1_{intern.NCAM+/+} reaches the level of GluR1_{intern.NCAM-/-} in neurons stimulated with glycine at 120 min following glycine stimulation. $n > 30$ neurons from 3 cultures were analysed in each group.

Project 2. The role of the cell adhesion molecule close homologue of L1 (CHL1) in regulation of clathrin-dependent synaptic vesicle recycling

2.1 CHL1 is accumulated in the presynaptic plasma membrane

Biochemical experiments show that CHL1 is enriched in synaptosomes; the level of CHL1 is approximately six times higher in synaptosomes and synaptic plasma membrane when compared with brain homogenates. CHL1 also could be detected in the crude synaptic vesicle fraction. In synaptic plasma membrane and synaptic vesicle fractions, CHL1 cofractionates with Hsc70. Here we have further analysed localisation of CHL1 at the subsynaptic level. We have labelled CHL1 with antibodies in cultured hippocampal neurons without permeabilization of the plasma membrane with detergent. Immunolabelling was localized to thin neurites negative for the dendritic marker MAP2 and positive for the axonal marker L1 (Fig. 15A), indicating that CHL1 is enriched in the axonal plasma membrane. After permeabilization of neurons with detergent, intracellular CHL1 was also detected in the somata of neurons and, to a lesser extent, in their dendrites (Fig.15B).



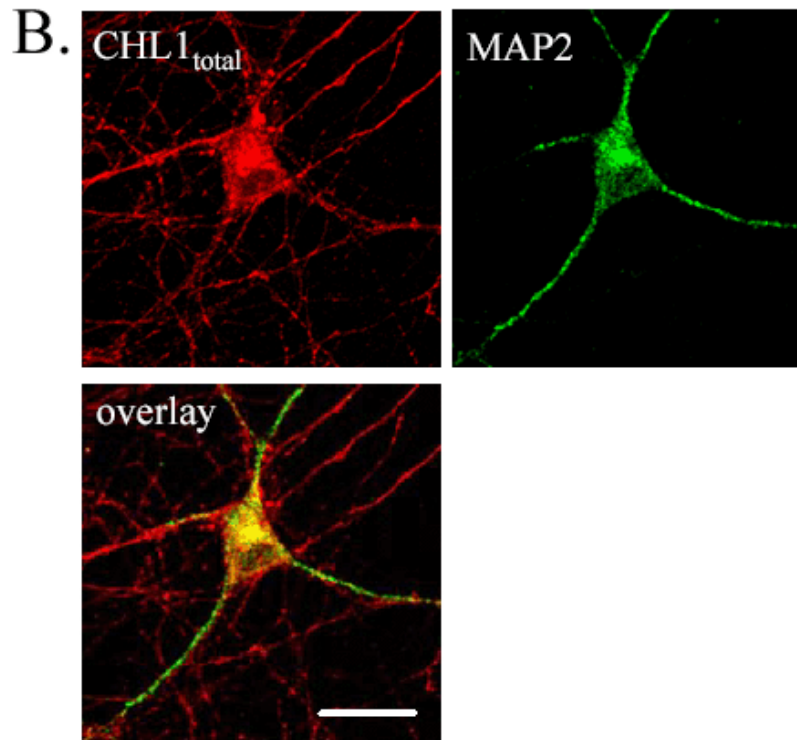


Figure 15. CHL1 is targeted to the axonal plasma membrane. A, B – Hippocampal neurons from CHL1^{+/+} mice were co-labelled with antibodies against CHL1 and the dendritic marker MAP2. In (A), labelling for axonally localized L1 was included. Antibodies against CHL1 and L1 were applied before (A) or after (B) permeabilization of the plasma membrane with the detergent Triton X-100. CHL1 at the cell surface localizes to thin L1 positive neurites identified as axons, a distribution that is distinct from dendritically localized MAP2 detected after permeabilization (A, B). After permeabilization of the plasma membrane, intracellular CHL1 is also detected in the soma and in dendrites (B). Bar = 20 μm (for A and B).

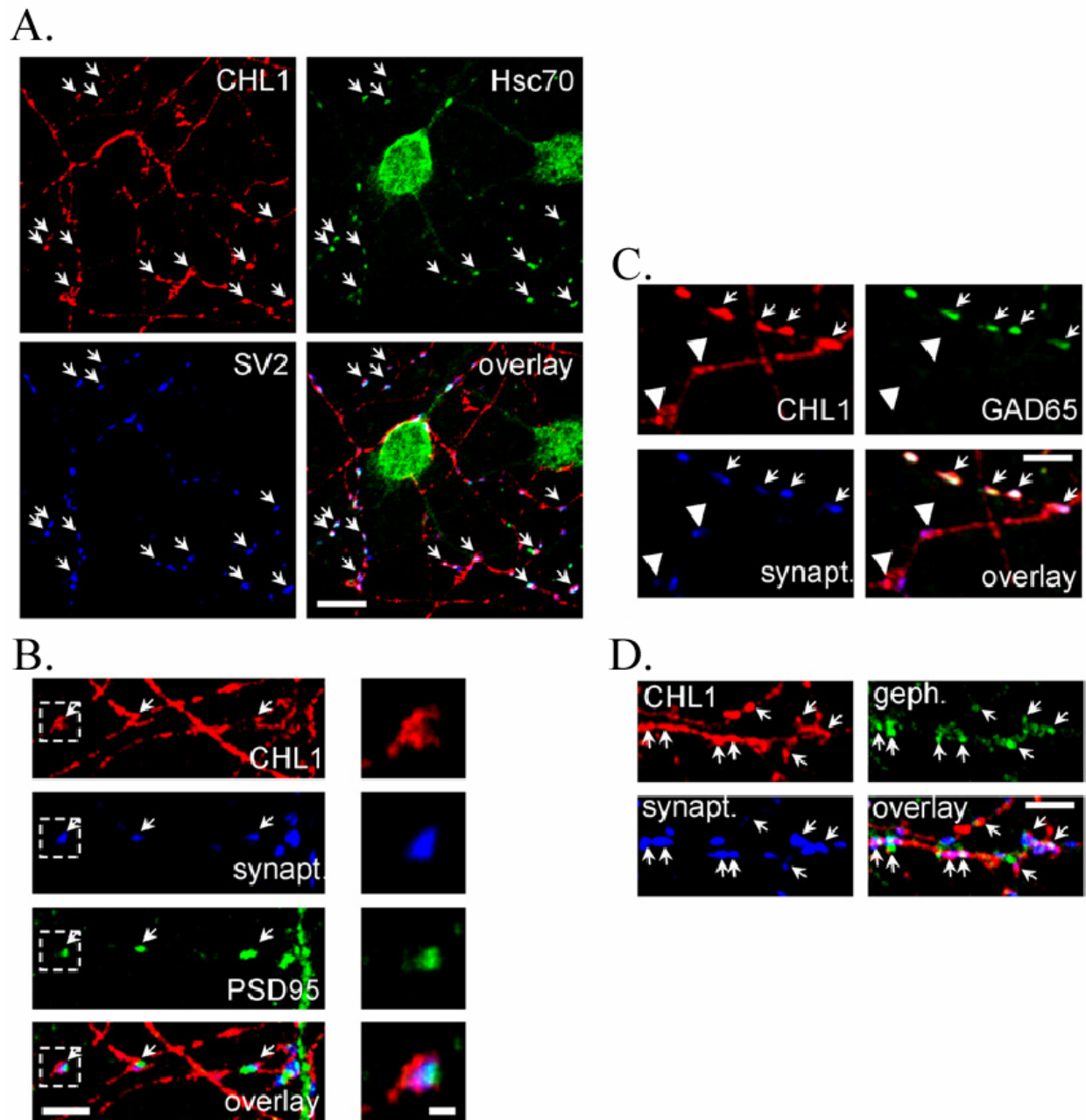


Figure 16. CHL1 accumulates at the presynaptic membrane. A.– C. - Hippocampal neurons were immunolabelled for cell surface exposed CHL1 and colabelled for Hsc70 and SV2 (A), synaptophysin and PSD95 (B), GAD65 (C), or gephyrin (D). CHL1 accumulates at sites of SV2 positive synaptic boutons containing Hsc70 (A, arrows). CHL1-positive synaptic boutons marked by synaptophysin are apposed to clusters of PSD95 (B, arrows) and gephyrin (D, arrows). CHL1-positive synaptic boutons are either positive (C, arrows) or negative (C, arrowheads) for GAD65. In (B), a higher magnification of the region marked with the dashed square is shown on the right. Bars = 10 μm (B), 5 μm (C–D), 1 μm (C, higher magnification).

We have also measured colocalization of CHL1 with Hsc70 and synaptic markers. Plasma membrane-associated CHL1 was highly expressed in presynaptic terminals visualized with antibodies against the synaptic vesicle protein SV2 where CHL1 was colocalized with Hsc70 (Fig. 16). CHL1 was detectable in both excitatory and inhibitory synapses, as indicated by apposition of CHL1 accumulations to the clusters of postsynaptic proteins of excitatory and inhibitory synapses (PSD95 and gephyrin, respectively) and by accumulation of CHL1 in synaptic boutons either positive or negative for GAD65, a presynaptic marker of inhibitory synapses (Fig. 16).

2.2 CHL1 recruits Hsc70 to synapses

Preliminary biochemical analysis indicated that Hsc70 protein levels were reduced in synaptosomes isolated from CHL1^{-/-} brains. To analyse levels of Hsc70 in presynaptic boutons, we labelled permeabilized cultured hippocampal neurons with Hsc70 antibody. Neurons were colabelled with synaptophysin antibody to identify presynaptic boutons, which were then graphically outlined to determine Hsc70 levels within the synaptophysin accumulations. Indeed, Hsc70 levels in synaptophysin accumulations were reduced in neurons derived from CHL1^{-/-} mice (Fig. 17A), indicating that CHL1 is involved in targeting of Hsc70 to synapses. Fluorescence intensity of the synaptic vesicle marker protein synaptophysin were the same in presynaptic boutons of cultured neurons from both wildtype (CHL1^{+/+}) and CHL1^{-/-} mice (Fig. 17A), showing that overall targeting of synaptic proteins to synaptic terminal was not affected in CHL1^{-/-} neurons.

To analyse the effect of CHL1 on the subcellular localization of Hsc70 in detail, we cotransfected cultured CHL1^{-/-} neurons together with Hsc70 tagged with green fluorescent protein (Hsc70GFP) and wild-type CHL1 or the tripeptide mutated CHL1 protein CHL1H1121Q in which binding site of CHL1 to Hsc70 is altered. Transfected full-length CHL1 showed a distribution similar to endogenous CHL1 expressed by CHL1^{+/+} neurons. Transfected CHL1 was enriched in axons and SV2 antibody-labelled synaptic boutons. Synaptic boutons of CHL1^{-/-} neurons transfected with wildtype CHL1 displayed two-fold enhanced concentration of Hsc70GFP labelling comparing to CHL1^{-/-} neurons transfected with an empty pcDNA3 vector. In contrast to transfection with wildtype form of CHL1 protein, transfection with the CHL1H1121Q mutant form of CHL1 did not enhance targeting of Hsc70GFP to SV2 positive synaptic boutons comparing to CHL1^{-/-} neurons

transfected with an empty pcDNA3 vector (Fig. 17B). This finding indicates that CHL1 enhances Hsc70 accumulation at synaptic boutons and the interaction between the HPD tripeptide of CHL1 and Hsc70 plays a crucial role in the CHL1-mediated recruitment of Hsc70 to synapses.

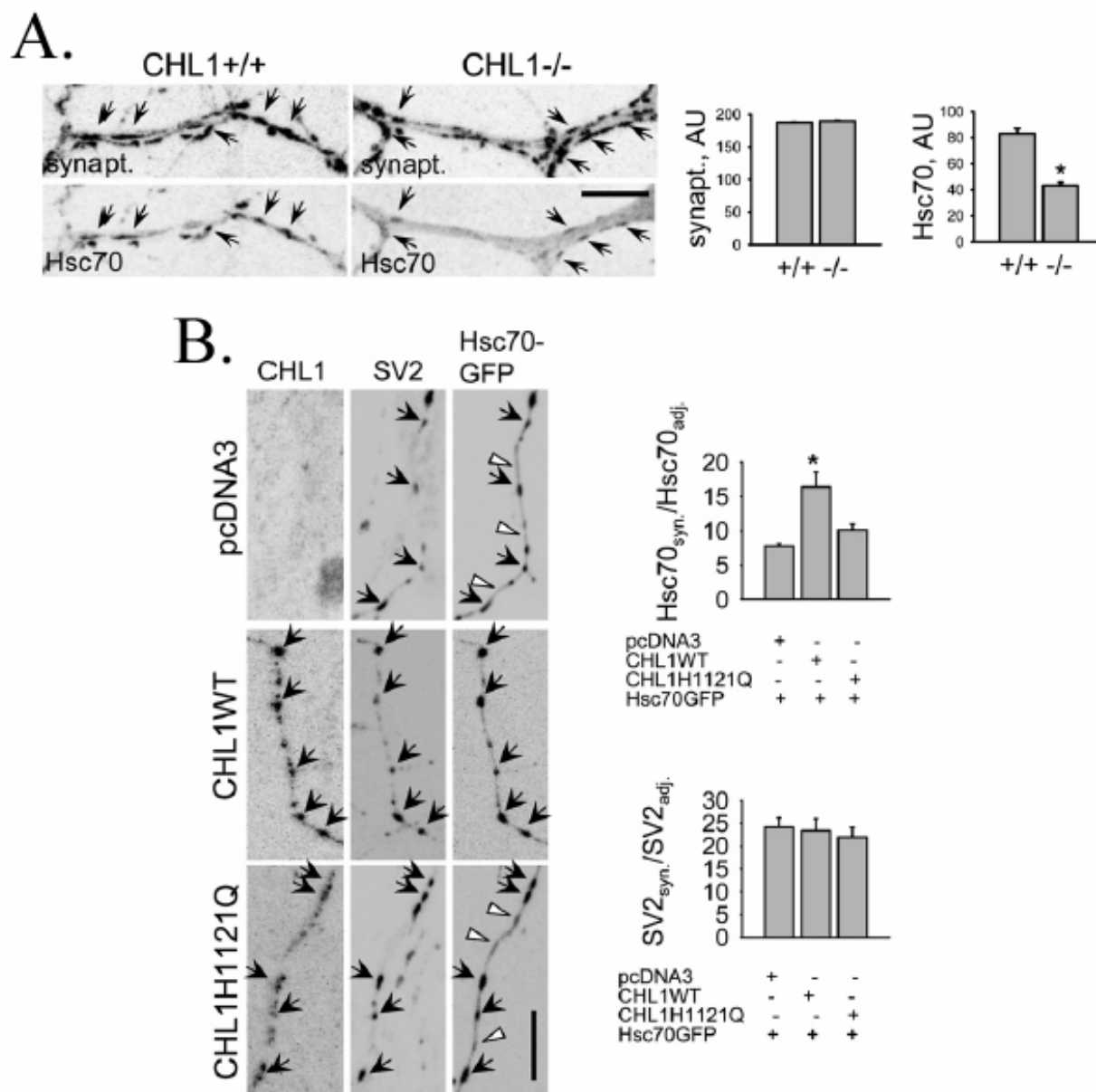


Figure 17. CHL1 recruits Hsc70 to synapses. A. - Neurons from CHL1^{+/+} and CHL1^{-/-} mice were colabelled with antibodies against synaptophysin (synapt.) and Hsc70. Immunofluorescence signals were inverted to accentuate differences in immunolabelling intensities between genotypes. Diagrams show mean intensity \pm SEM of Hsc70 and synaptophysin labelling in synaptophysin clusters. AU, arbitrary units. Levels of Hsc70 are reduced in CHL1^{-/-} versus CHL1^{+/+} synaptic boutons (arrows). Bar = 10 μ m. $n > 200$ synapses from images of 20 neurites from two coverslips analysed in each group. * $p < 0.05$, t test. B. -

CHL1^{-/-} neurons cotransfected with Hsc70GFP and the empty vector (pcDNA3) or vector containing full-length, wild-type CHL1 (CHL1WT) or CHL1H1121Q were colabelled with antibodies against SV2 and surface CHL1. Hsc70GFP, CHL1WT, and CHL1H1121Q accumulate in SV2 positive synaptic boutons (arrows). Inverted immunofluorescence signals are shown. Note increased extrasynaptic levels of Hsc70GFP in CHL1^{-/-} neurons cotransfected with pcDNA3 or CHL1H1121Q (arrowheads). Bar = 10 mm. Diagrams show mean values \pm SEM of the ratio of Hsc70GFP levels in the centre of the SV2 cluster to Hsc70 levels in the adjacent axon 3 mm away from the SV2 cluster centre. Cotransfection with CHL1WT enhances recruitment of Hsc70GFP to SV2 clusters, resulting in higher Hsc70_{syn}/Hsc70_{adj.} values. $n > 100$ synapses from ten neurons from two to three coverslips analysed in each group. Asterisk shows a statistically significant difference when compared with pcDNA3 cotransfected neurons ($p < 0.05$, t test).

It should be admitted that in CHL1^{-/-} and in CHL1^{-/-} neurons transfected with empty pcDNA3 vector or mutated CHL1, Hsc70GFP was still targeted to SV2 positive synaptic boutons. Concentration of Hsc70 in synaptic boutons was still significantly higher comparing to the adjacent axonal values in CHL1^{-/-} neurons. This finding indicates that cues other than CHL1 can recruit Hsc70 to synapses. A promising candidate for another protein that also recruits Hsc70 to synaptic boutons and could partially substitute CHL1 function in CHL1^{-/-} mice is a CSP protein. Interestingly, biochemical experiments shows that levels of CSP, an synaptic vesicle-associated protein that directly binds to Hsc70, were 2-fold higher in CHL1^{-/-} brain homogenates and synaptosomes correlating with increased mRNA levels of CSP in CHL1^{-/-} brains. Thus, Hsc70 may be recruited to CHL1^{-/-} synapses by CSP. However, CSP can not fully compensate CHL1 contribution in the Hsc70 recruiting since transfection with wild-type full-length CHL1 significantly enhanced the precision and degree of Hsc70GFP accumulation in synapses of CHL1^{-/-} neurons.

2.3 CHL1 is endocytosed to synapses in response to synapse activation

As a next step we tried to investigate the mechanisms that target CHL1 to synaptic vesicles. As a transmembrane protein, CHL1 can be delivered to synapses in trans-Golgi network-derived organelles, which are then transformed to synaptic vesicles (Hannah et al., 1999; Sytnyk et al., 2002; Zhai et al., 2001; Ahmari et al., 2000). However, considering the high levels of CHL1 in the presynaptic plasma membrane (Figure 16), a more potent pathway for CHL1 accumulation in synaptic vesicles could be its endocytosis during synaptic vesicle recycling. To test the latter possibility, we analysed the sites of CHL1

endocytosis and recycling in cultured hippocampal neurons by visualizing CHL1-mediated uptake of cell surface bound CHL1 antibodies to intracellular organelles (Carroll et al., 1999). CHL1 antibodies were applied to live cultured neurons in culture medium, and neurons were then allowed to incorporate CHL1 antibodies either at resting conditions in the presence of nominal potassium or in the presence of high potassium concentration buffer applied to stimulate exo- and endocytosis of synaptic vesicles by depolarising neuronal plasma membranes and inducing Ca²⁺ influx (Virmani et al., 2003). Antibodies bound to CHL1 at the cell surface were then removed by exposure to 0.5M NaCl/0.2M acetic acid, a procedure that did not result in abnormal swelling or degeneration of cells (not shown). Following permeabilization of neurons with detergent, internalised CHL1/CHL1 antibody complexes, resistant to acid stripping, were detected with fluorescence-labelled secondary antibodies (Figure 18A); (Carroll et al., 1999). Colabelling with SV2 antibodies showed that the major sites of CHL1 antibody uptake colocalized with SV2 accumulations (Figure 18). CHL1 was endocytosed to synaptic boutons even at resting conditions, probably due to antibody induced cross-linking of CHL1 at the cell surface, followed by internalisation and/or basal synaptic activity in cultures. However, stimulation with high potassium enhanced CHL1 endocytosis to synaptic boutons: levels of CHL1 antibody internalised to SV2 positive synaptic boutons of neurons stimulated by high potassium were approximately two times higher than those of non-stimulated neurons (Figure 18B). CHL1 is likely to be endocytosed with clathrin coated vesicles, thus CHL1 immunoreactive structures often appeared aside the major synaptic vesicle cluster labelled with antibodies against SV2 (Figure 18A), as has been reported before for CCSVs (Bloom et al., 2003). Also biochemical analysis shows CCSV to be positive for CHL1.

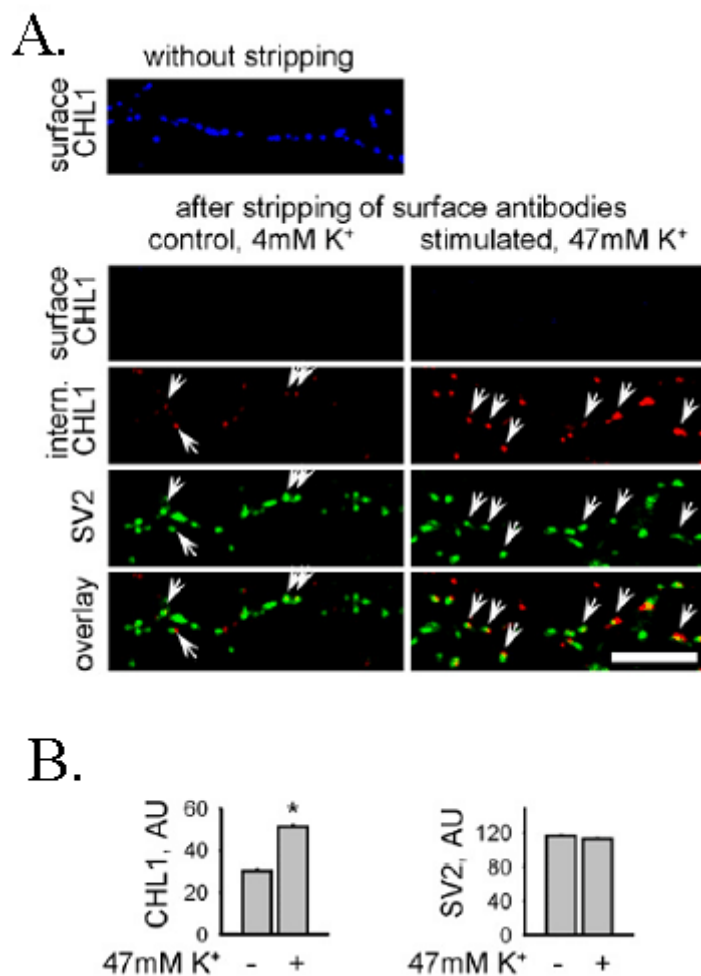


Figure 18. CHL1 is endocytosed to synaptic boutons in an activity-dependent manner.

A. - Live neurons were incubated with antibodies against CHL1 and allowed to internalise the antibodies in the presence of nominal (4 μ M) or high (47 μ M) K⁺. Immunolabelling of surface bound antibodies (surface CHL1) in neurons fixed without stripping shows that the antibodies bound to the surface. Surface bound antibodies were then stripped. The surface bound antibodies are not detectable in neurons after stripping. Accumulations of internalised CHL1 antibodies (intern. CHL1) overlap with SV2 positive synaptic boutons.

B. - Diagrams show mean intensity \pm SEM of SV2 labelling and endocytosed CHL1 labelling in SV2 clusters. AU, arbitrary units. Levels of internalised CHL1, but not of endogenous SV2, in SV2 positive synaptic boutons are higher after high K⁺ stimulation, indicating that SV recycling induced by high K⁺ enhances CHL1 endocytosis in synapses. Bar = 10 μ m. n > 1600 synapses from 20 neurons from two coverslips analysed in each group. *p < 0.05, t test.

2.4 Number of clathrin-coated vesicles is increased in synaptic terminals of CHL1 -/- mice

In neurons and non-neuronal cells, Hsc70 is the major ATPase mediating clathrin uncoating from clathrin coated vesicles (Newmyer and Schmid, 2001). In synapses, Hsc70 uncoats clathrin from synaptic vesicles, which are recycling via a clathrin-dependent pathway (Zinsmaier and Bronk, 2001; Morgan et al., 2001). Biochemical experiments performed in our laboratory demonstrated that protein and mRNA levels of clathrin were higher in CHL1-/- brain homogenates and levels of clathrin protein were increased in CHL1-/- synaptosomes and purified synaptic vesicles. Also the uncoating of clathrin coated vesicles purified from CHL1-/- brain homogenates was drastically inhibited in *in vitro* biochemical assay. All these facts indicated that CHL1, probably via Hsc70 recruitment, is involved in the regulation of uncoating of clathrin-coated vesicles. We therefore investigated by means of electron microscopy whether abnormalities in subcellular distribution of Hsc70 in CHL1-/- neurons may affect synaptic ultrastructure and, in particular, number of clathrin-coated and synaptic vesicles in the presynaptic terminals of CHL1-/- neurons. The organisation of the CA1 stratum radiatum in hippocampus analysed by electron microscopy showed no gross abnormalities in CHL1-/- mice when compared with wild type mice. We did not observe any difference between CHL1+/+ and CHL1-/- mice in the number of excitatory synapses in the CA1 stratum radiatum. The number of synaptic vesicles in synaptic terminals was also similar in both genotypes. However, the number of clathrin coated vesicles was slightly increased by 7% in synaptic terminals in CHL1-/- mice when compared to wild type littermates (Fig. 19). The difference became more evident when the number of CCSV was normalized to the number of synaptic vesicles present in the terminal. A similar tendency of increased numbers of clathrin-coated vesicles could be seen in presynaptic boutons of CHL1-/- versus CHL1+/+ hippocampal neurons maintained in cultures.

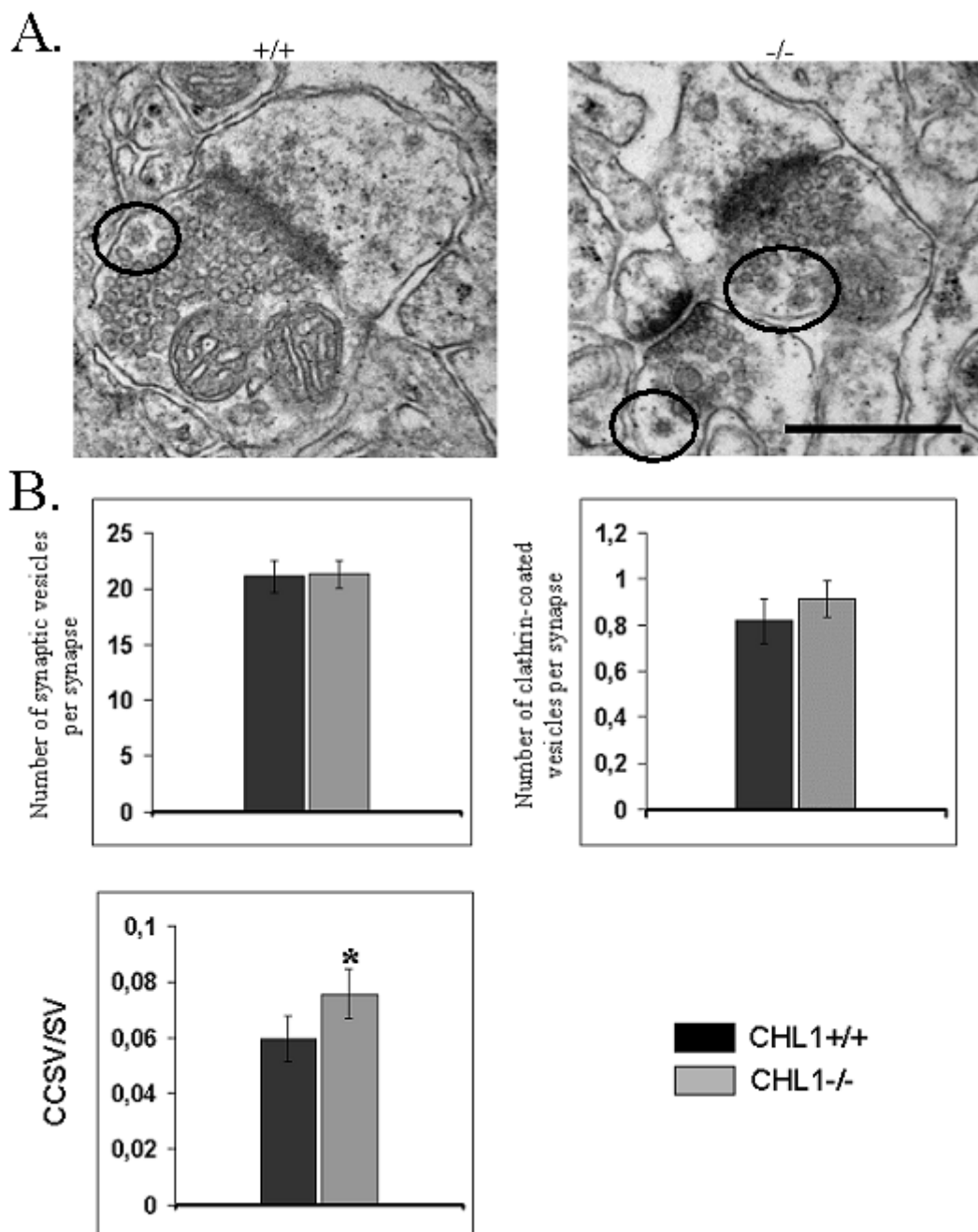


Figure 19. Numbers of clathrin-coated vesicles (CCSV) are slightly increased in presynaptic boutons in synapses of CHL1^{-/-} brains. A. Electron micrographs illustrating examples of hippocampal excitatory synapses in the CA1 stratum radiatum of CHL1^{+/+} and CHL1^{-/-} mice. Black circles mark clathrin-coated vesicles. Scale bar 0,5 μ m. B. Diagrams show average numbers of synaptic vesicles, clathrin-coated vesicles and ratios of clathrin-coated vesicles to synaptic vesicles in synaptic boutons of CHL1^{+/+} and CHL1^{-/-} synapses. $n > 200$ synapses from 4 brains were analysed in each group. * $p < 0.05$, t test.

2.5 Activity-induced formation of CCSVs is reduced in CHL1^{-/-} neurons.

In order to investigate whether abnormalities in clathrin release in CHL1^{-/-} neurons affect formation of CCSVs in an activity-dependent manner, we analysed ultrastructure of synapses in non-treated versus stimulated with high (47 mM) potassium concentration containing solution CHL1^{+/+} and CHL1^{-/-} neurons by means of electron microscopy. To analyse dynamics of clathrin-coated vesicle formation in CHL1^{+/+} and CHL1^{-/-} neurons under conditions stimulating synaptic vesicle exo- and endocytosis we have set six groups of each genotype: control cultures in Tyrode buffer with nominal 4 mM potassium concentration; cultures stimulated with high potassium concentration for 10 seconds; 30 seconds; 90 seconds; 90 seconds of stimulation + 1 minute of recovery in Tyrode buffer containing nominal concentration of potassium; and 90 seconds stimulation followed by 5 minutes of recovery in Tyrode buffer with nominal potassium concentration.

The number of CCSVs was increased in presynaptic boutons of morphologically identified synapses of non-stimulated CHL1^{-/-} versus CHL1^{+/+} neurons (Fig. 20), indicating that uncoating of CCSVs formed under conditions of normal spontaneous neuronal activity in culture was inhibited CHL1^{-/-} synapses.

Already 10 s after application of high potassium containing buffer (the earliest time tested), the number of CCSVs increased in CHL1^{+/+} boutons, reached a peak at 30 s after high application, and slightly declined by 90 s at the end of stimulation. Five minutes after exchanging the high potassium buffer to the nominal potassium buffer, the number of CCSVs in CHL1^{+/+} boutons declined to the level observed in non-stimulated neurons. In contrast, the number of CCSVs in CHL1^{-/-} boutons only slightly increased in response to high potassium buffer and remained at this level until the end of stimulation, suggesting that inhibition of uncoating of CCSVs in CHL1^{-/-} boutons hampered activity-induced formation of new CCSVs. This effect was particularly evident when activity-induced changes in the numbers of CCSVs normalised to the control values of CCSVs were compared: in CHL1^{+/+} boutons, the number of CCSVs increased by a factor of 2.6 in response to high potassium, whereas in CHL1^{-/-} neurons, the number of CCSVs increased by only a factor of 1.6 (Fig. 20). Inhibited formation of CCSVs was not related to a defect in synaptic vesicle exocytosis, since a reduction in the total number of SVs in response to high potassium (indicative of SVs that had fused with the plasma membrane) was similar in CHL1^{+/+} and CHL1^{-/-} synapses (Fig.20). Similarly, exocytosis was normal in CHL1^{-/-} synapses as measured by electrophysiological recordings (Nikonenko et al., 2006). Other

parameters with impact on the efficacy of neurotransmission, such as number of mitochondria, lengths of active zones in CHL1^{-/-} synapses, and number of perforated synapses in CHL1^{-/-} neurons were also normal (Fig. 21).

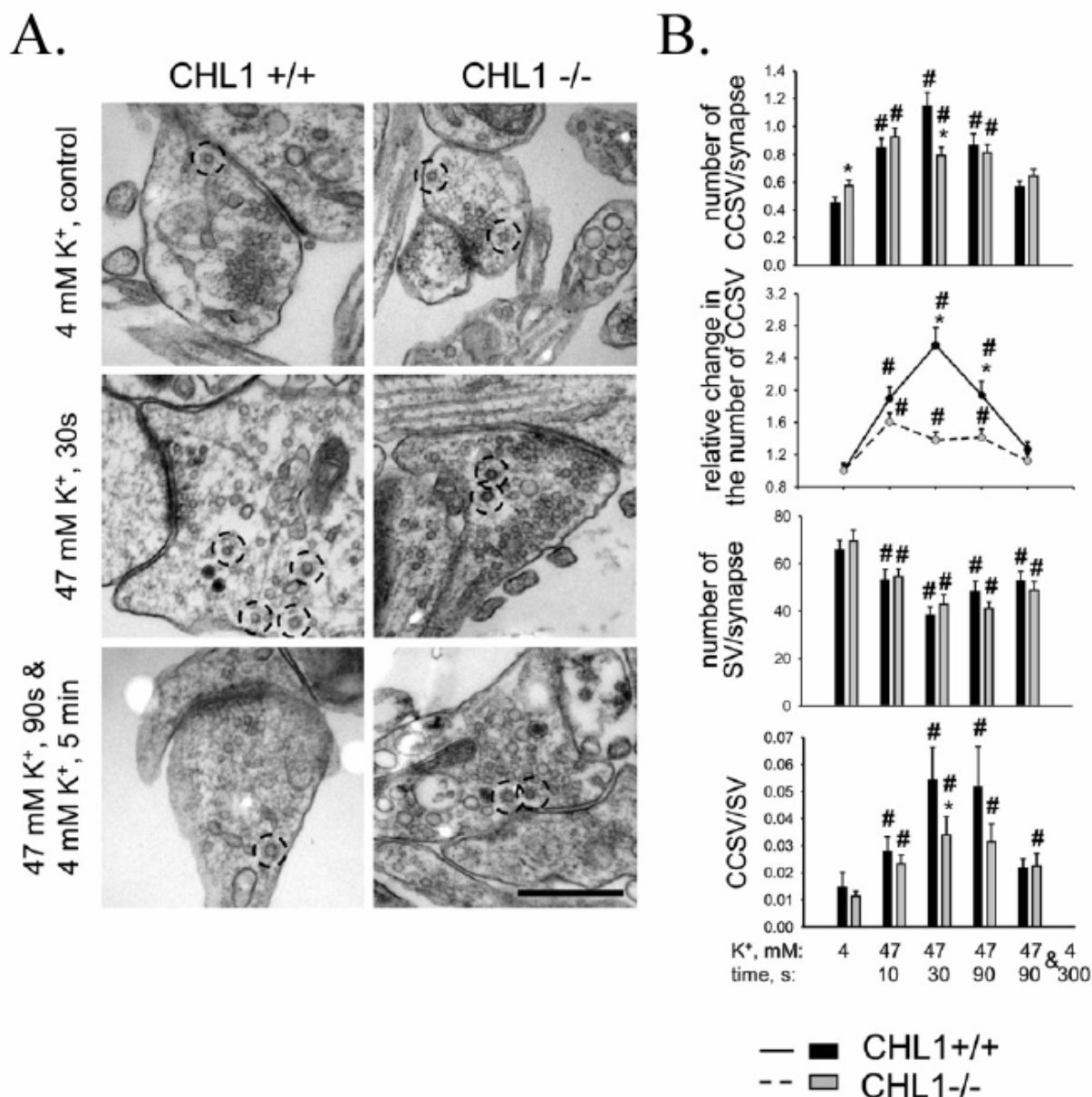


Figure 20. Activity-induced formation of clathrin-coated synaptic vesicles is inhibited in CHL1^{-/-} synapses. CHL1^{+/+} and CHL1^{-/-} neurons were incubated in modified Tyrode solution containing 4 mM K⁺ (control) or 47 mM K⁺ for the indicated time intervals or allowed to recover for 5 min at 4 mM K⁺ before fixation. Neurons were fixed for electron microscopy. (A) - representative electron micrographs of synapses from cultured CHL1^{+/+} and CHL1^{-/-} neurons for conditions indicated on images are shown. CCSVs are marked with dashed circles. Bar = 0.5 μ m. (B) - diagrams show numbers of CCSVs per synaptic bouton profile, changes in the number of CCSVs with respect to control neurons, total number of SVs, and the ratio of CCSV number to total SV number. Mean numbers \pm SEM are shown. Note increased

numbers of CCSVs in control and reduced increase in numbers of CCSVs in response to high K⁺ in CHL1^{-/-} neurons. $n > 200$ synapses from at least four coverslips were analysed in each group. Symbol (*) indicates statistically significant differences ($p < 0.05$, t test) between CHL1^{-/-} and CHL1^{+/+} neurons and (#) shows statistically significant difference ($p < 0.05$, t test) when neurons of a particular genotype are compared with the control group of neurons of this genotype.

The relatively mild phenotype of CHL1^{-/-} synapses at resting conditions could be explained by compensatory mechanisms. In particular, while mRNA and protein levels of Hsp70, an inducible counterpart of Hsc70, were slightly decreased in CHL1^{-/-} brain homogenates, Hsp70 protein levels were increased by approximately 60% in CHL1^{-/-} synaptosomes and synaptic vesicles (Leschyns'ka et al., 2006), suggesting that Hsp70 is recruited to CHL1^{-/-} synapses instead of Hsc70, thus at least partially substituting for Hsc70—a phenomenon observed in an Hsc70-4 *Drosophila* mutant (Bronk et al., 2001).

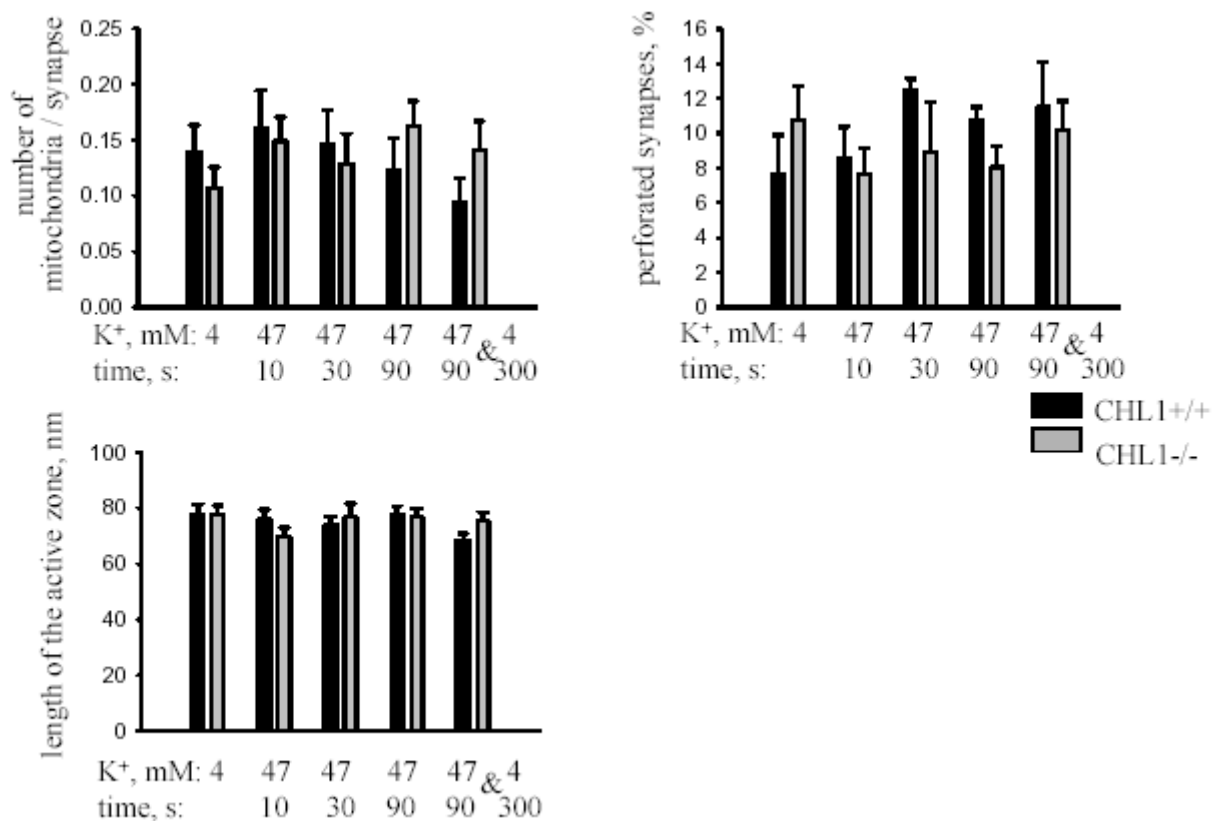


Figure 21. Percentage of perforated synapses in CHL1^{-/-} neurons and numbers of mitochondria and lengths of active zones in CHL1^{-/-} synapses are not changed. Graphs show mean percentage \pm SEM of perforated synapses in CHL1^{+/+} and CHL1^{-/-} cultures and mean number \pm

SEM of mitochondria and mean length \pm SEM of the active zones in synapses of CHL1^{+/+} and CHL1^{-/-} neurons. N>100 synapses from at least 4 coverslips were analyzed in each group. *p<0.05, t-test.

2.6 Activity-induced formation of CCSVs is reduced in CHL1^{+/+} neurons after acute CHL1/Hsc70 complex disruption

To analyse the consequences of an acute CHL1/Hsc70 complex disruption, we introduced a peptide derived from the intracellular domain of CHL1 containing an HPD tripeptide (HPDpeptideCHL1) into live neurons, thus interfering with Hsc70 binding to CHL1 in a dominant-negative fashion (Leschyns'ka et al., 2006). An acute CHL1/Hsc70 complex disruption by introduction of HPDpeptideCHL1 was intended to overcome compensatory reactions of neurons with ablated CHL1. Loading neurons with HPDpeptideCHL1, but not with QPDpeptideCHL1, or mock treatment of neurons with the peptide delivering reagent resulted in a 2-fold increase in the number of CCSVs at resting conditions and a profound reduction of CCSV formation in response to high potassium (Fig. 22). Furthermore, in neurons loaded with HPDpeptideCHL1, the total number of synaptic vesicles was reduced at resting conditions. This finding probably reflects an inhibition of synaptic vesicle regeneration due to the inhibition of CCSV uncoating. The total number of synaptic vesicles in HPDpeptideCHL1-loaded synapses decreased in response to high potassium, indicating that synaptic vesicles exocytosis was not blocked. However, the amplitude of this decrease was smaller in HPDpeptideCHL1-loaded synapses when compared with mock- or QPDpeptideCHL1- treated neurons again suggesting that the number of synaptic vesicle ready for exocytosis is decreased due to the inhibition of synaptic vesicle regeneration.

Western blot analysis of lysates of the peptide-treated cultures showed that the total levels of CSP and Hsp70 were not changed in HPDpeptideCHL1-loaded neurons, indicating that compensatory mechanisms were not active at the time the cultures were analysed (Leschyns'ka et al., 2006).

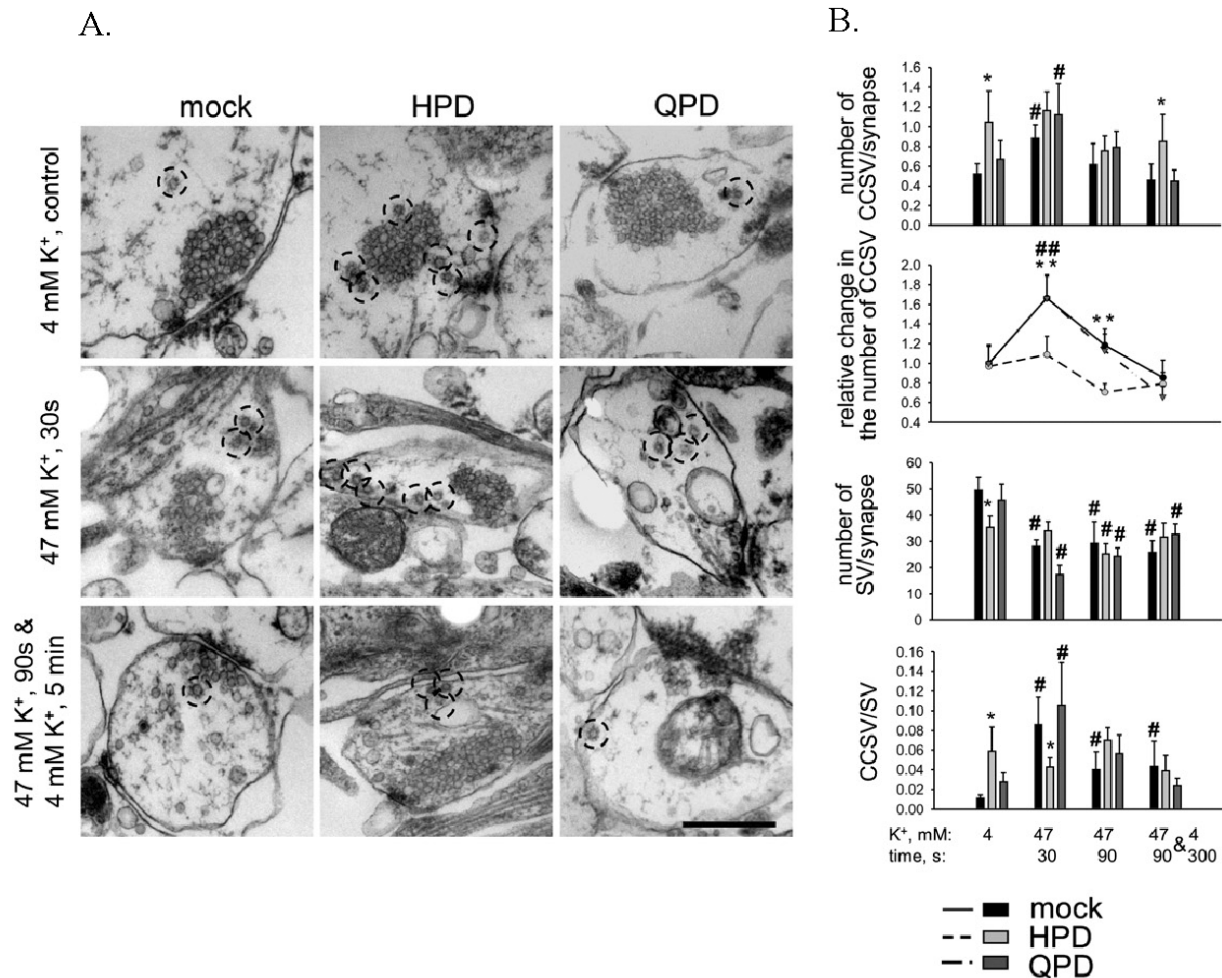


Figure 22. Activity-induced formation of clathrin-coated synaptic vesicles is inhibited in CHL1^{+/+} synapses in which the CHL1/Hsc70 Complex was disrupted. CHL1^{+/+} neurons loaded with HPDpeptideCHL1 (HPD) or QPDpeptideCHL1 (QPD), or mock treated with the peptide delivering reagent, were incubated in modified Tyrode solution containing 4 mM K⁺ (control) or 47 mM K⁺ for the indicated time intervals or allowed to recover for 5 min at 4 mM K⁺ before fixation. Neurons were fixed for electron microscopy. (A) - representative electron micrographs of synapses for conditions indicated are shown. CCSVs are marked with dashed circles. Bar = 0.5 μ m. (B) Diagrams show numbers of CCSVs per synaptic bouton profile, changes in the number of CCSVs with respect to control neurons, total number of SVs, and the ratio of CCSV number to total SV number. Mean numbers \pm SEM are shown. Note increased numbers of CCSVs in control and reduced increase in numbers of CCSVs in response to high K⁺ in HPDpeptideCHL1-loaded CHL1^{+/+} neurons. $n > 200$ synapses from at least four coverslips analysed in each group. Symbol (*) indicates statistically significant differences ($p < 0.05$, t test) between HPDpeptideCHL1- and mock-loaded neurons and (#) shows statistically significant difference ($p < 0.05$, t test) when neurons loaded with a particular peptide are compared with the control group loaded with this peptide.

2.7 Disruption of the CHL1/Hsc70 complex inhibits activity-induced recruitment of clathrin and Hsc70 into synaptic terminals

To answer the question whether the activity-dependent changes in the numbers of CCSVs correlated with the changes in the levels of Hsc70 and clathrin at synapses we decided to analyze the dynamics of clathrin and Hsc70 protein content at synapses following synaptic stimulation in neurons with intact CHL1/Hsc70 interaction and neurons in which CHL1/Hsc70 complex was disrupted by HPDpeptideCHL1. Neurons from CHL1^{+/+} hippocampal cultures loaded with HPDpeptideCHL1 were compared with QPDpeptideCHL1 loaded neurons or neurons treated with the peptide delivering reagent alone (mock-treatment). Control neurons from three groups were incubated in the modified Tyrode solution containing nominal potassium concentrations. Similar to the previous experiments, stimulation of neurons was carried out either by application of solution with high potassium concentration for 30 seconds followed by fixation or for 90 seconds followed by recovery for 5 min at nominal potassium concentration before fixation. Fixed neurons were colabelled with antibodies against synaptophysin, Hsc70, and clathrin. Immunofluorescence levels of Hsc70 and clathrin were measured in synaptophysin accumulations. Indeed, changes in the levels of Hsc70 and clathrin in synaptophysin accumulations in neurons treated with high potassium correlated with the changes in the numbers of CCSVs (Figure 22). In mock- or QPDpeptideCHL1-loaded neurons, synaptic levels of Hsc70 and clathrin increased 30 s after application of high potassium buffer and returned to initial levels after recovery for 5 min in buffer with nominal potassium concentration (Fig. 23). This activity driven increase in the Hsc70 and clathrin levels was strongly inhibited in HPDpeptideCHL1 loaded neurons. In non-stimulated neurons loaded with HPDpeptideCHL1, levels of clathrin were slightly increased, whereas levels of Hsc70 were decreased in synaptophysin clusters (Fig. 23). This also correlates with the electron microscopical observations indicating an increase in the number of clathrin coated vesicles at synapses of HPDpeptideCHL1 loaded neurons.

Decreased levels of Hsc70 at synapses in neurons loaded with HPDpeptideCHL1 and a prominent increase in the amount of Hsc70 at synapses following stimulation in control neurons not loaded with HPDpeptideCHL1 indicates that CHL1 recruits Hsc70 to synaptic boutons not only at resting conditions, but even more efficiently after activation, allowing neurons to immediately react to dynamic changes in clathrin levels at the synapse in response to synaptic activity.

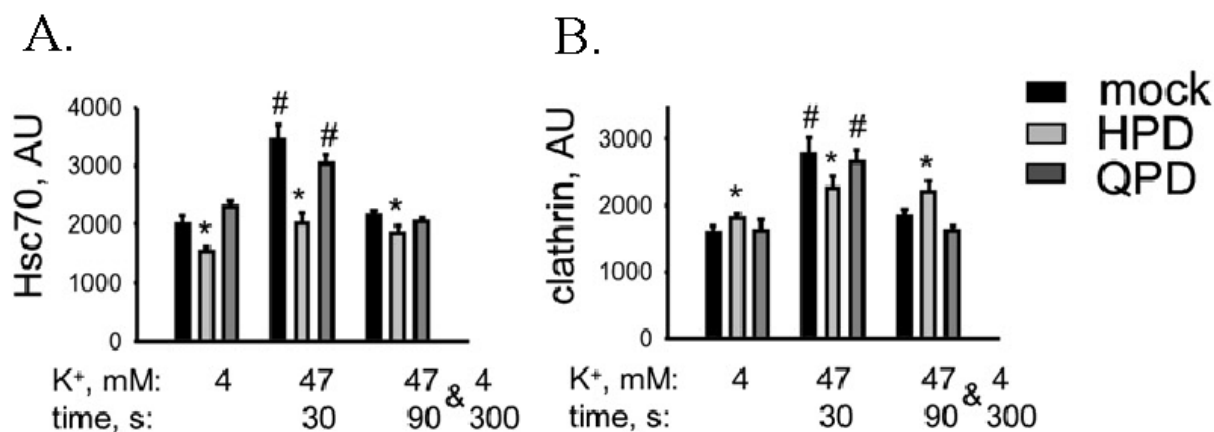


Figure 23. Disruption of CHL1/Hsc70 complex inhibits activity-induced clathrin and Hsc70 accumulation at synapses. CHL1^{+/+} neurons loaded with HPDpeptideCHL1 (HPD) or QPDpeptideCHL1 (QPD), or mocktreated with the peptide delivering reagent, were incubated in modified Tyrode solution containing 4 mM K⁺ (control) or 47 mM K⁺ for the indicated time intervals or allowed to recover for 5 min at 4 mM K⁺ before fixation. Neurons were fixed for immunofluorescence analysis. Neurons were colabelled with antibodies against synaptophysin, Hsc70, and clathrin. Levels of Hsc70 (A) and clathrin (B) were measured in synaptophysin accumulations. Mean numbers \pm SEM are shown. Note slightly increased levels of clathrin and reduced levels of Hsc70 in HPDpeptideCHL1-loaded neurons at resting conditions, and reduced increase of synaptic Hsc70 and clathrin levels in these neurons in response to high K⁺. $n > 5000$ synapses from 30 neurons from three coverslips were analysed in each group. Symbol (*) indicates statistically significant differences ($p < 0.05$, t test) between HPDpeptideCHL1- and mock-loaded neurons and (#) shows statistically significant difference ($p < 0.05$, t test) when neurons loaded with a particular peptide are compared with the control group loaded with this peptide.

V. DISCUSSION

Project 1. The role of NCAM in maintaining of the cytoskeleton-dependent structural integrity of post-synaptic densities and regulation of the AMPA receptor recycling

1.1 The role of NCAM/spectrin organised cytoskeleton in the regulation of PSD structure and postsynaptic endocytosis.

Cell adhesion molecules, and NCAM in particular, promote stabilization of axo-dendritic contacts (Sytnyk et al., 2002), followed by synapse and PSD formation (Dityatev et al., 2004; Sytnyk et al., 2006). We now show that NCAM is also required for the maintenance of the ultrastructural integrity of PSDs in synapses. We found that dissociation of NCAM/spectrin complex by NCAM ablation, application of β I-2,3 spectrin peptide, transfection with β I-spectrin siRNA, pharmacologically-induced dissociation of spectrin-actin organized cytoskeleton increases the number of synapses with PSDs of complex shape, which are previously reported to be partially or completely segmented. Several mechanisms for PSD perforation have been proposed, including PSD perforation by plasma membrane expansion through exocytosis or perforation by actin polymerisation. These, however, could not be verified in the present study. Instead, our data suggest a model according to which perforation of the PSD occurs via local disassembly of the NCAM associated spectrin meshwork, an event required and sufficient for PSD perforation (Fig. 9). To maintain PSD integrity, NCAM associates with and assembles the spectrin meshwork, which interacts with the intracellular domains of NCAM140 and NCAM180 (Leshchyn'ska et al., 2003). Interestingly, an increase of NCAM-mediated adhesion by removal of polysialic acid, a highly negatively charged carbohydrate carried by NCAM, reduced the percentage of synapses with perforated PSDs formed in response to long term potentiation, indicating that enhanced NCAM-dependent adhesion in the synaptic cleft stabilizes synapses and prevents perforation of PSDs (Dityatev et al., 2004).

While the functions of PSD perforations are not known, several intriguing possibilities for their role in synapses may be derived from the known functions of the spectrin meshwork. The spectrin meshwork beneath the plasma membrane prevents fusion of transport vesicles with the membrane (Portis et al., 1979; Sato et al., 1995). Sites of PSD perforations will thus facilitate delivery of integral membrane proteins, such as ligand-

gated neurotransmitter receptors or ion channels, to PSDs that could account for the observed increase in levels of these proteins in perforated synapses (Luscher et al., 2000). Since endocytosis of cell surface proteins also requires disassembly of the spectrin meshwork (Kamal et al., 1998), PSD perforations may serve as sites of intense local membrane recycling. Indeed, budding clathrin coated vesicles have often been observed at sites of PSD perforations (Toni et al., 2001; Fig. 12).

PSDs are remarkably stable structures that may impede membrane turnover in the postsynaptic membrane. In accordance with this idea, the spectrin meshwork inhibits endocytosis of cell surface proteins in fibroblasts (Kamal et al., 1998). We show that knock-down of β I spectrin expression by siRNA or abnormally low β I spectrin accumulation in PSDs of NCAM^{-/-} neurons are accompanied by increased numbers of clathrin-coated vesicles in the vicinity of PSDs and higher AMPA receptor internalisation rates suggesting that PSD perforations open additional endocytic zones for AMPARs within PSDs. In accordance with this hypothesis, we observed that GluR1 containing AMPARs enter PSD perforations and are found in endocytic zones formed at perforation sites. Additionally, partial digestion of the spectrin meshwork may release spectrin and actin monomers into the cytoplasm providing new sites of actin nucleation to form actin filaments that are required for endocytosis and endosomal transport. In extreme cases actin filaments may penetrate the “weakened” site of perforation to form a spinule. Since calpains are activated by Ca^{2+} influx in response to synapse activation (Faddis et al., 1997; del Cerro et al., 1994), remodelling of the calpain-depolymerised spectrin meshwork will be increased in activated synapses correlating with an increased number of perforations. Extracellular proteolysis of NCAM observed after long-term potentiation of synapses and kainic acid induced seizures (Hoffman et al., 1998) may also contribute to PSD perforations in activated synapses by weakening extracellular adhesive forces. PSD perforations may thus reflect PSD restructuring mechanism required for the efficient turnover of the postsynaptic machinery. Active turnover will be especially relevant for large PSDs that form following LTP induction and may impose a significant diffusion barrier for PSD components and it is noteworthy that largest PSDs usually accommodate perforations. Enhanced exocytosis of postsynaptic components immediately after LTP induction (Park et al., 2006) in these synapses could be compensated by increased endocytosis of postsynaptic components via PSD perforations that form at later stages to restore balance of postsynaptic machinery.

Our data also show that synapse activation is not the only way to induce PSD perforation. Abnormalities in adhesion and/or cytoskeleton organization may also result in perforation of PSDs in the absence of synapse activation and Ca^{2+} influx. An important conclusion from our observations is that whereas activation of synapses likely leads to perforations, it may be precocious to consider perforation of PSDs as a marker of synaptic activity since abnormal expression of or mutations in NCAM and spectrin molecules have been observed in brain pathologies including schizophrenia, bipolar disorder, epilepsy and ischemia (Vawter, 2000; Sato et al., 2001, 2003; Ringger et al., 2004; Najm et al., 1992; Kitamura et al., 1998), correlating with an increased percentage of perforated synapses (Jourdain et al., 2002; Leite et al., 2005). Whether an abnormally high rate of PSD perforations that result in increased membrane endocytosis in synapses contributes to brain pathology is an intriguing issue to pursue.

1.2 The model of PSD perforation formation and its role in synaptic function.

An increase in the size of activated spines occurs during the first 20 min following LTP induction (Toni et al., 2001, Park et al., 2006) whereas PSD perforation formation is a subsequent event that becomes evident at 30 minutes or later following stimulation (Toni et al., 2001; Stewart et al., 2005; Geinisman et al., 2002; Fig. 14). That is why it is not likely that PSD perforation formation is directly associated with the transport vesicle exocytosis and thus with spine membrane extension underlying spine growth as suggested by Spacek and Harris (2004). An initial increase in the size of activated spines correlates with the accumulation of AMPA receptors at spines (Park et al., 2004) that are responsible for the expression of initial phases of LTP (Malinow and Malenka 2002). Further development of LTP requires activation of additional mechanisms including new synapse formation and protein expression in activated spines (Toni et al., 2001; Ostroff et al., 2002). Interestingly, an increase in the number of perforated synapses is a transient event and the number of returns to the basal level at 1 up to 2 hours following LTP stimulation in brain slices (Toni et al., 2001; Harris et al., 1992). Taking in the consideration transient nature of PSD perforations following LTP induction it is likely that initially activated spines with perforated PSDs are converted back into non-perforated state. PSD perforations are often seen to be associated with clathrin coated pits and vesicles (Toni et al., 2001; own observations – Fig. 12) that provide an evidence of intensive membrane and

protein endocytosis at perforated synapses. We show that AMPA receptors could be internalised at sites of PSD perforations. We also show that the reduction of spectrin accumulation at PSDs either by spectrin siRNA or by inhibition of NCAM-dependent spectrin recruitment can induce PSD perforation formation. We suggest that partial spectrin-cytoskeleton dissociation can lead to the segmentation of postsynaptic densities facilitating the release and endocytosis of proteins bound to the PSD. This process could be important for regulation of the membrane and protein amount at the activated spine, removal of proteins that were involved in the initialisation of the LTP but not required for the late expression of LTP at activated synapses.

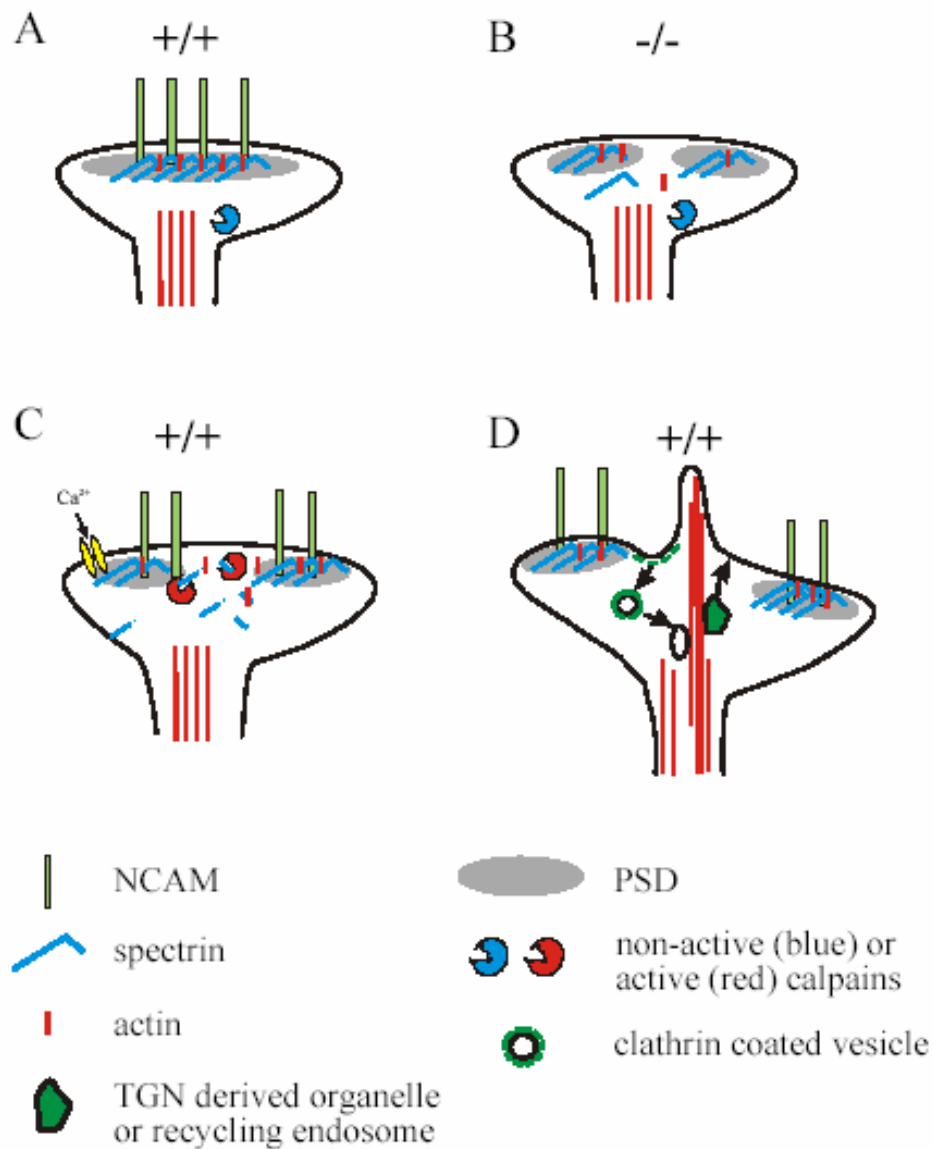


Figure 24. A proposed model of formation of perforated post-synaptic densities and their functional role in local membrane recycling at the synapse. (A) – In wild type (NCAM+/+) synapses, the NCAM-assembled spectrin cytoskeleton maintains structural integrity of the post-synaptic density (PSD). (B) – Local instability of the spectrin meshwork in synapses of NCAM-deficient (NCAM-/-) mice results in PSD perforation. (C) – In NCAM+/+ synapses, activation of calpains also results in local disassembly of the spectrin meshwork and PSD perforation. (D) – Disassembled by calpains spectrin meshwork releases actin monomers providing sites for actin nucleation and formation of actin filaments that form a spinule. Disassembly of the spectrin meshwork also facilitates vesicle endo- and exocytosis at the site of perforation.

Project 2. The role of the cell adhesion molecule close homologue of L1 (CHL1) in regulation of clathrin-dependent synaptic vesicle recycling

In the present study we were able to show the role of CHL1 in the regulation of uncoating of CCSVs in synaptic terminals and the effect of CHL1/Hsc70 complex disruption on activity-induced formation of CCSVs. This study was a part of a larger project on CHL1 and Hsc70 interaction performed in the collaboration with other members from our laboratory implying different morphological, cell biological and biochemical techniques. Results obtained in current study were published along with observation obtained by other colleagues in article by Leschyn'ska and colleagues (2006). In this discussion I summarise our observations with other data obtained on the interaction of CHL1 with Hsc70 in order to describe a model of CHL1 involvement in clathrin uncoating and synaptic vesicle recycling.

2.1 Role of CHL1 in the regulation of clathrin uncoating from synaptic vesicles.

Our observation that CHL1 immunofluorescence concentrated in axons (Fig.15) where CHL1 was colocalized with Hsc70 supports the finding that Hsc70 cofractionate with CHL1 in the synaptic membrane fraction indicating that Hsc70 may form a complex with CHL1 directly in the plasma membrane even before CHL1 internalisation into synaptic vesicles. Biochemical experiments show that CHL1-mediated recruitment of Hsc70 is significantly enhanced in the presence of ADP, whereas CHL1/Hsc70 complex is

dissociated by ATP. ATP-depleting, and thus ADP-producing, reactions accompany fusion of synaptic vesicles (Sollner et al., 1993) and initiation of clathrin coat assembly (Schmid and Smythe, 1991) and should result in a local increase in ADP concentration beneath the plasma membrane of synaptic terminal. It is thus tempting to speculate that this increase in ADP concentration promotes activity-dependent CHL1/Hsc70 complex formation as observed in isolated synaptosomes, thereby inducing an initial CHL1-dependent recruitment of Hsc70 to the synaptic plasma membrane similarly to another Hsc70 binding partner auxilin that is also initially recruited to the growing clathrin cages and budding vesicles at the cell surface (Massol et al., 2006). Following ATP-independent invagination of clathrin-coated pits (Mahaffey et al., 1989; Smythe et al., 1989) and ATP/GTP-dependent budding of the vesicles (Carter et al., 1993; Schmid and Smythe, 1991), CCSVs are translocated to the synapse interior away from the ATP-depleted area beneath the plasma membrane. This should result in an increase in ATP concentration that would dissociate the CHL1/Hsc70 complex and promote binding of Hsc70 to auxilin, accompanied by ATP-dependent clathrin release.

This scenario would suggest that CHL1 is endocytosed to synaptic vesicles. Indeed, endocytosis of CHL1 into synaptic vesicles has been proven by the presence of CHL1 in a highly purified fraction of synaptic vesicles and by our experiment that illustrates internalisation of CHL1 antibodies in response to synapse activation (Fig.18). The recycling pool of synaptic vesicles in hippocampal synapses comprises only 10%–20% of all synaptic vesicles at synaptic terminal, with an even smaller fraction of synaptic vesicles recycling via the clathrin-dependent pathway (Rizzoli and Betz, 2005; Harata et al., 2001). Thus, only a subpopulation of synaptic vesicles should contain CHL1, which is targeted to recycling synaptic vesicles from the axonal plasma membrane by endocytosis. The intracellular domain of CHL1 contains binding motif for the adaptor protein AP2 that could recruit CHL1 to the budding CCSVs. This adaptor protein, which is enriched in the presynaptic membrane (Yao et al., 2002), coordinates clathrin coat assembly and recruitment of the cargo proteins to the budding clathrin coated vesicles (Schmid, 1997). Indeed presence of CHL1 in CCSVs could be shown in purified CCSV fraction. Biochemical studies also show that ADP promotes not only CHL1/Hsc70, but also CHL1/clathrin, complex formation, indicating that ATP-consuming, and thus ADP-producing, fusion of synaptic vesicles may promote redistribution of the CHL1/Hsc70 complex to clathrin-coated pits and budding vesicles. The CHL1/clathrin complex

dissociates in the presence of ATP, indicating that an increase in ATP concentration in the vicinity of the CHL1-containing CCSVs should induce not only dissociation of Hsc70, but also of clathrin, from CHL1, thus further promoting clathrin release from the vesicle.

We show that levels of Hsc70 recruited to synaptic terminal are strongly reduced in CHL1^{-/-} mice (Fig.17). Levels of Hsc70 associated with the fraction of synaptic vesicles are also strongly reduced in CHL1^{-/-} mice, indicating that CHL1 not only recruits Hsc70 to synaptic plasma membrane, but also maintains high levels of Hsc70 associated with synaptic vesicles. However Hsc70 is still targeted to the synaptic vesicles, though less efficiently. Interestingly, levels of CSP, another synaptic vesicle associated protein that directly binds to Hsc70, were 2-fold higher in CHL1^{-/-} brain homogenates and synaptosomes correlating with increased mRNA levels of CSP in CHL1^{-/-} brains. This compensatory up-regulation of CSP concentration could indicate that CSP can partially substitute for CHL1 and provide a targeting cue for Hsc70 in CHL1^{-/-} vesicles. Although levels of Hsc70 associated with synaptic vesicles were not found to be abnormal in CSP-deficient mice (Tobaben et al., 2001), compensatory binding of Hsc70 to CSP in absence of CHL1 may explain rather mild phenotype of CHL1^{-/-} mice and residual targeting of endogenous or over-expressed Hsc70 to synapses in the absence of CHL1.

2.2 Effects of disregulated clathrin uncoating on synaptic vesicle recycling and overall synapse function in CHL1^{-/-} synapses.

Despite compensatory mechanisms, decreased efficiency of clathrin uncoating in CHL1^{-/-} synapses can inhibit synaptic vesicle recycling. Indeed, analysis of FM dye uptake in CHL1^{-/-} synapses illustrates reduced uptake and release rates of FM dyes suggesting that synaptic vesicle recycling is slowed down in CHL1^{-/-} mice. This observation supports our finding that, while CHL1^{-/-} synaptic boutons accumulate abnormally high numbers of CCSVs under conditions of spontaneous activity in cultured hippocampal neurons, formation of new CCSVs in CHL1^{-/-} synaptic boutons in response to a new stimulus, such as high K⁺ application, is inhibited. It is likely that reduced rates of clathrin coat release from CCSVs results in slower processing of synaptic vesicles via the recycling pathway. Slowed recycling rates may reflect the lack of availability of essential coat proteins to form new CCSVs in an activity-dependent manner: clathrin, AP180, and

AP2 could be trapped in CCSVs formed during previous cycles of neuronal activity, and would thus be unavailable to form new CCSVs.

Besides regulating uncoating of CCSVs, Hsc70 also plays a role in synaptic vesicle exocytosis in cooperation with CSP (Bronk et al., 2001). Normal synaptic vesicle exocytosis in CHL1^{-/-} mice may be related to increased levels of CSP and Hsp70, which may partially compensate for abnormal Hsc70 function. It is interesting in this respect that when the CHL1/Hsc70 complex is acutely disrupted in neurons by an interfering peptide, a smaller reduction in the number of synaptic vesicles in response to high potassium is observed, suggesting that fewer synaptic vesicles fuse with the plasma membrane. However this decrease of synaptic vesicle fusion could also reflect a decrease in the number of vesicles ready for exocytosis due to inhibited synaptic vesicle recycling. Interestingly acute disruption of CHL1/Hsc70 complex reveals stronger phenotypical alterations than those observed in CHL1^{-/-} mice. Thus synaptic terminals of HPDpeptideCHL1 loaded neurons accumulate two-fold more CCSVs comparing with terminals from neurons of control groups whereas synaptic terminals of CHL1^{-/-} neurons have only 7 to 10% more CCSVs when compared with CHL1^{+/+} neurons. Furthermore there is a 20% reduction in the number of synaptic vesicles in terminals of HPDpeptideCHL1 loaded neurons whereas no change in the number of synaptic vesicles in CHL1^{-/-} synapses could be observed. HPDpeptideCHL1 nearly completely blocked activity-induced formation of CCSVs. As it was mentioned above up-regulation of CSP expression and probably some other proteins might partially compensate CHL1 ablation.

However, a reduced rate of synaptic vesicle recycling may affect proper functioning of neural circuits and information processing in the brain, manifested by abnormalities in behaviour in CHL1^{-/-} mice. Two independent studies have shown a positive correlation between a missense polymorphism in the CHL1 gene and schizophrenia in humans (Chen et al., 2005; Sakurai et al., 2002), a finding that could not be explained by a molecular mechanism so far. Whereas an understanding of the many molecular mechanisms underlying schizophrenia remains presently rudimentary, it is well established that schizophrenia is a complex and predominantly genetic disorder. It is not characterized by a single causative gene; alterations in different critical genes predispose a subject in various ways, but in a convergent fashion, to a central pathophysiological process: an alteration in synapse function and an eventual disruption of neural circuits (Harrison and Weinberger, 2005). In this respect, it is interesting that alterations in at least one other gene, Epsin 4,

encoding the clathrin-associated protein entropin, also cause genetic susceptibility to schizophrenia (Pimm et al., 2005). Furthermore, expression levels of Hsc70 were also changed in animal models of schizophrenia (Fatemi et al., 2005), suggesting that abnormalities in Hsc70 function and clathrin recycling pathways may contribute to an aspect of schizophrenia etiology. Additional analyses are required to establish the mechanisms by which mutations in CHL1, and alterations in clathrin-dependent synaptic vesicles recycling, contribute to abnormalities in information processing in the brain that eventually result in neurological disorders.

VI. SUMMARY

Project 1. The role of NCAM in maintaining of the cytoskeleton-dependent structural integrity of post-synaptic densities and regulation of the AMPA receptor recycling

Glutamatergic synapses with postsynaptic densities (PSD) of complex shape, often referred as perforated, have attracted attention due to the transient increase of their percentage following neural activity, such as induction of long-term potentiation. Moreover, they are often considered as morphological landmarks of synaptic remodelling and increased synapse activation in brain pathologies. In spite of the fact that models of PSD perforation have been widely discussed, mechanisms inducing perforation of PSDs and the role of this structural rearrangement in PSD function are poorly understood. Cell adhesion molecules and associated cytoskeletal elements are likely to play an important role in such rearrangements. The neural cell adhesion molecule NCAM has been implicated in synaptic plasticity and recruits its binding partner spectrin to synaptic contacts providing an anchoring scaffold for synaptic proteins. We show that numbers of perforated synapses are increased in the CA1 stratum radiatum of the hippocampus of NCAM deficient (NCAM^{-/-}) versus wild type (NCAM^{+/+}) mice and in cultured NCAM^{-/-} versus NCAM^{+/+} hippocampal neurons. Disruption of the spectrin meshwork in cultured NCAM^{+/+} hippocampal neurons by antimycin or latrunculin or by transfection with spectrin siRNA increases the percentage of perforated synapses in these neurons to the level seen in NCAM^{-/-} neurons, suggesting that the NCAM-assembled spectrin cytoskeleton maintains structural integrity of PSD. We demonstrate that PSD perforations contain endocytic zones involved in alfa-amino-3-hydroxy-5-methyl-4-isoxazolepropionic acid (AMPA) receptor internalisation. AMPA receptor internalisation in NCAM^{-/-} neurons is increased by 30% compared to NCAM^{+/+} neurons indicating that the NCAM assembled postsynaptic spectrin scaffold is important for inhibition of AMPA receptor endocytosis. An abnormally high AMPA receptor endocytosis being accompanied by structural abnormalities in PSD may contribute to alterations in synaptic plasticity and brain pathologies associated with ablation or mutations in NCAM and spectrin genes.

Project 2. The role of the cell adhesion molecule close homologue of L1 (CHL1) in regulation of clathrin-dependent synaptic vesicle recycling

Mutations in human analogue of murin CHL1 gene – CALL correlate with the occurrence of schizophrenia. Schizophrenia is a neuropsychiatric disorder associated with abnormal neurocircuits and functioning of synapses. Although these findings suggest that CHL1 regulates synapse functioning, the role of CHL1 in the organization of the synaptic machinery has not been fully analysed. Pilot experiments show that CHL1 interacts with 70 kDa heat shock cognate protein (Hsc70) that is a constitutively expressed member of the heat shock inducible Hsp70 protein family. Hsc70 regulates uncoating of clathrin coated vesicles in the clathrin-dependent synaptic vesicles recycling pathway.

In the present study, we were able to show that CHL1 localizes in axons where it recruits Hsc70 to the synaptic terminals. Numbers of clathrin coated vesicles were increased in synaptic terminals of CHL1^{-/-} neurons suggesting that clathrin uncoating is slowed down under conditions of reduced levels of Hsc70. Conversely, activity-induced formation of clathrin-coated vesicles in response to high potassium stimulation was inhibited in CHL1^{-/-} compared with CHL1^{+/+} synapses. This can suggest that reduced rates of clathrin coat release from CCSVs may result in lack of availability of essential coat proteins to form new CCSVs in an activity-dependent manner: clathrin, AP180, and AP2 could be trapped in CCSVs formed during previous cycles of neuronal activity, and would thus be unavailable to form new CCSVs. Hsc70 is still recruited into the synapses of CHL1^{-/-} neurons probably via CSP, another vesicle Hsc70 binding protein. Levels of this protein are elevated in CHL1^{-/-} mice. To overcome this compensatory mechanism we have loaded CHL1^{+/+} neurons with a HPD peptide, which competitively interferes with CHL1/Hsc70 interaction. Disruption of CHL1/Hsc70 interaction showed an even more pronounced effect than CHL1 deficiency itself. HPD peptide induced two-fold increase in the numbers of clathrin coated vesicles and 20% decrease in the number of synaptic vesicles in non-stimulated synapses, nearly completely blocked activity-induced CCSV formation and significantly inhibited activity-induced synaptic vesicle fusion. Our results demonstrate that deficiency in CHL1/Hsc70 interaction inhibits uncoating of CCSVs and thus slower processing of synaptic vesicles recycling. This can contribute to synapse dysregulations contributing to a set of neuropsychiatric disorder including schizophrenia.

VII. REFERENCES

- Adesnik H, Nicoll RA, England PM. (2005) Photoinactivation of native AMPA receptors reveals their real-time trafficking. *Neuron*. 48:977-985.
- Ahmari SE, Buchanan J, Smith SJ. (2000) Assembly of presynaptic active zones from cytoplasmic transport packets. *Nat Neurosci*. 3:445-451.
- Allison DW, Chervin AS, Gelfand VI, Craig AM (2000) Postsynaptic scaffolds of excitatory and inhibitory synapses in hippocampal neurons: maintenance of core components independent of actin filaments and microtubules. *J Neurosci* 20:4545-4554.
- Angeloni D, Lindor NM, Pack S, Latif F, Wei MH, Lerman MI. (1999) CALL gene is haploinsufficient in a 3p- syndrome patient. *Am J Med Genet*. 86:482-485.
- Angeloni, D, Wei M, Lerman MI. (1999) Two single nucleotide polymorphisms (SNPs) in the CALL gene for association studies with IQ. *Psychiatr. Genet*. 9:165-167.
- Appel F, Holm J, Conscience JF, Schachner M. (1993) Several extracellular domains of the neural cell adhesion molecule L1 are involved in neurite outgrowth and cell body adhesion. *J. Neurosci*. 13: 4764-4775.
- Atkinson SJ, Hosford MA, Molitoris BA. (2004) Mechanism of actin polymerization in cellular ATP depletion. *J Biol Chem* 279:5194-5199.
- Baines AJ, Keating L, Phillips GW, Scott C. (2001) The postsynaptic spectrin/4.1 membrane protein "accumulation machine". *Cell Mol Biol Lett* 6:691-702.
- Blanpied TA, Scott DB, Ehlers MD. (2002) Dynamics and regulation of clathrin coats at specialized endocytic zones of dendrites and spines. *Neuron*. 36:435-449.
- Bliss TV, Collingridge GL. (1993) A synaptic model of memory: Longterm potentiation in the hippocampus, *Nature* 361:31-39.
- Bloom O, Evergren E, Tomilin N, Kjaerulff O, Low P, Brodin L, Pieribone VA, Greengard P, Shupliakov O. (2003) Colocalization of synapsin and actin during synaptic vesicle recycling. *J Cell Biol*. 161:737-47.
- Bodrikov V, Leshchyn'ska I, Sytnyk V, Overvoorde J, den Hertog J, Schachner M. (2005) RPTPalph is essential for NCAM-mediated p59fyn activation and neurite elongation. *J Cell Biol*. 168:127-39

- Bronk P, Wenniger JJ, Dawson-Scully K, Guo X, Hong S, Atwood HL, Zinsmaier KE. (2001). *Drosophila* Hsc70-4 is critical for neurotransmitter exocytosis in vivo. *Neuron* 30, 475–488.
- Buchs P, Muller D. (1996) Induction of long-term potentiation is associated with major ultrastructural changes of activated synapses. *Proc Natl Acad Sci USA* 93:8040-8045.
- Buhusi M, Midkiff BR, Gates AM, Richter M, Schachner M, Maness PF. (2003) Close homolog of L1 is an enhancer of integrin-mediated cell migration. *J Biol Chem.* 278:25024-25031.
- Bukalo O, Fentrop N, Lee AYW, Salmen B, Law JWS, Wotjak CT, Schweizer M, Dityatev A, Schachner M (2004) Conditional ablation of the neural cell adhesion molecule reduces precision of spatial learning, long-term potentiation, and depression in the CA1 subfield of mouse hippocampus. *J Neurosci* 24:1565-1577.
- Carroll RC, Beattie EC, Xia H, Luscher C, Altschuler Y, Nicoll RA, Malenka RC, von Zastrow M. (1999) Dynamin-dependent endocytosis of ionotropic glutamate receptors. *Proc Natl Acad Sci U S A.* 96:14112-7.
- Carter LL, Redelmeier TE, Woollenweber LA, Schmid SL. (1993) Multiple GTP-binding proteins participate in clathrin-coated vesicle-mediated endocytosis. *J Cell Biol.* 120:37-45.
- Chamberlain LH, Burgoyne RD. (1997) The molecular chaperone function of the secretory vesicle cysteine string proteins. *J Biol Chem.* 272:31420-31426.
- Chen QY, Chen Q, Feng GY, Lindpaintner K, Chen Y, Sun X, Chen Z, Gao Z, Tang J, He L. (2005) Case-control association study of the close homologue of L1 (CHL1) gene and schizophrenia in the chinese population. *Schizophr Res.* 73:269-74.
- Chen S., Mantei N., Dong L., Schachner M. (1999) Prevention of neuronal cell death by neural adhesion molecules L1 and CHL1. *J Neurobiol* 38: 428-439.
- Cole GJ, Akeson R. (1989). Identification of a heparin binding domain of the neural cell adhesion molecule N-CAM using synthetic peptides. *Neuron* 2, 1157-1165.
- Cooney JR, Hurlburt JL, Selig DK, Harris KM, Fiala JC. (2002) Endosomal compartments serve multiple hippocampal dendritic spines from a widespread rather than a local store of recycling membrane. *J Neurosci.* 22:2215-2224.
- Cremer H, Chazal G, Goridis C, Represa A. (1997). NCAM is essential for axonal growth and fasciculation in the hippocampus. *Mol. Cell Neurosci.* 8, 323-335.

- Cremer H, Lange R, Christoph A, Plomann M, Vopper G, Roes J, Brown R, Baldwin S, Kraemer P, Scheff S. (1994) Inactivation of the N-CAM gene in mice results in size reduction of the olfactory bulb and deficits in spatial learning. *Nature* 367:455-459.
- Crossin KL, Krushel LA. (2000). Cellular signaling by neural cell adhesion molecules of the immunoglobulin superfamily. *Dev. Dyn.* 218, 260-279.
- del Cerro S, Arai A, Kessler M, Bahr BA, Vanderklish P, Rivera S, Lynch G. (1994) Stimulation of NMDA receptors activates calpain in cultured hippocampal slices. *Neurosci Lett* 167:149-152.
- Delling M, Wischmeyer E, Dityatev A, Sytnyk V, Veh RW, Karschin A, Schachner M. (2002) The neural cell adhesion molecule regulates cell-surface delivery of G-protein-activated inwardly rectifying potassium channels via lipid rafts. *J Neurosci.* 22:7154-64.
- Demyanenko GP, Schachner M, Anton E, Schmid R, Feng G, Sanes J, Maness PF. (2004) Close homolog of L1 modulates area-specific neuronal positioning and dendrite orientation in the cerebral cortex. *Neuron.* 44:423-37.
- Derkach V, Oh M, Guire E, Soderling T. (2007) Regulatory mechanisms of AMPA receptors in synaptic plasticity. *Nat Rev Neurosci* 8:101-113.
- Dityatev A, Dityateva G, Schachner M. (2000) Synaptic strength as a function of post-versus presynaptic expression of the neural cell adhesion molecule NCAM. *Neuron* 26:207–217.
- Dityatev A, Dityateva G, Sytnyk V, Delling M, Toni N, Nikonenko I, Muller D, Schachner M. (2004) Polysialylated neural cell adhesion molecule promotes remodeling and formation of hippocampal synapses. *J Neurosci* 24:9372-9382.
- Doherty P, Walsh FS. (1992). Cell adhesion molecules, second messengers and axonal growth. *Curr. Opin. Neurobiol.* 2, 595-601.
- Edwards FA. (1995) Anatomy and electrophysiology of fast central synapses lead to a structural model for long-term potentiation. *Physiol Rev* 75:759-787.
- Ehlers MD. (2000) Reinsertion or degradation of AMPA receptors determined by activity-dependent endocytic sorting. *Neuron.* 28:511-25.
- Faddis BT, Hasbani MJ, Goldberg MP. (1997) Calpain activation contributes to dendritic remodeling after brief excitotoxic injury in vitro. *J Neurosci* 17:951-959.

- Fatemi SH, Pearce DA, Brooks AI, Sidwell RW. (2005) Prenatal viral infection in mouse causes differential expression of genes in brains of mouse progeny: a potential animal model for schizophrenia and autism. *Synapse*. 57:91-9.
- Fiala J, Feinberg M, Popov V, Harris K. (1998) Synaptogenesis via dendritic filopodia in developing hippocampal area CA1. *J Neurosci* 17:8900–8911.
- Fischer M, Kaeck S, Wagner U, Brinkhaus H, Matus A. Glutamate receptors regulate actin-based plasticity in dendritic spines. *Nature Neurosci.* 3, 887–894 (2000).
- Frints SG, Marynen P, Hartmann D, Fryns JP, Steyaert J, Schachner M, Rolf B, Craessaerts K, Snellinx A, Hollanders K, D'Hooge R, De Deyn PP, Froyen G. (2003) CALL interrupted in a patient with non-specific mental retardation: gene dosage-dependent alteration of murine brain development and behavior. *Hum Mol Genet.* 12:1463-74.
- Gaidarov I, Santini F, Warren RA, Keen JH. (1999) Spatial control of coated-pit dynamics in living cells. *Nat Cell Biol.* 1:1-7.
- Ganeshina O, Berry RW, Petralia RS, Nicholson DA, Geinisman Y. (2004) Synapses with a segmented, completely partitioned postsynaptic density express more AMPA receptors than other axospinous synaptic junctions. *Neuroscience*.125:615-23.
- Geinisman Y, deToledo-Morrel L, Morrel F. (1991) Induction of long-term potentiation is associated with an increase in the number of axo-spinous with segmented postsynaptic densities. *Brain Res* 566:77-88.
- Geinisman Y. (1993) Perforated axospinous synapses with multiple, completely partitioned transmission zones: probable structural intermediates in synaptic plasticity. *Hippocampus.* 3:417-433.
- Granseth B, Odermatt B, Roylev S, Lagnado L. (2006) Clathrin-Mediated Endocytosis Is the Dominant Mechanism of Vesicle Retrieval at Hippocampal Synapses *Neuron* 51, 773–786
- Hannah MJ, Schmidt AA, Huttner WB. (1999) Synaptic vesicle biogenesis. *Annu Rev Cell Dev Biol.* 15:733-98.
- Harata N, Pyle JL, Aravanis AM, Mozhayeva M, Kavalali ET, Tsien RW. (2001) Limited numbers of recycling vesicles in small CNS nerve terminals: implications for neural signaling and vesicular cycling. *Trends Neurosci.* 24:637-643.

- Harata N, Ryan TA, Smith SJ, Buchanan J, Tsien RW. (2001) Visualizing recycling synaptic vesicles in hippocampal neurons by FM 1-43 photoconversion. *Proc Natl Acad Sci U S A.* 98:12748-12753.
- Harris K, Jensen F, Tsao B. (1992) Three-dimensional structure of dendritic spines and synapses in rat hippocampus (CA1) at postnatal day 15 and Adult ages: implication for the maturation of synaptic physiology and long-term potentiation. *J Neurosci* 12:2685-2705.
- Harrison PJ, Weinberger DR. (2005) Schizophrenia genes, gene expression, and neuropathology: on the matter of their convergence. *Mol Psychiatry.* 10:40-68
- Hillenbrand R, Molthagen M, Montag D, Schachner M. (1999) The close homologue of the neural adhesion molecule L1 (CHL1): patterns of expression and promotion of neurite outgrowth by heterophilic interactions. *Eur J Neurosci.* 11:813-826.
- Hoffman S, Edelman GM. (1983). Kinetics of homophilic binding by embryonic and adult forms of the neural cell adhesion molecule. *Proc. Natl. Acad. Sci. U. S. A* 80, 5762-5766.
- Hoffman KB, Larson J, Bahr BA, Lynch G. (1998) Activation of NMDA receptors stimulates extracellular proteolysis of cell adhesion molecules in hippocampus. *Brain Res.* 811:152-155.
- Holm J, Hillenbrand R, Steuber V, Bartsch U, Moos M, Lubbert H, Montag D, Schachner M. (1996) Structural features of a close homologue of L1 (CHL1) in the mouse: a new member of the L1 family of neural recognition molecules. *Eur J Neurosci* 8: 1613-1629.
- Hortsch M. (1996) The L1 family of neural cell adhesion molecules: old proteins performing new tricks. *Neuron* 17: 587-593.
- Howard CV, Reed MG. (1998) Unbiased stereology. Three-dimensional measurement in microscopy. Oxford: BIOS Scientific Publications.
- Hsieh H, Boehm J, Sato C, Iwatsubo T, Tomita T, Sisodia S, Malinow R. (2006) AMPAR removal underlies Ab-induced synaptic depression and dendritic spine loss. *Neuron* 52, 831–843
- Irintchev A, Koch M, Needham LK, Maness P, Schachner M. (2004) Impairment of sensorimotor gating in mice deficient in the cell adhesion molecule L1 or its close homologue, CHL1 *Brain Res.* 1029: 131-4.
- Jeffrey M, Halliday WG, Bell J, Johnston AR, MacLeod NK, Ingham C, Sayers AR,

- Brown DA, Fraser JR. (2000) Synapse loss associated with abnormal PrP precedes neuronal degeneration in the scrapie-infected murine hippocampus. *Neuropathol Appl Neurobiol* 26:41-54.
- Jiang R, Gao B, Prasad K, Greene LE, Eisenberg E. (2000) Hsc70 chaperones clathrin and primes it to interact with vesicle membranes. *J Biol Chem.* 275:8439-47.
- Jorgensen OS. (1995). Neural cell adhesion molecule (NCAM) as a quantitative marker in synaptic remodeling. *Neurochem. Res.* 20, 533-547.
- Jourdain P, Nikonenko I, Alberi S, Muller D. (2002) Remodeling of hippocampal synaptic networks by a brief anoxia-hypoglycemia. *J Neurosci* 22:3108-3116.
- Jourdi H, Yanagihara T, Martinez U, Bi X, Lynch G, Baudry M. (2005) Effect of positive AMPA receptor modulators on calpain-mediated spectrin degradation in cultured hippocampal slices. *Neurochem Int* 46:31-40.
- Kadmon G, Altevogt P. (1997) The cell adhesion molecule L1: species- and cell-type-dependent multiple binding mechanisms. *Differentiation* 61: 143-150.
- Kadmon G, Kowitz A, Altevogt P, Schachner M. (1990). Functional cooperation between the neural adhesion molecules L1 and N-CAM is carbohydrate dependent. *J. Cell Biol.* 110, 209-218.
- Kamal A, Ying Y, Anderson RG. (1998) Annexin VI-mediated loss of spectrin during coated pit budding is coupled to delivery of LDL to lysosomes. *J Cell Biol* 142:937-947.
- Kirov S, Harris K. 1999 Dendrites are more spiny on mature hippocampal neurons when synapses are inactivated. *Nat neuroscience* 2:878:883.
- Kiss JZ, Muller D. (2001). Contribution of the neural cell adhesion molecule to neuronal and synaptic plasticity. *Rev. Neurosci.* 12, 297-310.
- Kitamura N, Nishino N, Hashimoto T, Kajimoto Y, Shirai Y, Murakami N, Yang CQ, Lin XH, Yamamoto H, Nakai T, Mita T, Komure O, Shirakawa O, Nakai H (1998) Asymmetrical changes in the fodrin alpha subunit in the superior temporal cortices in schizophrenia. *Biol Psychiatry* 43:254-262.
- Kolkova K, Novitskaya V, Pedersen N, Berezin V, Bock E. (2000). Neural cell adhesion molecule-stimulated neurite outgrowth depends on activation of protein kinase C and the Ras-mitogen-activated protein kinase pathway. *J. Neurosci.* 20, 2238-2246.
- Kruse J, Mailhammer R, Wernecke H, Faissner A, Sommer I, Goridis C, Schachner M. (1984) Neural cell adhesion molecules and myelin-associated glycoprotein share a

- common carbohydrate moiety recognized by monoclonal antibodies L2 and HNK-1. *Nature* 311: 153-155.
- Landis DM, Reese TS. (1983) Cytoplasmic organization in cerebellar dendritic spines. *J Cell Biol* 97:1169-1178.
- Leite JP, Neder L, Arisi GM, Carlotti CG Jr, Assirati JA, Moreira, JE. (2005) Plasticity, synaptic strength, and epilepsy: what can we learn from ultrastructural data? *Epilepsia* 46:134-141.
- Leshchyn's'ka I, Sytnyk V, Morrow J, Schachner M. (2003) Neural cell adhesion molecule (NCAM) association with PKC β 2 via β 1 spectrin is implicated in NCAM-mediated neurite outgrowth. *J Cell Biol* 61:625-639.
- Leshchyn's'ka I, Sytnyk V, Richter M, Andreyeva A, Puchkov D, Schachner M. (2006) The adhesion molecule CHL1 regulates uncoating of clathrin-coated synaptic vesicles. *Neuron* 52, 1011–1025.
- Lipman DJ, Pearson WR. (1985) Rapid and sensitive protein similarity searches. *Science* 227: 1435-1441.
- Lledo, PM, Zhang X, Sudhof TC, Malenka RC, Nicoll RA. (1998). Postsynaptic membrane fusion and long-term potentiation. *Science*. 279:399–403.
- Lu, W., Man, H., Ju, W., Trimble, W.S., MacDonald, J.F., and Wang, Y.T. (2001). Activation of synaptic NMDA receptors induces membrane insertion of new AMPA receptors and LTP in cultured hippocampal neurons. *Neuron*. 29, 243-254.
- Lu W, Ziff EB. (2005) PICK1 interacts with ABP/GRIP to regulate AMPA receptor trafficking. *Neuron*. 47:407-421.
- Luscher C, Nicoll RA, Malenka RC, Muller D. (2000) Synaptic plasticity and dynamic modulation of the postsynaptic membrane. *Nat Neurosci* 3:545-550.
- Lynch G, Baudry M. (1987) Brain spectrin, calpain and long-term changes in synaptic efficacy. *Brain Res Bull* 18:809-815.
- Mackie K, Sorkin BC, Nairn AC, Greengard P, Edelman GM, Cunningham BA. (1989) Identification of two protein kinases that phosphorylate the neural cell-adhesion molecule, N-CAM. *J. Neurosci.* 9, 1883-1896.
- Mahaffey DT, Moore MS, Brodsky FM, Anderson RG. (1989) Coat proteins isolated from clathrin coated vesicles can assemble into coated pits. *J Cell Biol*. 108:1615-1624.
- Malenka R, Nicoll R. (1999) Long-term potentiation--a decade of progress? *Science*. 285:1870-4.

- Maletic-Savatic M, Malinow R. (1998) Calcium-evoked dendritic exocytosis in cultured hippocampal neurons. Part I: *trans*-Golgi network derived organelles undergo regulated exocytosis. *J Neurosci* 18:6803–6813.
- Malinow R, Malenka R. (2002) AMPA receptor trafficking and synaptic plasticity, *Annu. Rev. Neurosci.* 25:103–126.
- Maness P, Schachner M. (2007) Neural recognition molecules of the immunoglobulin superfamily: signaling transducers of axon guidance and neuronal migration *Nat neurosci* 1:19-26.
- Massol RH, Boll W, Griffin AM, Kirchhausen T. (2006). A burst of auxilin recruitment determines the onset of clathrin-coated vesicle uncoating. *Proc. Natl. Acad. Sci. USA* 103, 10265–10270.
- Milev,P., Friedlander,D.R., Sakurai,T., Karthikeyan,L., Flad,M., Margolis,R.K., Grumet,M., and Margolis,R.U. (1994). Interactions of the chondroitin sulfate proteoglycan phosphacan, the extracellular domain of a receptor-type protein tyrosine phosphatase, with neurons, glia, and neural cell adhesion molecules. *J. Cell Biol.* 127, 1703-1715.
- Milev,P., Maurel,P., Haring,M., Margolis,R.K., and Margolis,R.U. (1996). TAG-1/axonin-1 is a high-affinity ligand of neurocan, phosphacan/protein-tyrosine phosphatase-zeta/beta, and N-CAM. *J. Biol. Chem.* 271, 15716-15723.
- Molitoris BA, Dahl R, Hosford M (1996) Cellular ATP depletion induces disruption of the spectrin cytoskeletal network. *Am J Physiol* 271:790-798.
- Montag-Sallaz M, Baarke A, Montag D. (2003) Aberrant neuronal connectivity in CHL1-deficient mice is associated with altered information processing-related immediate early gene expression. *J Neurobiol.* 57:67-80.
- Montag-Sallaz M, Schachner M, Montag D. (2002) Misguided axonal projections, neural cell adhesion molecule 180 mRNA upregulation, and altered behavior in mice deficient for the close homolog of L1. *Mol Cell Biol.* 22:7967-81.
- Morgan JR, Prasad K, Jin S, Augustine GJ, Lafer EM. (2001) Uncoating of clathrin-coated vesicles in presynaptic terminals: roles for Hsc70 and auxilin. *Neuron.* 32:289-300.
- Muller D, Wang C, Skibo G, Toni N, Cremer H, Calaora V, Rougon G, Kiss JZ (1996) PSA-NCAM is required for activity-induced synaptic plasticity. *Neuron* 17:413-422.
- Najm I, el-Skaf G, Massicotte G, Vanderklish P, Lynch G, Baudry M (1992) Changes in

- polyamine levels and spectrin degradation following kainate-induced seizure activity: effect of difluoromethylornithine. *Exp Neurol* 116:345-354.
- Neuhoff H, Roeper J, Schweizer M (1999) Activity-dependent formation of perforated synapses in cultured hippocampal neurons. *Eur J Neurosci* 11:4241-4250.
- Newmyer SL, Schmid SL. (2001) Dominant-interfering Hsc70 mutants disrupt multiple stages of the clathrin-coated vesicle cycle in vivo. *J Cell Biol.* 152:607-20.
- Nicholson D, Trana R, Katz Y, Kath W, Spruston N, Geinisman Y (2006) Distance-dependent differences in synapse number and AMPA receptor expression in hippocampal CA1 pyramidal neurons. *Neuron* 50:431-442.
- Nicoll RA, Malenka RC. (1995) Contrasting properties of two forms of long-term potentiation in the hippocampus. *Nature* 377:115-8.
- Niethammer P, Delling M, Sytnyk V, Dityatev A, Fukami K, Schachner M. (2002) Cosignaling of NCAM via lipid rafts and the FGF receptor is required for neuritogenesis. *J Cell Biol.* 157:521-32.
- Nikonenko, A.G., Sun, M., Lepsveridze, E., Apostolova, I., Petrova, I., Irintchev, A., Dityatev, A., and Schachner, M. (2006). Enhanced perisomatic inhibition and impaired long-term potentiation in the CA1 region of juvenile CHL1-deficient mice. *Eur. J. Neurosci.* 23, 1839–1852.
- Nikonenko I, Jourdain P, Alberi S, Toni N, Muller D (2002) Activity-induced changes of spine morphology. *Hippocampus* 12:585-591.
- Olsen M, Krog L, Edvardsen K, Skovgaard LT, Bock E (1993) Intact transmembrane isoforms of the neural cell adhesion molecule are released from the plasma membrane. *Biochem J* 295: 833-840.
- Ono K, Tomaszewicz H, Magnuson T, Rutishauser U. (1994). N-CAM mutation inhibits tangential neuronal migration and is phenocopied by enzymatic removal of polysialic acid. *Neuron* 13, 595-609.
- Ostroff LE, Fiala JC, Allwardt B, Harris KM. (2002) Polyribosomes redistribute from dendritic shafts into spines with enlarged synapses during LTP in developing rat hippocampal slices. *Neuron.* 35:535-45.
- Park, M., Penick, E.C., Edwards J.G., Kauer, J.A. and Ehlers, M.D. (2004) Recycling endosomes supply AMPA receptors for LTP. *Science* 305: 1972-1975.
- Park M, Salgado JM, Ostroff L, Helton TD, Robinson CG, Harris KM, Ehlers MD. (2006) Plasticity-induced growth of dendritic spines by exocytic trafficking from recycling

- endosomes. *Neuron*. 52:817-830.
- Pielage J., Fetter R., and Davis G. (2005) Presynaptic spectrin is essential for synapse stabilization. *Curr Biology* 15:918-928.
- Pimm J, McQuillin A, Thirumalai S, Lawrence J, Quested D, Bass N, Lamb G, Moorey H, Datta SR, Kalsi G, Badacsonyi A, Kelly K, Morgan J, Punukollu B, Curtis D, Gurling H. (2005) The Epsin 4 gene on chromosome 5q, which encodes the clathrin-associated protein enthoprotin, is involved in the genetic susceptibility to schizophrenia. *Am J Hum Genet*. 76:902-907.
- Portis A, Newton C, Pangborn W, Papahadjopoulos D. (1979) Studies on the mechanism of membrane fusion: evidence for an intermembrane Ca²⁺-phospholipid complex, synergism with Mg²⁺, and inhibition by spectrin. *Biochemistry*. 18:780-90.
- Pratte M, Rougon G, Schachner M, Jamon M. (2003) Mice deficient for the close homologue of the neural adhesion cell L1 (CHL1) display alterations in emotional reactivity and motor coordination. *Behav Brain Res*. 147:31-9.
- Probstmeier, R., Kuhn, K., and Schachner, M. (1989). Binding properties of the neural cell adhesion molecule to different components of the extracellular matrix. *J. Neurochem*. 53, 1794-1801.
- Richards D., Guatimosim C., and Betz W. (2000) Two Endocytic Recycling Routes Selectively Fill Two Vesicle Pools in Frog Motor Nerve Terminals *Neuron*, Vol. 27, 551–559
- Richards DA, Bai J, Chapman ER. (2005) Two modes of exocytosis at hippocampal synapses revealed by rate of FM1-43 efflux from individual vesicles. *J Cell Biol*. 168:929-39.
- Ringger NC, O'Stehen BE, Brabham JG, Silver X, Pineda J, Wang KK, Hayes RL, Papa L (2004) A novel marker for traumatic brain injury: CSF alphaII-spectrin breakdown product levels. *J Neurotrauma* 21:1443-1456.
- Rizzoli SO, Betz WJ. (2005) Synaptic vesicle pools. *Nat Rev Neurosci*. 6:57-69.
- Rolf, B., Lang, D., Hillenbrand, R., Richter, M., Schachner, M., Bartsch, U. (2003) Altered expression of CHL1 by glial cells in response to optic nerve injury and intravitreal application of fibroblast growth factor-2. *J. Neurosci. Res*. 71, 835-843.
- Ruoslahti E., Pierschbacher M. D. (1987) New perspectives in cell adhesion: RGD and integrins. *Science* 238: 491-497.
- Saghatelyan AK, Nikonenko AG, Sun M, Rolf B, Putthoff P, Kutsche M, Bartsch U,

- Dityatev A, Schachner M (2004) Reduced GABAergic transmission and number of hippocampal perisomatic inhibitory synapses in juvenile mice deficient in the neural cell adhesion molecule L1. *Mol Cell Neurosci* 26:191-203.
- Sakurai K, Migita O, Toru M, Arinami T. (2002) An association between a missense polymorphism in the close homologue of L1 (CHL1, CALL) gene and schizophrenia. *Mol Psychiatry*. 7:412-415.
- Sanes JR, Lichtman J. (1999) Can molecules explain long-term potentiation? *Nat Neurosci*. 2:597-604.
- Sato K, Hayashi T, Sasaki C, Iwai M, Li F, Manabe Y, Seki T, Abe K (2001) Temporal and spatial differences of PSA-NCAM expression between young-adult and aged rats in normal and ischemic brains. *Brain Res* 922:135-139.
- Sato K, Iwai M, Zhang WR, Kamada H, Ohta K, Omori N, Nagano I, Shoji M, Abe K (2003) Highly polysialylated neural cell adhesion molecule (PSA-NCAM) positive cells are increased and change localization in rat hippocampus by exposure to repeated kindled seizures. *Acta Neurochir Suppl* 86:575-579.
- Sato K, Saito Y, Kawashima S. (1995) Identification and characterization of membrane-bound calpains in clathrin-coated vesicles from bovine brain. *Eur J Biochem*. 230:25-31.
- Schachner M, Martini R. (1995) Glycans and the modulation of neural-recognition molecule function. *Trends Neurosci*. 18:183-91
- Schachner M. (1997) Neural recognition molecules and synaptic plasticity. *Curr Opin Cell Biol*. 9:627-34.
- Schikorski T, Stevens CF. (1997) Quantitative ultrastructural analysis of hippocampal excitatory synapses. *J Neurosci* 17:5858–5867.
- Schmid SL, Smythe E. (1991) Stage-specific assays for coated pit formation and coated vesicle budding in vitro. *J Cell Biol*. 114:869-880.
- Schmid SL. (1997) Clathrin-coated vesicle formation and protein sorting: an integrated process. *Annu Rev Biochem*.66:511-48.
- Schuster T, Krug M, Hassan H, Schachner M. (1998) Increase in proportion of hippocampal spine synapses expressing neural cell adhesion molecule NCAM 180 following long-term potentiation. *J Neurobiol* 37:359-372.
- Schuster T, Krug M, Stalder M, Hackel N, Gerardy-Schahn R, Schachner M. (2001). Immunoelectron microscopic localization of the neural recognition molecules L1,

- NCAM, and its isoform NCAM180, the NCAM-associated polysialic acid, beta1 integrin and the extracellular matrix molecule tenascin-R in synapses of the adult rat hippocampus. *J. Neurobiol.* 49,142-158.
- Sharma K, Fong DK, Craig AM. (2006) Postsynaptic protein mobility in dendritic spines: long-term regulation by synaptic NMDA receptor activation. *Mol. Cell. Neurosci.* 31:702-712.
- Smythe E, Pypaert M, Lucocq J, Warren G. (1989) Formation of coated vesicles from coated pits in broken A431 cells. *J Cell Biol.* 108:843-53.
- Snyder EM, Philpot BD, Huber KM, Dong X, Fallon JR, Bear MF. (2001). Internalization of ionotropic glutamate receptors in response to mGluR activation. *Nat. Neurosci.* 4:1079–1085.
- Sollner T, Bennett MK, Whiteheart SW, Scheller RH, Rothman JE. (1993) A protein assembly-disassembly pathway in vitro that may correspond to sequential steps of synaptic vesicle docking, activation, and fusion. *Cell.* 75:409-418.
- Sorra KE, Fiala JC, Harris KM (1998) Critical assessment of the involvement of perforations, spinules, and spine branching in hippocampal synapse formation. *J Comp Neurol* 398:225–240.
- Spacek J, Harris KM. (2004) Trans-endocytosis via spinules in adult rat hippocampus. *J Neurosci* 24:4233-4241.
- Sterio DC. (1984) The unbiased estimation of number and sizes of arbitrary particles using the disector. *J Microsc* 134:127–136.
- Stewart MG, Medvedev NI, Popov VI, Schoepfer R, Davies HA, Murphy K, Dallerac GM, Kraev IV, Rodriguez JJ. (2005) Chemically induced long-term potentiation increases the number of perforated and complex postsynaptic densities but does not alter dendritic spine volume in CA1 of adult mouse hippocampal slices. *Eur J Neurosci* 21:3368-3378.
- Stork O, Welzl H, Cremer H, Schachner M. (1997). Increased intermale aggression and neuroendocrine response in mice deficient for the neural cell adhesion molecule (NCAM). *Eur. J. Neurosci.* 9, 1117-1125.
- Stork O, Welzl H, Wotjak CT, Hoyer D, Delling M, Cremer H, Schachner, M. (1999). Anxiety and increased 5-HT1A receptor response in NCAM null mutant mice. *J. Neurobiol.* 40, 343-355.
- Sytnyk V, Leshchyn'ska I, Delling M, Dityateva G, Dityatev A, Schachner M (2002)

- Neural cell adhesion molecule promotes accumulation of TGN organelles at sites of neuron-to-neuron contacts. *J Cell Biol* 159:649-661.
- Sytnyk V, Leshchyns'ka I, Dityatev A, Schachner M (2004) Trans-Golgi network delivery of synaptic proteins in synaptogenesis. *J Cell Sci* 117:381-388.
- Sytnyk V, Leshchyns'ka I, Nikonenko AG, Schachner M. (2007) NCAM promotes assembly and activity-dependent remodeling of the postsynaptic signaling complex. *J Cell Biol.* 174:1071-1085.
- Tardin C, Cognet L, Bats C, Lounis B, Choquet D. (2003) Direct imaging of lateral movements of AMPA receptors inside synapses. *EMBO J* 22:4656–4665.
- Tobaben S, Thakur P, Fernandez-Chacon R, Sudhof TC, Rettig J, Stahl B. (2001). A trimeric protein complex functions as a synaptic chaperone machine. *Neuron* 31, 987–999.
- Toni N, Buchs PA, Nikonenko I, Povilaitite P, Parisi L, Muller D. (2001) Remodeling of synaptic membranes after induction of long-term potentiation. *J Neurosci* 21:6245-6251.
- Tsai J, Douglas MG. (1996) A conserved HPD sequence of the J-domain is necessary for YDJ1 stimulation of Hsp70 ATPase activity at a site distinct from substrate binding. *J. Biol. Chem.* 271, 9347-9354.
- Turrigiano G, Leslie K, Desai N, Rutherford L, Nelson S. (1998) Activity-dependent scaling of quantal amplitude in neocortical neurons. *Nature* 391:892-895.
- Vawter MP. (2000) Dysregulation of the neural cell adhesion molecule and neuropsychiatric disorders. *Eur J Pharmacol* 405:385-395.
- Virmani T, Han W, Liu X, Sudhof TC, Kavalali ET. (2003) Synaptotagmin 7 splice variants differentially regulate synaptic vesicle recycling. *EMBO J.* 22: 5347-5357.
- Voglmaier S, Kam K, Yang H, Fortin D, Hua Z, Nicoll R, Edwards R. (2006) Distinct Endocytic Pathways Control the Rate and Extent of Synaptic Vesicle Protein Recycling *Neuron* 51, 71–84.
- Wilde A, Beattie EC, Lem L, Riethof DA, Liu SH, Mobley WC, Soriano P, Brodsky FM. (1999) EGF receptor signaling stimulates SRC kinase phosphorylation of clathrin, influencing clathrin redistribution and EGF uptake. *Cell* 96:677-87.
- Williams EJ, Mittal B, Walsh FS, Doherty P. (1995). A Ca²⁺/calmodulin kinase inhibitor, KN-62, inhibits neurite outgrowth stimulated by CAMs and FGF. *Mol. Cell Neurosci.* 6, 69-79.

- Yao PJ, Coleman PD, Calkins DJ. (2002) High-resolution localization of clathrin assembly protein AP180 in the presynaptic terminals of mammalian neurons. *J Comp Neurol.* 447:152-162.
- Young JC, Agashe VR, Siegers K, Hartl FU. (2004) Pathways of chaperone-mediated protein folding in the cytosol. *Nat Rev Mol Cell Biol.* 5:781-91.
- Yuste R, Bonhoeffer T. (2001) Morphological changes in dendritic spines associated with long-term synaptic plasticity. *Annu Rev Neurosci* 24:1071-1089.
- Zhai RG, Vardinon-Friedman H, Cases-Langhoff C, Becker B, Gundelfinger ED, Ziv NE, Garner CC. (2001) Assembling the presynaptic active zone: a characterization of an active zone precursor vesicle. *Neuron.* 29:131-143.
- Zhang Y, Roslan R, Lang D, Schachner M, Lieberman AR, Anderson PN. (2000) Expression of CHL1 and L1 by neurons and glia following sciatic nerve and dorsal root injury. *Mol Cell Neurosci* 16: 71-86.
- Zhou Q, Homma KJ, Poo MM. (2004). Shrinkage of dendritic spines associated with long-term depression of hippocampal synapses. *Neuron* 44:749–757
- Zhu J, Qin Y, Zhao M, Van Aelst L, Malinow R. (2002). Ras and Rap control AMPA receptor trafficking during synaptic plasticity. *Cell* 110:443-455.
- Ziff EB (1997) Enlightening the postsynaptic density. *Neuron* 19:1163-1174.
- Zinsmaier KE, Bronk P. (2001) Molecular chaperones and the regulation of neurotransmitter exocytosis. *Biochem Pharmacol.* 62:1-11.

VIII. ACKNOWLEDGEMENTS

I would like to thank the ZMNH, the University of Hamburg and Professor Schachner as a director of the “Institute for the Biosynthesis of Neural Structures” for the possibility for me to accomplish my PHD study. I especially acknowledge the work of people that supervised me during this years – Prof. Mellita Schachner, Dr. Alexandr Nikonenko, Dr. Vladymyr Sytnyk, Dr. Iryna Leshchyns’ka. I would also like to thank my supervisor from Hamburg University Prof. Renwrantz and all the people who kindly agreed to join my PhD defense committee. I thank Michaela Schweizer for technical hints and discussions. I want to acknowledge the secretary of the Biology Faculty, Frau Sült-Wüpping, for helping me organizing documents for the defense. I would like to sincerely thank to all members of Volodya and Iryna’s group and all other institute colleagues for help and friendly attitude. I would like to thank my family members in Ukraine for telepathy support. I would like to thank all the people with whom I have enjoyed a friendship relations and personal development. Considering an impact on the latter my special thanks go to Gaga Kochlamazashvili, Sven Löbrich, Anselm Eibert and Ian Belle Stein.

IX. APPENDIX**1. Abbreviations**

ADP	adenosine diphosphate
AMPA	α -amino-3-hydroxy-5-methyl-4-isoxazolepropionic acid
AP	adaptor protein
ATP	adenosine triphosphate
BSA	bovine serum albumine
CA	cornus ammonus
CAM	cell adhesion molecule
CCSV	clathrin coated synaptic vesicles
CCV	clathrin coated vesicles
CHL1	close homologue of L1
CNS	central nervous system
CSP	cystein-string protein
DMSO	dimethylsulfoxide
DRG	dorsal root ganglia
FGF	fibroblast growth factor receptor
HNK-1	human nature killer
Hsc	heat shock cognate
Hsp	heat shock protein
Ig	immunoglobulin
kb	kilo base pairs
LTD	long term depression
LTP	long term potentiation
NCAM	neural cell adhesion molecule
NMDA	N-methyl-D-aspartate
PBS	phosphate buffer saline
PSA	polysialic acid
PSD	postsynaptic density
RPTP	receptor-type phosphotyrosine phosphatases
SEM	standard error of the mean
siRNA	small interference ribonucleic acid

TetTX	tetanus toxin
TGN	trans-Golgi network
TTX	tetrodotoxin

2. Publications and poster presentations

Publications:

Leshchyns'ka I., Sytnyk V., Richter M., Andreyeva A., Puchkov D., and Schachner M. (2006) The adhesion molecule CHL1 regulates uncoating of clathrin-coated synaptic vesicles. *Neuron* 52, 1011–1025.

Puchkov D., Leshchyns'ka I., Nikonenko A., Schachner M. and Sytnyk V. Disassembly of the NCAM/spectrin complex enhances postsynaptic endocytosis and induces perforation of the postsynaptic density. In preparation.

Poster presentations:

Puchkov D., Leschyns'ka I., Nikonenko O., Schachner M. and Sytnyk V. NCAM maintains cytoskeleton-dependent structural integrity of post-synaptic densities. Meeting of the federation of european neuroscience societies (FENS), Vienna, 8th-12th July 2006.

3. Curriculum vitae

Name	Dmytro Puchkov
Degree	Diploma in biology
Date of birth	3.03.1980
Place of birth	Ukraine, Zaporijja
Citizenship	Ukraine

Education

1997-2002 – National Kyiv University, Biological Faculty, Department of cytology, histology and developmental biology

Diploma thesis: “Morphometric study of the neurocytes in the medial preoptical nucleus of hypothalamus of sexually matured rats, which have been undergone the effect of stress or hydrocortisone during prenatal period”

Employment

11.1999 – 02.2001 - Lab technician in the Institute of Oncology, Ukrainian Academy of Medical Sciences, Kyiv

09.2001 - 07.2002 – volunteer in the Physiology Institute of Bogomoletz, Department of General physiology of Nervous System, Kyiv

01.08.2002 – present day - PhD student at the ZMNH, Institute for the Biosynthesis of Neural Structures, Hamburg University

4. Erklärung

Hiermit versichere ich dass ich die vorliegende Arbeit selbstständig und ohne fremde Hilfe verfasst habe. Ich habe keine anderen als die angegebenen Hilfsmittel und Quellen benutzt und habe die entnommen Stellen als solche kenntlich gemacht. Soweit Fremde Hilfe in Anspruch genommen wurde, ist dies entsprechend im Text vermerkt.

Diese Arbeit ist zuvor keiner Prüfungsbehörde, weder in dieser noch in abgewandelter Form, zum Erwerb des Doktorgrades vorgelegt worden. Auch mit keiner anderen Arbeit habe ich mich zuvor um den Erwerb des Doktorgrades bemüht.

Hamburg, March 2008
Dmytro Puchkov